INFORMATION TO USERS

This manuscript has been reproduced from the microfilm master. UMI films the text directly from the original or copy submitted. Thus, some thesis and dissertation copies are in typewriter face, while others may be from any type of computer printer.

The quality of this reproduction is dependent upon the quality of the copy submitted. Broken or indistinct print, colored or poor quality illustrations and photographs, print bleedthrough, substandard margins, and improper alignment can adversely affect reproduction.

In the unlikely event that the author did not send UMI a complete manuscript and there are missing pages, these will be noted. Also, if unauthorized copyright material had to be removed, a note will indicate the deletion.

Oversize materials (e.g., maps, drawings, charts) are reproduced by sectioning the original, beginning at the upper left-hand corner and continuing from left to right in equal sections with small overlaps.

Photographs included in the original manuscript have been reproduced xerographically in this copy. Higher quality 6" x 9" black and white photographic prints are available for any photographs or illustrations appearing in this copy for an additional charge. Contact UMI directly to order.

ProQuest Information and Learning
300 North Zeeb Road, Ann Arbor, MI 48106-1346 USA
800-521-0600

IN VIVO ASSESSMENT OF THE RELATION BETWEEN TRABECULAR BONE STRUCTURE IN THE RADIUS AND GENDER, AGING, MECHANICAL LOADING AND FRACTURE

By

NORMA J. MACINTYRE

A Thesis

Submitted to the School of Graduate Studies

in Partial Fulfillment of the Requirements

for the Degree

Doctor of Philosophy

McMaster University

IN VIVO ASSESSMENT OF RADIAL BONE STRUCTURE USING PQCT

DOCTOR OF PHILOSOPHY (1999)
(Medical Sciences)

McMaster University
Hamilton, Ontario

TITLE: *In Vivo* Assessment of the Relation Between Trabecular Bone Structure in the Radius and Gender, Aging, Mechanical Loading and Fracture.

AUTHOR: Norma J. MacIntyre, M.Sc. (University of Western Ontario)

SUPERVISOR: Dr. Colin E. Webber

NUMBER OF PAGES: *xiv*, 226

ABSTRACT

Bone structure is compromised in individuals with osteoporosis. Indices of trabecular bone structure which reflect the connectivity (CI), the average dimensions of the marrow holes (H_A) and the area of the largest hole (H_M) at the distal radius can be determined *in vivo*. This work evaluates whether these structural indices 1) are influenced by gender, aging and mechanical loading and 2) aid in the discrimination of individuals with low bone mass most at risk for fracture.

Gender and age-related patterns of bone structure in the nondominant distal radius measured using peripheral quantitative computed tomography (pQCT) demonstrate the expected trends in a cross-sectional study of 145 healthy adults. Men have a better connected, less porous trabecular network. The age-related decrease in CI in men (-0.8% /yr, $p < 0.05$) is less pronounced than in women (-2.2% /yr, $p < 0.001$). Similarly, there are significant age-related increases in H_A (+2.2% /yr, $p < 0.01$) and H_M (+1.1% /yr, $p < 0.01$) in women but not in men.

To investigate the impact of mechanical loading associated with hand dominance on indices of bone structure, bilateral images for 106 healthy adults were acquired. For all subjects, H_M is significantly smaller in the dominant radius ($p < 0.01$). Right handed subjects ($n = 96$) have greater CI ($p < 0.05$) and smaller H_M ($p < 0.01$) in the dominant limb.

The effect of altered mechanical loading on bone structure was assessed by immobilizing the nondominant limb of 10 healthy volunteers in a plaster cast for 6 weeks

followed by a remobilization period of 1 year. H_M increases ($p = 0.04$) during immobilization and recovers within 3 months of remobilization.

The ability of indices of trabecular structure to discriminate individuals with recent wrist fracture ($n = 22$) from controls matched for bone density ($n = 22$) was evaluated. The fracture group has a larger mean H_A than the group without fractures ($p < 0.05$). The relative odds of wrist fracture is 6.9 (95% CI: 1.3 to 37.3) for individuals with a $H_A \geq 6$ mm^2.

These data show that indices of trabecular bone structure, derived from pQCT images, reflect the expected patterns with respect to gender, age and mechanical loading. Preliminary results suggest that measuring H_A at the distal radius may aid in the identification of individuals with low bone mass who will sustain a fracture.

ACKNOWLEDGEMENTS

I am grateful to a number of individuals for their contribution to this work. First, I would like to thank my supervisor, Dr. Colin Webber, who provided a great learning environment. His insight and enthusiasm for bone research (and beyond) are inspiring. I thank Dr. Chris Gordon for pioneering the groundwork for my thesis and taking an active interest in my work. Thank-you to the members of my advisory committee, Dr. C.J. (Joe) Blimkie and Dr. G. Coates, for guidance and support. I am grateful to Dr. Adachi for providing valuable input. I thank my fellow lab mates, past and present, for many helpful discussions. Thanks to Lesley Beaumont for sharing her resources and expertise. I would also like to thank the staff of the Department of Nuclear Medicine (HHSC, McMaster Site) who always found time to provide assistance, encouragement and laughter.

I am indebted to all of the volunteers who participated in my research studies - without them there would be no thesis. I am grateful to a number of individuals who assisted me with subject recruitment: L. Picard, M. Ackerman, L. Hastings, M. Muller, Dr. M. Bhandari, G. Walencik and Dr. Adachi. I thank Dr. Webber, R. Stewart and L. Hastings for valuable input and assistance during the writing of my thesis. I could not have done it without you. I am grateful to Dr. M. Pierrynowski, Dr. C.J. Blimkie, R. Fraser, R. Cunningham, J. Moroz, Dr. V. Galea for aid in establishing techniques and designing/calibrating equipment. Thanks to Dr. M. Bhandari for applying plaster casts.

The support of all my family has been a welcome constant in my life. Over the past 5 years, their overwhelming love and generosity have carried me through some tough times and have made the good times even better. Especially, I thank my mother for encouraging my every endeavor and for her faith in my abilities and dreams. A special thanks to my "oldest" Hamilton friend, Laura Hastings, who has been an important part of my work and my play! Finally, I am grateful to Ron Stewart for contributing to this work (in ways too numerous to mention) with endless encouragement, love and friendship.

Financial support from the Father Sean O'Sullivan Research Centre (Studentship Award, 1996-1999) is gratefully acknowledged.

To my father, Donald Cameron MacIntyre (1933 - 1996),

who lived life with a merry heart and a mindful curiosity.

A merry heart doeth good like a medicine:
but a broken spirit drieth the bones.

- PROVERBS 17: 22

TABLE OF CONTENTS

LIST OF FIGURES

LIST OF TABLES

CHAPTER ONE
INTRODUCTION

1.1 Historical Perspective

Osteoporosis is a condition which results in an increased risk of fracture due to a loss of bone material and a deterioration in structural integrity making the skeleton less competent to withstand imposed forces imparted to it (Consensus Development Conference 1993). Osteoporosis is responsible for a substantial burden to our health care system; in Canada, there were 60,000 osteoporosis-related fractures in 1993 (Goeree et al 1996). Although age-related bone loss is a universal process, expression of osteoporosis is most frequent in postmenopausal women because women generally have smaller skeletons and experience accelerated bone loss with estrogen deficiency (Riggs and Melton 1986). Typically, the earliest clinical manifestation of postmenopausal osteoporosis is the fracture of the distal radius (Eastell 1996; Earnshaw et al. 1998). For a 50 year old women, there is a 16% lifetime risk of distal forearm fracture, with a peak incidence between the ages of 60 and 70 years (Goeree et al. 1996). The incidence of other common osteoporotic fractures (vertebrae and proximal femur) increases later in life (Riggs and Melton 1995). While there is no cure for osteoporosis, the early detection of individuals at risk permits interventions to preserve bone quality before it is critically compromised. Thus the ability to detect early changes associated with osteoporosis using an accessible, reliable, noninvasive technique is essential.

The identification of individuals most at risk for osteoporosis-related fractures is facilitated by quantifying correlates of bone strength. Bone mass and structure are two independent predictors of bone strength (Hui, Slemenda, and Johnston 1988; Mosekilde 1989). Bone mass can be measured noninvasively and is closely related to osteoporotic fracture risk on a population basis (Marshall, Johnell, and Wedel 1996). While measurement of bone mass is an accepted surrogate measure of bone strength, there are large overlaps in values for individuals with and without osteoporotic fracture limiting the ability to predict the fracture risk for a particular individual (Marshall, Johnell, and Wedel 1996; Webber 1998). Clearly, other assessment techniques are needed to identify individuals with low bone mass at risk for osteoporotic fracture. Another determinant of bone strength is bone structure and, recently, the technology permitting the simultaneous, noninvasive assessment of bone density and structure at the distal radius has become available (Müller, Rüegsegger, and Rüegsegger 1989; Gordon et al. 1996). It seems plausible that *in vivo* assessment of bone structure at the distal radius may aid in the early identification of individuals with low bone mass who will sustain an osteoporotic fracture.

1.2 Objectives and Experimental Approach

The overall purpose of this study was to evaluate the utility of *in vivo* distal radius trabecular bone structure measurements, derived from peripheral quantitative computed tomography (pQCT) images, in the identification of individuals at risk for fracture at the distal radius. To this end, a series of experiments has been completed.

The first objective was to determine if the indices of bone structure can be measured reliably. To achieve this, replicate pQCT scans obtained for 25 volunteers on two occasions (separated by approximately 7.7 days) were compared. The influence of controlled movement on the reproducibility of the structure measurements was also investigated in a subset of 16 volunteers.

The second objective was to test the hypothesis that these indices of bone structure would demonstrate the anticipated trends associated with gender and aging. This was done by assessing the gender and age-related patterns in trabecular bone structure in the nondominant radius in a cross-sectional study of 145 men and women between the ages of 20 and 84 years. The patterns determined for bone structure were compared with those for bone mass, density and geometry.

Thirdly, the impact of habitual mechanical loading on indices of trabecular bone structure assessed *in vivo* was determined and compared to the impact on bone mass, density and geometry. A cross-sectional study of 106 volunteers was completed to determine if structural differences exist between limbs which may be related to differential loading of the dominant limb. As well, 10 subjects completed a 13.5 month trial which altered the mechanical loading of the radius in the nondominant wrist. The structure of the trabecular bone was assessed to determine the response to a 6 week period of immobilization in a plaster cast and a subsequent 1 year period of remobilization.

The fourth objective was to assess the contribution of *in vivo* measurements of trabecular bone structure in the discrimination of individuals with low bone mass most at risk for fracture. This involved the completion of a case-control study to compare the

trabecular bone structure in the uninjured radius of 22 women with recent wrist fractures to that measured in matched controls with no history of fracture.

1.3 Organization of the Thesis

A review of the relevant literature is presented in Chapter 2. The description of the equipment and protocol used to determine the indices of trabecular bone structure measured using pQCT are presented in Chapter 3. As well, factors affecting reproducibility of these measurements are examined in that chapter. Chapters 4 and 5 describe cross-sectional studies which characterize the patterns of trabecular bone structure associated with gender, age and hand dominance. Chapter 6 details the impact of changes in mechanical loading due to cast immobilization and subsequent remobilization on trabecular radial bone structure. In Chapter 7, the results of the study to determine whether these indices of bone structure aid in the identification of individuals at risk for osteoporotic fracture are presented. The relevant findings are discussed in each of Chapters 3 to 7 with a general summary of the work presented in Chapter 8.

CHAPTER TWO
ASSESSING RADIAL BONE STRENGTH AND FRACTURE RISK

2.1 Introduction

A fracture occurs when the strength of the bone is insufficient to withstand the forces to which the bone is subjected. While there are many factors which contribute to fracture risk, anything which compromises bone strength will increase the likelihood that the bone will break. Osteoporosis is a common condition which is characterized by a loss of bone quality resulting in increased bone fragility and susceptibility to fracture (World Health Organization 1994). This has severe consequences for both the individual and the health care system. Therefore, considerable effort has been invested in determining which variables influence bone strength and how they can be measured in order to target high risk individuals for early intervention. The purpose of this chapter is to review the factors which have been identified as contributing to the strength of the adult skeleton and to discuss current *in vivo* methods of estimating fracture risk at the distal radius. The first section provides a brief overview of the problems associated with osteoporosis, focusing primarily on fractures of the distal forearm. The second section discusses determinants of bone strength, the "mechanostat" theory which proposes the mechanism(s) by which bone strength is regulated and the pathophysiology of postmenopausal osteoporosis. The third

section describes *in vivo* techniques which assess determinants of bone strength and evaluate the ability of these techniques to predict an individual's risk for fracture.

2.1 Epidemiology of Osteoporotic Fracture of the Distal Radius

In Canada, it is estimated that 1.8 million women had osteoporosis in 1993 and 60,000 osteoporotic fractures were documented that year (Goeree et al. 1996). There is an age-related increase in the incidence of fracture and one of the key risk factors is low bone mass. Although bone loss in the adult skeleton is a universal process, women, with typically smaller skeletons and an accelerated rate of bone loss associated with estrogen deficiency, are twice as likely as men to develop osteoporosis (Melton et al. 1992). The distal forearm is the site most frequently fractured in women under 75 years of age (Owen et al. 1982). In contrast, fractures of the spine and hip are experienced later in life (Riggs and Melton 1986). Consequently, osteoporotic fractures are most common in postmenopausal women and fracture of the distal forearm may be the earliest clinical manifestation of general osteoporosis (Mallmin and Ljunghall 1994).

Individuals with distal forearm fractures have significantly low bone mass compared to normal controls (Hesp, Klenerman, and Page 1984; Harma and Karjalaminen 1986; Crilly et al. 1987; Smith et al. 1990; Ooms et al. 1993; Mallmin and Ljunghall 1994; Eastell 1996). A correlation between bone quality (measured as cortical bone width in the 2nd metacarpal) and post fracture deformity has been identified (Dias, Wray, and Jones 1987). In the normal population there is a good correlation between bone mass measurements at different skeletal sites (Mazess and Barden 1990). In contrast,

differential bone loss has been observed in individuals with fractures in either the distal forearm or the spine (Eastell et al. 1989). Postmenopausal women with fractured wrists had a preferential bone loss in the distal radius; the women with fractures of the lumbar spine had a preferential bone loss in the spine; the women with fractures at both sites had a similar magnitude of bone loss in both sites. Regardless of the fracture site, the fracture group had lower bone mass at all sites than the normal postmenopausal women (Eastell et al. 1989). In a prospective study, Earnshaw et al. (1998) recruited 106 consecutive postmenopausal Colles' fracture patients and found that 50% had osteoporosis at the spine, hip or contralateral radius. Others found generalized bone loss in the nonfractured forearm, the spine and the hip of patients with fractures of the distal forearm who had no prior history of fracture (Mallmin and Ljunghall 1994). In fact, a single measurement of bone mass at the distal forearm acquired using single photon absorptiometry (SPA) can successfully predict various types of fragility fractures over a period of 25 years (Düppe et al. 1997). In women between the ages of 40 and 70 years, a decrease of 1 standard deviation (SD) in bone mineral density at the distal radius was associated with a relative risk of 1.66 [95 % confidence interval (95% CI): 1.13 to 2.46] for hip fracture, 1.79 (95% CI: 1.22 to2.62) for a vertebral fracture, and 1.33 (95% CI: 1.20 to1.73) for all fractures. Findings such as these suggest that measurements of bone mass at the distal radius represent a useful method of identifying individuals at risk for osteoporotic fracture.

Measurements of bone mineral density successfully predict fracture risk (Gärdsell, Johnell, and Nilsson 1991; Black et al. 1992; Cummings et al. 1993). A recent meta-analysis looked at the results of 229 prospective studies published between 1985 and

1995 which used densitometry methods to measure baseline bone mineral density in women and documented subsequent fractures (Marshall, Johnell, and Wedel 1996). Regardless of the site measured, the relative risk for fracture was approximately 1.5 (95% CI: 1.4 to 1.6) for a decrease in bone mineral density of 1 SD below age adjusted mean. The predictive ability was improved when site specific measurements were used to determine fracture risk at that site. Bone mineral density measurements are helpful to physicians when estimating the fracture risk of a patient. However, Marshall, Johnell, and Wedel conclude that while measurements of bone mineral density at fracture prone sites predict fracture risk on a population basis, they do not predict which individual with low bone mass will experience a fracture (1996). Thus, the implementation of an osteoporosis screening program using absorptiometry techniques was not recommended. A technique which quantifies bone strength *in vivo* and permits the early diagnosis of osteoporosis in individual patients is needed.

2.2 Determinants of Bone Strength in the Adult Skeleton

A number of factors have been identified which are associated with bone strength in the adult skeleton and characterize the natural history of bone turnover across the life span. One determinant of bone quality and fracture risk is the amount of mineralized bone present at a particular skeletal site. Bone mass can be described in absolute terms, bone mineral content (BMC) in g or mg. This does not take the size of the skeleton into account. Bone quantity also can be described in terms of the amount of bone in a given area, bone mineral density (BMD) in g/cm^2, or in terms of the amount of mineral in a

given volume of bone tissue, bone density (BD) in mg/cm^3. Two factors which contribute to the amount of bone present in the adult skeleton are peak bone mass and rate of bone loss. Bone geometry and structure are other factors associated with the strength of bone.

2.2.1 Peak Bone Mass and Rate of Bone Loss

The relation between bone quantity and fracture risk is evident in population studies. Two main determinants of bone mass in the mature skeleton are the peak amount of mineral accretion and the rate of bone loss (Seeman 1994). Controversy exists regarding the age at which peak bone mass is achieved in the maturing skeleton but it is generally accepted that about half is acquired during puberty (Parfitt 1994). Cross-sectional studies have investigated the accumulation or maintenance of bone mass in young adults and suggest that peak bone mass may be achieved as late as the third and possibly the fourth decade at some skeletal sites (Tylavsky et al. 1989; Halioua and Anderson 1990). Bonjour et al. (1993) have suggested that predominantly trabecular sites such as the spine achieve peak bone mass prior to cortical sites such as the shaft of long bones. Matkovic et al. (1994) measured BMC and BMD in 265 premenopausal Caucasian women and reported that most of the mineralized tissue in the spine and proximal femur is accumulated by late adolescence. At the distal forearm, bone mineral accumulation was estimated to be completed by the age of 22 years. Based on BMD measurements of the third lumbar vertebra corrected for bone size estimated from anteroposterior and lateral spine projection images, these investigators predicted that BD (g/cm^3) of the lumbar spine peaked towards the end of the third decade. As well, gender differences have been

identified demonstrating that the female skeleton typically achieves a lower peak bone mass than the male skeleton with calcium accretion ceasing by the age of 24 years in women and continuing beyond the age of 26 years in men (Garn 1972; Hui, Johnston, and Mazess 1985). Longitudinal studies provide a higher level of evidence but there are few such studies which investigate the age at which peak bone mass is achieved. One prospective study followed 156 healthy women (varying in age between 18.5 and 26 years at entry) for 5 years and found that increases of 12.5% occurred in total body BMD during the third decade and regionally BMD increased by 4.8% at a site in the radius, which consists of primarily cortical bone, and by 6.8% in the lumbar spine, which consists of primarily trabecular bone (Recker et al. 1992). Recker et al. (1992) estimated that the accretion of skeletal mass ceased between the ages of 28.3 and 29.5 years at the various sites measured in their study population while noting that fewer women over the age of 25 years gained bone mass compared to younger women. Despite the controversy concerning when peak bone mass is achieved, it is clear that the gains observed in early adulthood are substantially smaller than those observed during the adolescent growth spurt (Parfitt 1994). Thus, the peak bone mass of the adult skeleton is largely influenced by genetics, pubertal age and nutritional and physical activity factors accompanying puberty (Kannus et al. 1995; Hawker 1996).

An accelerated rate of bone loss is another factor which can contribute to low bone mass and, consequently, weaker bones. In the mature skeleton, bone is constantly being turned over by means of a process called 'remodeling' which involves the tightly coupled activity of basic multicellular units within a temporary anatomic structure known

as a bone remodeling unit (BRU) or bone metabolic unit (BMU). Following activation of a BRU, the old bone is demineralized by osteoclasts and creates a resorption cavity which is subsequently filled with new organic matrix by osteoblasts. This becomes mineralized and the process is complete. The entire process takes 3 to 6 months to complete one remodeling cycle (25 to 35 days for resorption and over 100 days for formation and mineralization) (Parfitt 1979). In a healthy skeleton of average size, one new BRU is initiated and one new structural unit is completed about every 10 seconds (Parfitt 1979; Schultheis 1991). In contrast to the positive balance that occurs during growth, the resorption cavity in the adult skeleton may not be completely filled by new bone. The accumulation of these small deficits contributes to a gradual age-related loss of bone.

Gender differences exist with respect to the rate of bone loss. Men experience a steady age-related decrease in bone mass following the attainment of peak bone mass while women experience a three phase loss (Riggs and Melton 1986). Women between the ages of 35 years and the menopause lose no or very little bone mass, reflecting a protective influence of estrogen on the rate of bone loss (Riggs et al. 1987; Mazess and Barden 1991). An accelerated rate of loss occurs during the first 10 years of estrogen deficiency associated with menopause. During this second phase there is an increase in the number of activated BRUs and an increase in the depth of the resorption pits (Parfitt 1984). During the final phase there is a more gradual rate of loss which approximates the age-related rate observed in men (Riggs and Melton 1986). A cross-sectional study was recently conducted to look at patterns of cortical and trabecular bone loss in women by measuring BD of these compartments in the distal metaphyseal region of the radius

(Martin and Reid 1999). There appears to be a regional difference in duration of the accelerated bone loss phase. Martin and Reid (1999) found preferential bone loss in early postmenopausal women in the subcortical bone at the radius whereas trabecular bone loss occurred at a less pronounced but steady rate in women up to 40 years postmenopause. In a longitudinal study of age-related changes in forearm BD in 81 healthy postmenopausal women, most women (75%) lost bone between the initial visit and the second visit (1 to 3 years later) with 43% to 45% of the women demonstrating a rapid loss (> 2.5% per year change) of both cortical and trabecular bone (Hernández et al. 1997). The gender differences in patterns of bone loss result in a lifetime reduction in bone mass of 30% to 50% for women and 20% to 35% for men (Riggs and Melton 1986).

2.2.2 Bone Geometry and Trabecular Bone Structure

Bone quantity does not explain all of the variance in measurements of bone strength; the organization of bone material also contributes to the regional competency of the skeleton (Kleerekoper et al. 1985; Mosekilde 1986; Hui, Slemenda, and Johnston 1988). Cross-sectional studies have reported an age-related change in bone geometry. At the distal radius, there is a significant increase in cross-sectional area for the whole bone and for trabecular bone with aging in healthy women, whereas cortical bone cross-sectional area decreases (Bouxsein et al. 1994; Gatti et al. 1996; Wapniarz et al. 1997). The age-related increase in cross-sectional area in the shaft of the radius with periosteal bone apposition and endosteal bone resorption is more pronounced in men than in women (Burr and Martin 1983). The changes in bone geometry have been confirmed in a

longitudinal study by Heaney et al. (1997) using standardized x-ray films to quantify age-related dimensional changes in the metacarpals, radius and femur of 191 Caucasian women over a period of 21 years. Large increases in external diameter were observed in the shaft and neck of the femur. Small but significant decreases in external diameter were observed at the distal ¼ site of the radius and the metacarpal bones. A similar pattern was observed for measurements of cortical area which were significantly increased in the femoral shaft and decreased in the radius and metacarpals with age. An age-related decrease in cortical thickness was observed at all sites but was most pronounced in the nonweightbearing bones.

Bone biopsies from the iliac crest and necropsy specimens have made it possible to determine the natural history of bone structure and its contribution to mechanical competency in response to physical loading. In transiliac bone biopsies there is little change in the mean trabecular thickness with aging, whereas in the vertebrae there is a steady increase in the distance between horizontally oriented trabeculae which is slightly more pronounced in aging women than in aging men (Mosekilde 1988, 1989). In samples obtained from women over 75 years of age, there was an increased frequency of perforation of the trabecular network which was not observed in samples from males (Mosekilde 1989). There is no gender difference associated with age-related thinning of horizontal trabeculae (Mosekilde 1988, 1989). Similar information regarding connectedness and spacing of trabecular elements is not yet available for the distal radius. However, there is a recent *ex vivo* study which looked at the association between 2-dimensional indices of trabecular bone structure and mechanical failure of the distal

radius (Gordon, Webber, and Nicholson 1998). Using multiple regression analysis, Gordon, Webber and Nicholson (1998) demonstrated that the peak load at fracture is predicted by a combination of two variables which characterize the spacing of trabecular elements at the distal radius ($R^2 = 0.82$, $p = 0.006$). These data support the hypothesis that, similar to the bones in the spine and the pelvis, the organization of bone material contributes to the regional competency of the distal radius.

2.2.3 The Mechanostat Theory: A Putative Mechanism for Regulating Bone Strength

Four factors have been identified which contribute to the competency of the adult skeleton. These are: 1) genetics; 2) endocrinology; 3) nutrition; and 4) mechanical loading. Twin studies have shown that heredity accounts for as much as 80% of the variance in BMD (Pocock et al. 1987). Factors which alter the normal hormonal environment or the bioavailability of calcium and vitamin D are associated with altered bone mass (Johnston and Slemenda 1993). The "mechanostat" theory suggests that the factors related to genetics, endocrinology and nutrition modulate a "set point" within the effector bone cells (most likely the lining cells and osteocytes) which determines whether the bone maintains homeostasis, activates the modeling process, or activates the remodeling process (Frost 1987; Burr and Martin 1989). The "mechanostat" theory proposes that mechanical loading (through muscle action and anti-gravity weightbearing) controls the set point such that a decreased strain on the skeleton associated with disuse would activate the remodeling process to produce a site specific decrease in the amount of bone (Frost 1988; Frost, Ferretti, and Jee 1998). Skeletal homeostasis is re-established

when the perceived strain again falls within the physiological range determined by the set point. Conversely, increased mechanical forces would produce strains perceived to exceed the upper threshold for the physiological range determined by the set point for the loaded bone. Subsequent skeletal adaptations would occur to increase bone strength such that the perceived strain would again fall within the normal physiological range (Frost 1987; Burr and Martin 1989).

2.2.3 i Mechanical Loading Protocols With Osteogenic Characteristics

In response to induced strain, there are skeletal changes in both the physical properties, such as mass, density and structure, and mechanical properties, such as the amount of energy stored and amount of loading required to reach the bending and breaking points in bone (Lanyon 1987; Woo et al. 1981; Raab et al. 1990). Strain refers to the fractional geometric deformation of bone caused by loading. For example, a 0.1% change in bone length (for example) corresponds to 1,000 microstrain. Whereas *in vivo* characterization of the strain environment is difficult to quantify (Hinsenkamp et al. 1981), normal activity is associated with compressive strain between 200 and 2500 microstrain (Turner et al. 1991).

Work by Lanyon and Rubin has demonstrated characteristics of mechanical loading which have osteogenic effects. These investigators functionally isolated skeletally mature avian ulnae for a 6 to 8 week period and found that the associated decrease in normal mechanical loading (below 100 microstrain) caused a decrease in BMC and cross-sectional area, as well as cortical thinning due to endosteal resorption and intracortical

porosis associated with incomplete filling of Haversian canals (Rubin and Lanyon 1984, 1985). By applying controlled strain environments, a dose-response increase in bone mass accompanied increasing peak strain magnitudes in the functionally isolated turkey ulnae (Rubin and Lanyon 1985). In porcine bone, increases in the magnitude of peak strain have been achieved by removing the ulna from one forelimb and evaluating the response to increased functional loading in the remaining radius during ambulation (Goodship, Lanyon, and McFie 1979). When the peak strain magnitude was maintained within the normal physiological range and applied with consistent on/off rates but varied in load cycles, bone mass was preserved in rooster ulnae with a minimum of 4 X 0.5-hertz cycles per day and increased with loading cycles of at least 36 X 0.5-hertz cycles per day due to the altered strain distribution (Rubin and Lanyon, 1984). Static and dynamic strains were evaluated in isolated turkey ulnae to determine osteogenic effects and it was found that a static compressive strain applied daily for short periods induced bone loss similar to that associated with disuse, whereas dynamic compressive strains with an equivalent peak magnitude and loading protocol increased bone formation (Lanyon and Rubin 1984). Using the sheep model, a dose-response relation was found for bone formation and strain rates (O'Conner and Lanyon 1982) and high strain rates were required to induce an osteogenic response when strains of high magnitude were applied over a short period of time (Lanyon et al. 1982). Based on these studies, the strain characteristics which are optimal for bone preservation and accretion are associated with a few cycles of locally applied loads which impose dynamic strains having a high peak magnitude and rate and a novel distribution within the bone.

2.2.3 ii Decreased Mechanical Loading Reduces Bone Strength

Support for the postulate that reduced loading causes a reduction in bone strength comes, in part, from observations of naturally occurring bone loss in individuals who have medical conditions resulting in limb paralysis or astronauts who have been exposed to zero gravity. In such cases, there is no local change in the genetic, hormonal, or nutritional environment but bone mass decreases due to the altered mechanical loading of the affected skeleton.

The bone loss in individuals who suffer spinal cord injuries is quite rapid and marked (Garland et al. 1992). This may be due to the extreme lack of loading experienced by the skeleton due to virtual elimination of weightbearing, impact loading and muscle tension. However, it is possible that the musculoskeletal changes observed in this population are due to factors specific to the injury as well. Frost (1981) has described such a "regional acceleratory phenomenon" in a number of injury-induced animal models of disuse including amputation, tendonectomy, or surgical denervation. To determine the response of healthy bone to mechanical unloading, a number of animal and human models of disuse have been developed which fall along a continuum ranging from bedrest/ microgravity to tape/ cast immobilization.

Animal studies demonstrate that the bone loss which occurs with immobilization is influenced by age as well as by the duration and type of unloading. When the hindlimb of growing rats was taped to immobilize the knee in 100° of flexion and the ankle in 60° of plantarflexion for 3 weeks, the bone mass and density in the unloaded tibia averaged 9.6% below the values for the contralateral limb (Kannus et al. 1994). When a plaster cast

was applied for a 2 week period, a greater between-limb difference in bone density (as measured by ash weight) was observed with a decrease of approximately 15% in the immobilized hindlimb of immature rats (Tuukkanen, Peng, and Väänänen 1992). In mature rat tibia, when the hindlimb was secured to the thorax by elastic tape for 6 weeks, metaphyseal trabecular bone volume and trabecular number decreased, intertrabecular spacing increased and the diaphyseal periosteal surface of cortical bone had more eroded surfaces and fewer mineralization surfaces (Maeda et al. 1993). The same protocol for hindlimb immobilization of mature rats was used by Li et al. (1990) and histomorphometric changes indicative of trabecular bone loss and structural deterioration were detected within 2 weeks. Immobilization for 10 weeks was required before a significant decrease in BMD was detected in the proximal and distal femur (-8% and -13%, respectively) (Li et al. 1990). Reduced loading resulted in continual bone loss until a steady state was reached at 18 weeks which was maintained until the end of the 26 week period of immobilization (Li et al. 1990). Rat studies such as these suggest that the changes induced by reduced mechanical loading are observed primarily as histomorphometric deterioration of trabecular bone with minimal change in the cortical bone compartment unless the bone is growing.

In young adult dogs, immobilization of the forelimb by taping the flexed limb to the thorax for 16 weeks resulted in significantly less bone mineral density in the proximal radius (78.1%), than in the midshaft of the radius (83.1%) (Lane et al. 1996). The former has a large trabecular bone component and the latter is composed of cortical bone. The impact of immobilization on cortical bone is also observed in adult monkeys restrained in

a semi-recumbant position (Young, Niklowitz, and Steele 1983; Young et al. 1986). Young and colleagues (1983, 1986) observed resorption cavities in the endosteal region of the proximal tibia after 1 month of unloading with progressive cortical bone loss extending to the intracortical and subperiosteal regions throughout immobilization periods of up to 7 months. Taken together, the animal models of disuse show that the trabecular bone compartment of weightbearing bones is most responsive to unloading but given sufficient duration and extent of immobilization, cortical bone loss also occurs. Apart from studies of the functionally isolated avian ulna, no data concerning the response of nonweightbearing bone to reduced mechanical loading is available in the literature using animal models of disuse.

In humans, upper limb mobility and strength are essential for the performance of functional activities. These activities require muscular forces but rarely involve ground reaction forces associated with weightbearing. The skeleton of the upper limb must adapt to the loading history in order to optimize bone strength. Table 2.1 summarizes the changes observed at mature human nonweightbearing skeletal sites following periods of disuse. In studies which investigate the impact of disuse associated with various medical conditions, the effect of the decreased loading is difficult to isolate from changes related to pathology (Prince et al. 1988; Garland et al. 1992; Sato et al. 1996; Sievänen et al. 1996). Studies of healthy bones of the upper limb exposed to conditions of decreased loading due to spaceflight and bedrest report that bone is not lost (Vogel and Whittle 1976; LeBlanc et al. 1990; Hangartner 1995; Collet et al. 1997). It may be that the sample size used in these studies is too small to detect changes in nonweightbearing bone.

TABLE 2.1

RESPONSE OF HUMAN NONWEIGHTBEARING BONE TO DECREASED MECHANICAL LOADING [a,b]

Disuse Model	n[a]	Duration	Site [Measurement[b]]	Results
Ligament Injury				
Sievänen et al. 1996	1	18 wk	patella [BMD (DXA)]	↓ BMD for 4 mo; recovered 2 yr post injury
Hemiplegia				
Prince et al. 1988	74	from 1mo to 15 yr	radius [BMC (quantitative x-ray)]	positive relation between BMC and duration of stroke (distal site) and functional level (midshaft)
Sato et al. 1996	87	> 1 mo	hand (2nd metacarpal) [optical density (x-ray)]	↑ between-limb difference compared to controls (n=28)
Quadriplegia:				
Garland et al. 1992	23	~114 d (n=12) & > 5 yr (n=11)	arms [BMC (DPA)]	↓ BMC compared to controls (n=10) & men with paraplegia (n=22)
Spaceflight				
Vogel and Whittle 1976	3	56 d	distal radius & ulna [BMC (SPA)]	no change
Collet et al. 1997	2	1 & 6 mo	midradius [BD (QCT)]	no change
Bedrest:				
LeBlanc et al. 1990	6	17 wk	proximal & distal radius & ulna [BMC (SPA)]	no change
Hangartner 1995	5	3 wk	distal radius [BD (QCT)]	no change

[a] n = sample size

[b] BMD (DXA) = areal bone mineral density (g/cm^2) measured using dual energy x-ray absorptiometry; BMC (quantitative x-ray) = bone mineral content (g/cm); optical density = reported as microdensitometric scores; BMC (DPA) = bone mineral content (g) measured using dual photon absorptiometry; BMC (SPA) = bone mineral content (g/cm) measured using single photon absorptiometry; BD (QCT) = apparent bone density (g/cm^3) measured using quantitative computed tomography.

Alternatively, the loading patterns which the upper limbs experience in these models of disuse may not be significantly different from the typical loads experienced under nonexperimental conditions.

2.2.3iii Increased Mechanical Loading Influences Nonweightbearing Bone Strength

Muscle activity produces the primary mechanical forces experienced in nonweightbearing bone and such forces are critical to the maintenance of strong bones in adulthood (Frost 1987; Kannus, Sievänen, and Vuori 1996). Hand grip dynamometry is a simple measure of muscle strength and has been used to explore the relation between muscle force and BMD in the radius. Pocock et al. (1989) recruited 73 women between the ages of 20 and 75 years and found that nondominant grip strength was a significant predictor of BMC in the distal radius (10 % site) of the nondominant arm. However, grip strength did not predict BMC at this site in the subgroup (n = 45) of premenopausal women (Pocock et al. 1989). Another study of 59 premenopausal women found that nondominant grip strength was the strongest predictor of BMD at the midradius of the nondominant limb (Snow-Harter et al. 1990). The latter study also reported that dominant hand grip strength was the strongest predictor of lumbar spine BMD and the relation was superior to that between isokinetic muscle strength of muscles with attachments local to the lumbar spine (Snow-Harter et al. 1990). Similar findings have been reported by others (Bevier et al. 1989; Kritz-Silverstein and Barrett-Conner 1994). Bevier et al. showed that BMD at the nondominant midradius is associated with hand grip strength (dominant, $r = 0.47$, $p < 0.005$; nondominant, $r = 0.37$, $p < 0.05$) and back strength ($r = 0.46$, $p < 0.01$) in

men. These data suggest that grip strength may be a correlate of global functional physical strength which influences bone mass more than measures of maximum force exerted by isolated muscle groups. This postulate seems plausible since investigations in postmenopausal women have shown that both dominant and nondominant grip strength predict BMD in the midradius (Bevier et al. 1989) and distal radius (Kritz-Silverstein and Barrett-Conner 1994) of the nondominant arm. Kritz-Silverstein and Barrett-Conner (1994) studied bilateral grip strength and BMD at the lumbar spine, hip and nondominant radius (midshaft and distal 10% sites) in 649 women over the age of 65 years and, after adjusting for confounding variables, found that both dominant and nondominant grip strength were significantly associated with BMD at all sites measured with the exception of dominant grip strength and BMD at the nondominant midradius ($p = 0.06$).

Controversy exists regarding the association between grip strength and bone mass at the midradius. Bevier et al. (1989) found no relation whereas Sinaki, Wahner, and Offord (1989) reported an association in the nondominant limb ($r = 0.46$, $p < 0.001$) but found that it was an inferior predictor compared to age ($r = -0.52$, $p < 0.001$). The relation between grip strength and bone mass is influenced by the magnitude of the individual's grip strength such that no association is seen among those with lower ranges of grip strength (Sinaki, Wahner, and Offord 1989; Kritz-Silverstein and Barret-Conner 1994). Vico et al. (1995) used pQCT to measure trabecular bone in the ultra distal radius and cortical bone at the midshaft in 55 postmenopausal women and reported that volumetric bone density (BD) in trabecular sites is associated with physical ability while cortical bone in the midshaft of the radius is solely influenced by height and weight.

Computed tomography permits the assessment of BD and geometric variables, and has been employed to study the relation between grip strength and both midradius BD and cross-sectional area in a study of 255 inactive early postmenopausal women (Sandler et al. 1989). Positive associations were observed between grip strength and both bone variables; however, after adjusting for confounding variables including age, height and body mass index, a positive association was observed for grip strength and the geometric variable only (Sandler et al. 1989). These cross-sectional studies demonstrate that grip strength is a marker of functional physical strength which significantly predicts BMD locally (at the radius) and at remote skeletal sites and may have a stronger association with local geometric and trabecular bone properties of nonweightbearing bone than with bone mass.

Evidence regarding the influence of mechanical loading on nonweightbearing bone comes from studies comparing bone mass in the upper limbs of athletes with that of sedentary individuals. Alfredson et al. (1998) compared 11 volleyball players who trained 8 hours per week with an equal number of inactive young women and found no difference in BMD in the distal radius, as determined by DXA. Colletti et al. (1989) measured BMD of the midradius in 12 men who had been involved in a weight training program of at least 1 year duration for a minimum of 45 minutes 2 times per week and in 50 age-matched controls and found no difference between groups in midradius BMD. Shimegi et al. (1994) compared the BMD of weightbearing and nonweightbearing skeletal sites among three groups of Japanese postmenopausal women (11 volleyball players, 5 joggers and 9 controls). Whereas group differences were found in weightbearing bones, no

difference was observed in the proximal or distal radius (Shimegi et al. 1994). In contrast, others have shown site specific increases, compared to sedentary individuals, in the playing arms of elite squash players and tennis players (Haapasalo et al. 1994; Kannus et al. 1995; Calbet et al. 1998). Kannus et al. (1995) reported that the magnitude of the difference in measurements of radial bone BMC between athletes and controls was greater when the athletes started playing before or at menarche; thus, differences in the duration of training and age at which sport training was initiated in these groups of athletes could account for the conflicting findings.

Studies using cross-sectional designs can not determine causal influences of physical activity on bone properties because of confounding variables such as genetic, hormonal and nutritional factors on bone. A number of studies have sought to control for these confounding variables by investigating differences in bone quality associated with differential loading patterns within subjects. In these studies, the between-limb differences in BMD and BMC in the arms of elite athletes playing racquet sports were significant at every site measured (with the between-limb difference most evident in the humerus) and significantly greater than the between-limb differences found in the sedentary controls (Haapasalo et al. 1994; Kannus et al. 1994; Kannus et al. 1995; Alfredson et al. 1998). These studies demonstrate that the influence of increased mechanical loading is site specific and that differences in BMC are more pronounced than differences in BMD (Haapasalo et al. 1994; Kannus et al. 1994; Kannus et al. 1995; Alfredson et al. 1998).

Two studies have investigated the between-limb difference in large groups of individuals with moderate to low activity levels to determine the effect of hand dominance on BD and bone mass (Rico et al. 1994; Walters et al. 1999). Rico et al. (1994) observed that the cortical bone at the distal radius of the dominant limb was more dense (11%) than in the nondominant limb and the trabecular BD was not different between limbs in a group of 50 young adults. Walters et al. (1999) compared bilateral measurements of the distal forearm for 140 young adult women and found that the dominant forearm had significantly higher BMC and bone area. These data suggest that in nonathletes, long term loading patterns associated with preferential use of the dominant limb may result in the development or maintenance of larger and more dense bone.

Studies investigating the effect of increased mechanical loading on the radius in osteoporotic women are limited in number and report conflicting results (Krølner et al. 1983; Simkin, Ayalon, and Leichter 1987; Beverley et al. 1989). Brief forearm loading (15 to 20 min) 3 times per week for 5 months increased trabecular BD by 3.8% in an exercise group (Simkin, Ayalon, and Leichter 1987) and BMC increased in the midradius by 3.4% in response to two daily sessions of brief (30 seconds) high intensity loading for 6 months compared to no significant change in the contralateral nonexercised arm (Beverley et al. 1989). Aerobic exercise with brief periods of forearm loading 2 times per week for 8 months induced no significant change in the radius (Krølner et al. 1983). These conflicting results may be due to differences in the extent of osteoporosis among the study samples. Alternatively, osteoporotic bone may respond to mechanical loads that

are site specific and of sufficient strain magnitude, rate and frequency (i.e., no less than 3 times per week).

Most of the studies undertaken to investigate the effectiveness of exercise interventions on reducing the rate of bone loss have targeted healthy postmenopausal women since they are safe to exercise and concerned about minimizing their risk for developing osteoporotic fractures. Bérard, Bravo, and Gauthier (1997) completed a meta-analysis of the literature published between 1966 and 1996 which investigated the influence of physical activity on BMD of the lumbar spine, proximal femur, heel and radius in postmenopausal women. They concluded that physical activity (involving either ground reaction forces or joint reaction forces) significantly reduced the loss of lumbar BMD (Bérard, Bravo, and Gauthier 1997). The effectiveness of physical activity in the prevention of bone loss at other sites was not clear since the ability to pool data and summarize results was limited by small sample sizes and the lack of uniformity in the interventions and outcome measurements.

Table 2.2 summarizes the longitudinal studies which determined the response of nonweightbearing radial bone in healthy postmenopausal women to increases in mechanical loading associated with specific exercise interventions. A number of studies which report no beneficial effect of exercise at the radius did not use training protocols which increased loading of the upper limb (Aloia et al. 1978; Sandler et al. 1987; Prince et al. 1991; Nelson et al. 1991; Martin and Notelovitz 1993; Bassey and Ramsdale 1995). Given the site specific effect of mechanical loading on the skeleton, these studies provide

TABLE 2.2

RESPONSE OF ADULT NONWEIGHTBEARING BONE TO INCREASED MECHANICAL LOADING IN HEALTHY INACTIVE POSTMENOPAUSAL WOMEN[a-c]

Authors	Design[a] & Sample size	Loading Protocol [b]	Measurement at Radius[c]	Results
Ryan et al. 1998	NR n = 12 (no control)	RT (n = 12) X 16 wk F: 3X /wk I: 1 set of 10-15 reps T: 60 min	BMD in the ultra distal and 1/3 distal regions (DXA)	no change
Khort et al. 1997	NR n = 39 (control = 12)	RT (n = 13) X 9 mo F: 3.4X /wk I: fatigue after 8-12 reps (+ rowing X 15-20 min at 80-85% HRmax) T: 3- 4 sets /exercise Aerobic (n = 14) X 9 mo F: 3.4 X /wk I: ~70 - 85% HRmax T: 24 - 52 min / session	BMD in the ultra distal and 1/3 distal regions (DXA)	no change & no between group differences
Kerr et al. 1996	R n = 46 (final) unilateral training with alternate limb serving as control	RT1 (n = 21) X 1 yr F: 3X /wk I: 3 sets of 20 RM T: 20-30 min RT 2 (n = 25) X 1 yr F: 3X /wk I: 3 sets of 8 RM T: 45 - 60 min	BMD in the ultra distal, 1/3 distal and middle regions (DXA)	RT 1: ↑BMD in middle region (+0.1 ± 1.4 %, $p < 0.01$) RT2: ↑BMD in ultra distal region (+2.4 ± 4.3%, $p < 0.01$) no between-limb difference at other regions
Preisinger et al. 1995	RCT n = 146 (final) (control = 64)	RT and Aerobic (n = 82) X ~3yr F: ≥3 X /wk I: not reported T: ≥ 20 min /session (subgrouped by level of compliance)	BMD proximal (33%) and distal (10%) sites (SPA)	Compliant exercisers (n = 39) had a reduced rate of loss at the proximal site and no loss at the distal site. All others lost BMD

TABLE 2.2 (CONTINUED)

Authors	Design[a] & Sample size	Loading Protocol [b]	Measurement at Radius[c]	Results
Bassey and Ramsdale 1995	RCT n = 44 (final)	High impact aerobic & heel drops (n = 20) X 1 yr F: daily heel drops & 1X /wk high impact aerobics I: peak force ~2-3.5 N/N (ground reaction force / body weight) T: 50 heel drops / session Low impact aerobics control X 1 yr	BMD of distal radius (DXA)	loss of BMD in both groups
Martin & Notelovitz 1993	RCT n = 55	Aerobic X 1 yr F: 3X /wk I: 70 - 80% VO_{2max} T: 30 min (n = 20); 45 min (n = 16) + warm up	BMC of proximal (33%) and ultra distal (1.5 cm proximal to ulnar styloid) sites (SPA)	no change
Pruitt et al. 1992	NR n = 26 (final) (control = 9)	RT (n = 17) X 9 mo Upper limb - F: 3X /wk I: 1 set at 10-12 RM T: 1 hour	BMC of distal radius (~10%) site (SPA)	no change, no between group difference
Notelovitz et al. 1991	RCT n = 20 (final) (control = 11)	RT circuit plus estrogen treatment (n = 9) X 1 yr F: 3X /wk I: 1 set at 8RM T: 15 - 20 min / session Control group was on estrogen treatment alone	BMD and BMC of the nondominant midshaft (SPA)	exercise caused ↑ BMD (3.8 ± 3.5 %, p = 0.006) and ↑ BMC (4.1 ± 4.3 %, p = 0.01) which was significantly > control (p = 0.009 and p = 0.017) who had a non significant ↓ in BMD and BMC
Nelson et al. 1991	NR n = 36 (final) (control = 18)	Aerobic walking program (n = 18) X 1 yr F: 4 X /wk I: 75 - 80 % of HRmax T: 50 min / session	BMD of the nondominant midshaft (SPA)	no change in BMD; no between group difference
Prince et al. 1991	RCT n = 145 (final) (control = 42)	Low Impact Aerobic (n = 103; n = 35 ex alone) F: 3 X /wk I: "brisk" T: 30 min (walk) & 1 hr class (18 min of arm ex)	BMD of the nondominant radius (ultra distal, distal and proximal sites) (SPA)	rate of bone loss was similar in control group and exercise alone group.

TABLE 2.2 (CONTINUED)

Authors	Design[a] & Sample size	Loading Protocol [b]	Measurement at Radius[c]	Results
Rikli and McManis 1990	NR n = 31 (final) (control = 11)	Aerobic (n = 10) X 10 mo F:≥ 3X /wk I: 60 - 70 % HRmax T: 50 min Aerobics plus RT (n = 10) X 10 mon as above plus 20 min of resisted upper body exercise 3X/wk; no specifics given re: progression of weights, repetitions and sets	BMC and BMD at the proximal (33%) site (SPA)	no between group differences in BMC pooling the exercise groups, showed a significant loss in BMC (- 2.50%) and BMD (- 2.58%) in the control group but not the exercise group
Smith et al. 1989	NR n = 65 (control = 30	Aerobic + upper body RT: (n = 35) X 4 yr F: 3 X /wk I: 70 -85% of HR reserve X 30 min each yr ↑ upper body work using light resistance T: 45 min	BMC, W, and BMD of both radii - proximal (33%) site (SPA)	↓ rate of loss of left radius BMC and W & right radius BMC and BMD with exercise vs control group
Sandler et al. 1987	RCT n = 255 (control = 125)	Aerobic (n = 130) X 3 yr F: 2 X /wk I: not specified T: ≥ 7 miles /wk	midshaft (proximal site) BD and cross-sectional area (Computed Tomography)	no between-group differences
Aloia et al. 1978	NR n = 18 (control = 9)	Aerobic: (n = 9) X 1 yr F: 3 X / wk I: progressed to level 4 out of 5 T: 1 hr / session	BMC and BMD of the distal (~10%) site of the radius (SPA)	the ↑ in BMC and BMD in the exercise group and the ↓ in BMC and BMD in the control group were not statistically significant

[a] NR = nonrandomized group assignment; R = randomized group assignment (within subject control); RCT = randomized control trial; n = number of subjects completing the study.

[b] RT = resistive training; F = frequency; I = intensity; T = time; reps = repetitions; HRmax = maximum heart rate; RM = repetition maximum.

[c] Abbreviated terms as shown for Measurements[b] in Table 2.1; W = bone width (cm); BMD (SPA) = BMD (SPA) normalized for W (g/cm^2).

little information regarding the adaptability of healthy nonweightbearing bone to increased usage postmenopause. Of the 8 studies with training protocols designed to increase the load on the upper limb, only 3 are randomized trials. Thus, there is a dearth of studies designed to provide the highest level of evidence regarding the effectiveness of an exercise intervention on nonweightbearing bone.

Training protocols designed to load the arms have produced conflicting results. Ryan et al. (1998) found no change in radial BMD following 16 weeks of moderately intense resistive training and concluded that the exercise prevented bone loss. However, this study did not include a control group so conclusions regarding the effectiveness of the exercise are not clear. Moderate to high intensity resistive training in the upper limb has been associated with no benefit to the radius (Rickli and McManis 1990; Prince et al. 1991; Pruitt et al. 1992; Khort et al. 1997), while others have found reduced bone loss (Smith et al. 1989) or increased radial BMD (Notelovitz et al. 1991; Kerr et al. 1996). Where appropriate osteogenic training protocols are used and benefits are observed, the changes are small (0.1% to 2%). One randomized controlled trial followed 146 women over 3 years and reported that exercise (a combination of resistive training and aerobics) reduced the rate of loss at the midshaft of the radius only in a subgroup of compliant exercisers (Prince et al. 1991). This underlines the difficulty in determining effectiveness of exercise since sedentary individuals randomly assigned to exercise programs typically exhibit poor adherence. This is not surprising given the fact that 41% of postmenopausal women who self selected exercise over hormone replacement therapy and calcium

supplementation in a 12 month decision support intervention study did not adhere to the exercise program (Rothert et al. 1997).

The effectiveness of exercise in reducing bone loss among postmenopausal women is similar to that for groups of women who are not subdivided according to menopausal status. Smith et al. (1984) evaluated the effect of light resistive training loads on the BMC, bone width and BMD at the midshaft of the radius in women varying in age from 35 to 65 years over a 4 year period. The exercise group demonstrated a small (< 2%) but significant gain in BMC. Comparable findings were obtained using a similar training protocol in a group of 77 premenopausal women, of whom 45 exercised and demonstrated significantly smaller decreases in BMC at the midshaft of the radius bilaterally compared to controls (Smith et al. 1989). In contrast, no change in BMC at the midshaft of the radius was observed in a group of inactive premenopausal women between the ages of 30 and 40 years (n = 50) who were randomly assigned to perform 3 sets of 10 repetitions of resistive exercise thrice weekly over a 3 year trial period (Sinaki et al. 1996). Similarly, Lohman et al. (1995) studied the effect of moderate to high intensity resistive training over 18 months in a group of 66 inactive premenopausal women (varying in age from 28 to 30 years) and found no change in upper extremity BMD in the 22 women comprising the exercise group. The adherence rate for the exercise group was 84% for those who completed the study but a total of 35 subjects with this group assignment withdrew (Lohman et al. 1995). The conflicting findings may be explained by differences in adherence rates among the study subjects in the exercise groups. It seems probable that increased mechanical loading, by means of regular, high

intensity, site specific exercises, helps maintain bone in nonweightbearing skeletal sites in premenopausal women who have not previously been engaged in regular exercise programs. Clearly, it is a challenge to convince healthy sedentary premenopausal women to adhere to exercise programs designed for osteogenic effects and this factor suggests that such exercise interventions may not be practical.

The effect of exercise interventions such as those described in the studies on upper limb bone strength would be more clear if the study subjects were randomized to an exercise group and persuaded to adhere to a training protocol which was designed to load the forearm. Unless these studies are completed, it is difficult to discern whether increased mechanical loading does produce benefits such as bigger, more dense or architecturally improved bone and thus help to prevent osteoporotic fracture. It seems that an exercise intervention may be more successful if it is initiated at puberty when the skeleton is developing rather than after the bone has become osteoporotic. Certainly long term commitment to a progressive exercise program is required and such changes in habitual activity levels may be more difficult for aging women.

2.2.4 Pathophysiology of Osteoporosis

The turnover of bone is predominantly a surface-based phenomenon, and the rate of bone turnover is determined by the number of BRUs activated within a given space. While cortical bone comprises 80% of the adult skeleton, it accounts for 20% of the exposed surface area. Trabecular bone (making up 20% of the adult skeleton) has a large surface to mass ratio and accounts for a far greater percentage of bone turnover since it

comprises 80% of the bone surface area exposed to extracellular fluids. Therefore, trabecular bone is more responsive to most metabolic perturbations and exchanges ions with the extracellular calcium pool most readily (Riggs and Melton, 1995). Bone loss is a normal feature of aging; however, the frequency of activation of the remodeling process as well as the depth of the resorption pits also influence the rate at which bone is lost (Parfitt 1994). Typically osteoclasts create a groove in trabecular bone which is 65 micrometers in depth and create a tunnel in cortical bone which is 100 micrometers in length (Recker et al. 1988). Since remodeling is a surface phenomenon, when bone removal (resorption) exceeds replacement (formation), the effects are most apparent within trabecular bone compartments. When the depth of the resorption pits exceeds the thickness of trabeculae, loss of bony struts can occur. If many bone struts are lost, there is a reduction of surfaces on which remodeling can occur. Consequently, once an individual becomes osteoporotic there is no way to truly rebuild much of the structure and mass which has been lost. Interventions may increase the amount of bone by thickening the outer shell and remaining trabecular struts but the inner supporting struts are lost and structural weakness may persist.

2.3 Methods of Estimating the Risk of a Distal Forearm Fracture *In Vivo*.

Typically fracture in the appendicular skeleton occurs as a result of trauma such as falling. Clearly, fracture risk is multifactorial and depends on extraskeletal factors as well as factors related to bone strength. It is beyond the scope of this review to discuss trauma-related factors such as the propensity to fall, characteristics of the fall, and the extent to

which soft tissue attenuates the forces transmitted to the bone. In situations where the forces imparted to the skeleton exceed the strength of the bone, fracture occurs. The most direct method of quantifying bone strength at fracture prone sites would be to measure the amount of force which is required to bend and break the bone. From this information, force - deformation curves can be plotted which describe the elastic properties of the bone. Alternatively, bone strength can be estimated by considering determinants of mechanical quality which can be measured by noninvasive methods.

Bone strength depends on the amount of mineralized tissue present, material properties of the skeletal components which contribute to "intrinsic stiffness" and the spatial distribution of the mineralized tissue in relation to the axis of loading forces (Ferretti 1998). Standard noninvasive techniques, including bone absorptiometry and pQCT, are available which permit the *in vivo* assessment of these determinants of bone strength in the forearm. These technologies are discussed below (sections 2.3.1 to 2.3.3) with respect to their utility in estimating an individual's risk for forearm fracture.

2.3.1 Quantifying the Amount of Mineralized Bone in the Radius

Measurements of the amount of mineralized bone present in a particular region can be derived from projected imaging techniques (Genant et al. 1996). In 1963, Cameron and Sorensen developed the single photon absorptiometry (SPA) scanner to replace radiographic optical density techniques which were limited by high precision errors (coefficients of variation of 9 to 10%) (Morgan et al. 1967). Figure 2.1 shows the radius and ulna of the forearm with the distal (10%), proximal (33.3%) and midshaft (50%) sites

(which are determined from the ulnar length) where scans are typically acquired using SPA. Based on the linear attenuation of radiation by the tissue in the region of the scan, bone mineral content is measured in units of g/cm. Some investigators report the amount of bone mineral determined using SPA as bone mineral density (BMD) in units of g/cm^2 calculated by normalizing BMC to the width of the radius (Aloia et al. 1978; Rikli and McManis 1990). More recently, the gamma source used in SPA has been replaced by an x-ray beam (SXA) and multiple scan paths are used to improve the precision of the technique (Kelly, Crane, and Baran 1994).

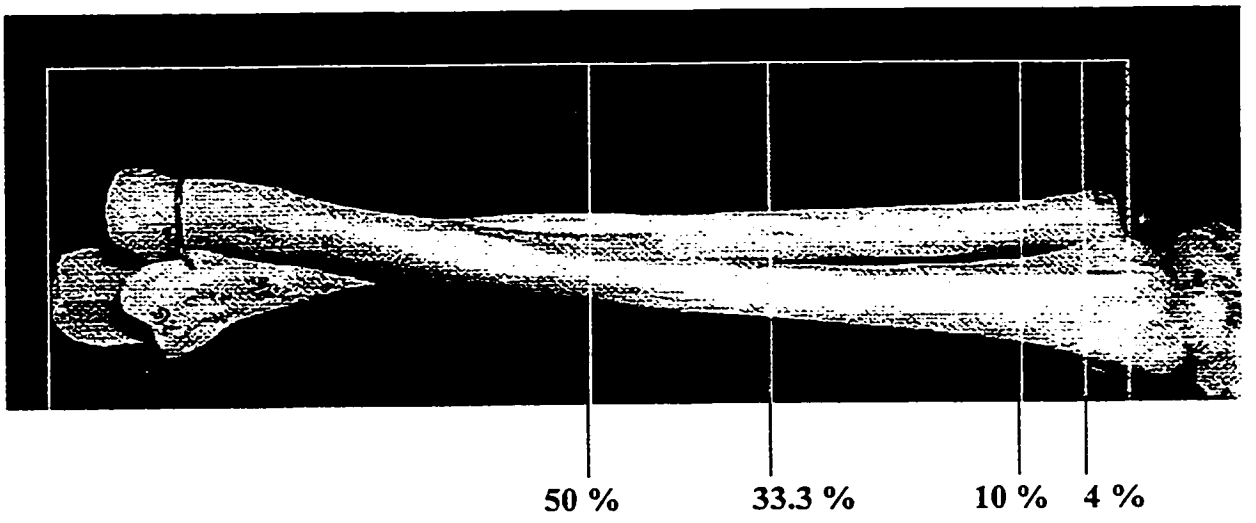

Figure 2.1 Illustration of the location of scan sites in the nondominant forearm calculated from ulnar length.

Densitometry techniques using radiation sources with two different energy levels (dual photon absorptiometry, DPA, and dual energy x-ray absorptiometry, DXA) were developed to permit the measurement of bone mineral at nonperipheral sites (Mazess et al. 1988). When the same skeletal site was measured, there was an excellent level of agreement between measurements derived using SPA and DXA (Weinstein, New, and Sappington 1991) but DXA required shorter scan times and eliminated the need for water baths or soft tissue equivalents and for frequent replacement of decayed radionuclide sources. Table 2.3 compares the single and dual energy projectional techniques for evaluating bone mineral in the forearm with respect to scanning time, precision and radiation exposure. With DXA and DPA, bone mass is measured and reported as areal bone mineral density (BMD) in g/cm^2 and bone mineral content (BMC) in g. Figure 2.2 depicts the region scanned using the DXA forearm scanning protocol. The region of interest is set by the operator so that the most distal reference line is level with the ulnar styloid. The software centers the 1/3 distal region around the scan line which corresponds with 1/3 of the length of the ulna and both boundaries shown are included in the 1/3 distal region. The ultra distal region includes a 10 to 20 mm length of the radius and is automatically set at a specific distance proximal to the ulnar styloid process. The middle region is the portion of bone which lies between the ultra distal and distal 1/3 regions. All 3 of these regions are included in the calculation of BMD and BMC in the total region of the distal radius.

TABLE 2.3

COMPARISON OF SINGLE AND DUAL ENERGY PROJECTIONAL TECHNIQUES USED TO QUANTIFY THE AMOUNT OF BONE MINERAL IN THE FOREARM[a,b]

Technique[a]	Acquisition Time	*In Vivo* Precision Error	Radiaton Dose[b]
SPA	10 - 15 min	1% (midshaft and proximal sites) 2-3% (distal site)	50 - 150 μ Sv
SXA	4 min	1-2%	17 μ Sv
DPA	25 min	~ 1.5%	30 - 40 μ Sv
DXA	< 2 min	1 %	20 - 200 μ Sv

[a] Abbreviations as described in the text and references as follows: SPA, Weinstein, New, and Sappington 1991; Kelly, Crane, and Baran 1994; DPA, von Wowern, Storm, and Olgaard 1988; DXA, Weinstein, New, and Sappington 1991; Leboff et al. 1992; Eiken et al. 1994.
[b] skin entrance dose.

Measurements of areal BMD and BMC determined using projectional densitometry techniques (SPA, SXA, DPA and DXA) are significantly correlated with mechanical bone strength (Faulkner et al. 1991; Genant et al. 1996). The amount of mineralized tissue is critical for withstanding compression loading along the central axis of the bone (Turner and Burr 1993). However, measurements of BMD and BMC have low predictive power for determining an individual's risk for forearm fracture (Marshall, Johnell, and Wedel 1996). These measurements of integral bone mineral are only partially corrected for bone size and do not provide information regarding material properties, spatial distribution of the bone tissue and separate cortical and trabecular bone compartments.

Figure 2.2 Image of a left forearm acquired using dual energy x-ray absorptiometry (DXA, Hologic QDR 4500A). The scan regions (distal 1/3, middle, ultra distal and total) are automatically calculated based on measurements of the ulnar length and placement of reference line at the tip of the ulnar styloid determined by the operator.

2.3.2 Quantifying 'True' Bone Density in the Radius

One of the material properties of bone which can be measured noninvasively *in vivo* is 'true' volumetric bone density (BD) of the mineralized tissue. Measurements of BD at the distal radius can be obtained using peripheral quantitative computed tomography (pQCT) which was developed in order to assess the cortical and trabecular bone compartments separately (Schneider et al. 1988; Rüegsegger, Durand, and Dambacher 1991). The standard scan location is at the 4 % site (Figure 2.1) based on the ulnar length and the image is obtained in the transverse plane. Image acquisition requires 5 minutes and, whereas the pixel resolution depends upon the scanning diameter, the *in vivo* resolution is reported to range from 0.2 (XCT 2000 and XCT 3000) to 0.8mm (XCT 960) for second generation scanners manufactured by Stratec and 0.2 mm for the high-resolution Densiscan machine. Precision error for pQCT derived measurements of BD at the radius varies from 0.22% to 2.1% depending upon the machine used and the population being assessed and the radiation dose is less than associated with most densitometry techniques (Grampp et al. 1995; Schneider and Reiners 1998). Ferretti et al. (1997) report that BMC determined from pQCT imaging was a strong predictor of fracture risk at the distal radius ($R^2 = 0.95$, $p < 0.00001$). Thus pQCT technology provides a noninvasive method for quantifying the amount of mineralized tissue as well as mass per unit volume; a bone variable which has a strong association with the elastic properties of the bone (Currey 1988; Ferretti, Capozza, and Zanchetta 1996). However, a number of other material properties which contribute to the intrinsic stiffness of a skeletal site can not be determined *in vivo* using absorptiometry techniques.

2.3.3 Quantifying the Architectural Integrity of the Radius

The bones in the upper limb typically experience bending or torsional loading forces created by muscle action. The factors which contribute most to mechanical strength under these kinds of loading conditions are the spatial arrangement of the bone tissue with respect to the axis that the force is acting through and the integrity of the trabecular network (Ott 1993; Mosekilde 1993). The cross-sectional images acquired using pQCT technology can be analyzed to provide information regarding bone geometry in the radius (Ferretti 1995). Also, commercial software is available which calculates the cross-sectional moment of inertia to quantify how the cortical bone is distributed around a reference axis (Ferretti, Capozza, and Zanchetta 1996).

Currently, there is no commercially available noninvasive technique for measuring trabecular structure at the distal radius. Clinically, bone structure is determined from 2 dimensional histomorphometric analysis of biopsied bone from the iliac crest. This is an invasive technique which does not permit the same volume of bone to be reanalyzed to evaluate changes due to interventions or medical conditions. Recently, preliminary work has been published which describes techniques developed to quantify radial bone trabecular structure noninvasively using whole body computed tomography (CT) imaging (Cortet et al. 1999), x-ray computed tomographic microscopy (Majumdar et al. 1997), micro CT (Müller et al. 1996), magnetic resonance imaging (Gordon et al. 1997; Majumdar et al. 1997) and pQCT (Gordon et al. 1996).

Cortet et al. (1999) quantified the trabecular network of the distal radius, imaged in the transverse and coronal planes, for 2 groups of postmenopausal women (20 with

osteoporosis and 21 healthy controls). The image analyses included structural analysis, statistical analysis and fractal analysis. The results demonstrate that reproducibility of the technique was better for the cross-sectional images. The variables which were statistically different between groups were obtained using a structural analysis which characterized the network length and the spacing between bone in the transverse plane (Cortet et al. 1999).

Majumdar et al. (1996) completed an *in vivo* study to compare the measurements of structure variables derived from magnetic resonance images or by x-ray computed microscopy imaging with the elastic properties of the bone. The resolution for the magnetic resonance images was 156 X 156 X 300 μm and as a result of a partial volume effect, the measurements of bone area, bone volume, fractal dimensions and trabecular width were overestimated and the intertrabecular spacing was underestimated when compared to the measurements acquired using x-ray computed tomographic microscopy. Despite the differences in absolute values, the addition of the structure measurements derived from magnetic resonance imaging to BMD contributed significantly in the prediction of elastic modulus quantified by nondestructive loading of the bone cubes.

Müller et al. (1998) compared the morphometric measurements derived from the 2 dimensional histological technique and a 3 dimensional micro CT imaging technique for quantifying radial bone structure and found correlations ranging from 0.84 for trabecular thickness to 0.91 for trabecular spacing and bone surface density. The 3 dimensional micro CT technique is a promising tool for the noninvasive evaluation of bone strength; it requires 10 minutes to obtain 60 high resolution images with a slice thickness of 0.28

mm, a voxel size of 0.165 mm and consecutive cross-sectional slices are acquired in steps of 0.165 mm (Müller et al. 1996). To date, the *in vivo* application of this technique has been limited because of the high radiation dose (mean skin dose = 0.8 mSv) (Laib and Rüegsegger 1999).

Work by Gordon et al. (1996) suggests that postprocessing of high resolution pQCT images can provide estimates of trabecular bone structure. The development of this technology and proposed indices of trabecular bone structure have been described in detail previously (Gordon 1997) and is reviewed briefly here. Figure 2.3A illustrates a pQCT image with an in-plane resolution of 0.36 mm and a slice thickness of 2.5 mm acquired at the 4 % site of the forearm according to the method of Gordon et al. (1996). This resolution is just sufficient to measure trabecular structure which is reported to have marrow pore spaces varying in width from 0.5mm to 2 mm and trabeculae which vary in thickness from 0.1 mm to 0.4 mm (Amstutz and Sissons 1969; Whitehouse 1977).

During postprocessing of the pQCT image, a region of interest is selected which isolates the radius and the trabecular bone is segmented (Figure 2.3B). A binary representation of the image is created (Figure 2.3C) and intertrabecular spacing is characterized by quantifying the mean hole size (H_A, mm^2) and maximum hole size (H_M, mm^2) which can be identified using region grow analysis. In a skeletonization step, illustrated in Figure 2.3D, the pixels attributed to trabecular bone are reduced to a width of one and information regarding the connectedness of the trabecular bone structure is quantified. Based on the skeletonized image, the junctions of the bony struts are counted

Figure 2.3 Indices of trabecular bone structure quantified using pQCT imaging and postprocessing techniques. A: The original pQCT image acquired at the 4 % site of the distal radius from a 25.6 year old male. B: The trabecular bone is segmented by a region grow step. C: A binary image is produced from which mean marrow pore size (H_A, mm^2) and maximum marrow pore size (H_M, mm^2) are derived. D: The skeletonized image from which trabecular connectivity index (CI) is derived.

as nodes, connecting 3 or more struts, free ends, having one end which is not connected to another strut, and isolated points, which appear as a single pixel with no connection to another strut. Based on these characterizations, an index of trabecular bone connectivity is calculated such that the number of free ends and isolated points are subtracted from the total number of nodes, normalized to network length and multiplied by 100. Calculated in this way, a higher value for the connectivity index (CI) represents a well connected trabecular structure with numerous nodes and comparatively few isolated points and free ends. Conversely, a trabecular network which has a low frequency of nodes and a comparatively high frequency of isolated points or free ends would have a low value for CI. Biologically, a CI value of 0 might suggest that there is no connected trabecular network; however, the calculated CI may assume a negative value, indicating that the number of nodes is less than the combined number of isolated points and free ends for a given network length. Whereas, a CI of 0 indicates that the combined frequency of isolated points and free ends is equivalent to the frequency of the nodes. Preliminary work has shown that these indices (H_A, H_M and CI) which characterize the 3 dimensional trabecular bone structure at the distal radius based on a 2 dimensional pQCT image are significant predictors of bone strength on mechanical testing (Gordon, Webber, and Nicholson 1998).

2.4 Implications for the Identification of Individuals at Risk for Forearm Fracture

The distal radius is a fracture prone site particularly among postmenopausal women and is one of the earliest clinical manifestations of osteoporosis. One determinant of

fracture risk is bone strength and there are a number of factors which contribute to the strength of the bone in the adult skeleton. Whereas it is not possible to directly quantify mechanical strength using noninvasive *in vivo* techniques, a number of bone variables can be measured in order to estimate fracture risk at the distal radius.

Ferretti et al. (1998) studied a large group of individuals with fractures of the distal radius and a matched control group with no history of fracture using pQCT and found that BD of the cortical bone compartment was not a strong predictor of fracture risk. The combination of measurements of cortical BD (reflecting material properties of the bone) and the cross-sectional moment of inertia (reflecting architectural characteristics of the bone) into a single score called the "bone strength index" improved the predictive strength (R^2 = 0.54) compared to BD of the total or cortical bone compartments. The strongest predictor was the pQCT derived BMC of the trabecular bone compartment (R^2 = 0.95). Spadaro et al. (1994) performed *in vitro* mechanical tests to determine the predictors of fracture at the distal radius (1994). Lower trabecular bone density, but not cortical bone density, was associated with failure of the distal radius. In contrast, geometry of the cortical bone at the 4% site of the distal radius was better correlated with fracture load than was geometry of the trabecular compartment. These findings suggest that trabecular bone contributes significantly to the strength of the distal radius but the geometric properties of cross-sectional area and moment of inertia do not describe the critical attributes of the trabecular compartment. It appears that the assessment of a combination of factors which contribute to bone strength would be advantageous in

estimating fracture risk. However, the optimal combination of variables has yet to be identified.

Prediction of fracture risk is currently based on population studies of bone mass measurements and large uncertainties are introduced when applied to a particular individual (Webber 1998). Whereas bone mass is a predictor of fracture risk, the consideration of other factors which contribute to bone strength may improve upon the ability to identify individuals at risk for osteoporotic fracture. Bone structure is an independent predictor of bone strength and the spatial distribution of mineralized trabecular bone at fracture prone sites such as the distal radius probably contributes to whether or not a bone will fail under a given mechanical stress. Images of trabecular bone structure can be obtained using pQCT. Previous work by Gordon et al. (1996) has made it possible to quantify the intertrabecular connectivity, the average dimensions of the holes in the trabecular network and the area of the largest hole observed in the imaged plane. With this recent technological advance it is possible to formulate the hypothesis that the indices of bone structure would demonstrate differences associated with gender, aging and altered mechanical loading, and that indices of structure may aid in the identification of individuals with low bone mass most at risk for fracture.

CHAPTER THREE
METHODOLOGY OF PQCT MEASUREMENTS OF BONE DENSITY AND STRUCTURE AT THE DISTAL RADIUS

3.1 Introduction

The technique of peripheral quantitated computed tomography (pQCT) was developed for the measurement of volumetric bone density (BD) of cortical and trabecular bone at the distal radius. Its use as a measurement tool to characterize and assess changes in BD at the distal radius is increasingly common worldwide. The precision of the pQCT technique is influenced by a number of factors inherent in the measurement situation and must be considered when measuring BD in a population of interest to evaluate longitudinal skeletal changes. Classical test theory holds that any observed measurement is equal to the true magnitude of the variable plus an error component. Measurement variation may originate from a number of sources such as the person acquiring the measurement, the subject(s) being measured, the environment in which the measurement is being acquired and from factors inherent to the pQCT instrument itself. To determine the precision errors characteristic of the pQCT technique, the important factors which may contribute to variation need to be identified.

Evaluation of short-term *in vivo* precision of pQCT measurements of BD has identified the operator, the study population and the repositioning of the subjects as

important sources of variation in the measurements (Grampp et al. 1995; Gatti et al. 1996). To minimize the variation which may be associated with the operator, most studies are designed such that all measurements are acquired by a single operator. The importance of the study population as a source of variation in the measurements has been demonstrated by comparing the precision error for pQCT measurements acquired in individuals with osteoporosis to the error for healthy premenopausal and postmenopausal women (Grampp et al. 1995). *In vivo* reproducibility was good but was influenced by the study group such that precision was worse in individuals with osteoporosis. This illustrates the necessity of characterizing the precision error of a technique for the population of concern.

Some studies have measured the reproducibility of pQCT measurements *in vivo* although the methods for calculating precision have been inconsistent or poorly defined making comparisons among studies difficult (Grampp et al. 1995; Sievänen et al. 1998). Table 3.1 summarizes some mathematical methods used to calculate the reproducibility of two measurements (x_1 and x_2) obtained for j subjects (i.e., $x_{1,1}$, $x_{2,1}$, $x_{1,2}$, $x_{2,2}$, $x_{1,3}$, $x_{2,3}$,...$x_{1,j}$, $x_{2,j}$). Precision has been described in absolute terms as the standard deviation (SD) of the repeated measurements (Sievänen et al. 1998). The standard deviation of the measurement (SD_{meas}) is comparable to the SD in meaning but reflects intrasubject variation. The standard error of the measurement (SE_{meas}) is a statistical test which estimates the likely standard deviation of the error for individual measurements. In addition, the short-term precision of repeated measurements can be described in absolute

TABLE 3.1

METHODS OF CALCULATING ABSOLUTE ESTIMATES OF PRECISION[a,b]

Statistical tests which estimate precision[a]	Mathematical equations[b]
SD (indicating biological variation)	$= \sqrt{\frac{\sum_{j=1} (\bar{x}_j - \bar{X})^2}{n-1}}$
SD_{meas} (indicating measurement error)	$= \frac{\sum_{j=1}^{n} \sqrt{\sum_{i=1}^{n_j} \frac{(x_{ij} - \bar{x}_j)^2}{n_j - 1}}}{n}$
SE_{meas} (indicating deviation of the observed measurement from the true measurement)	$= \sqrt{EMS}$ or $= SD\sqrt{1-\left(\frac{\sum(x_{1J} - \bar{X}_1)(x_{2J} - \bar{X}_2)}{\sqrt{\sum(x_{1J} - \bar{X}_1)^2}\sqrt{\sum(x_{2J} - \bar{X}_2)^2}}\right)}$
bias ± 95% limit of agreement	$= \frac{\sum^{n_j} x_{1.j} - x_{2.j}}{n} \pm 2SD_{meas}$

[a] abbreviated variables are described in the text.
[b] where n is the number of subjects, j is the subject index, i is the measurement index, $\bar{X}$ is the grand mean of the 2 sets of measurements, $\bar{x}$ is the mean of 2 measurements, $\bar{x}_1$ and $\bar{x}_2$ are the means of the first and second set of measurements, respectively, and EMS is the observed mean square for residual variation determined using ANOVA.

terms as the 95% limit of agreement which also gives information about the magnitude of change which is required in order to have confidence that a real change has occurred. The 95% limit of agreement between two measurements of a given variable is from 2 standard deviations below the average bias (or difference) to two standard deviations above the bias (Bland and Altman 1986). This approach is beneficial because it is independent of

the mean of a given variable within the sample population. Moreover, if the variable has a distribution of values which crosses zero as is the case for the connectivity index, the 95% limit of agreement permits discussion of reproducibility in absolute terms.

Table 3.2 summarizes methods of reporting precision or precision error as a proportionate measure. Precision error may be calculated using the coefficient of variation (CV%) of repeated measurements (Gatti et al. 1996; Hasegawa et al. 1997). When describing the precision of pQCT BD measurements in a group of subjects as a proportionate measure, it has been proposed that the average root mean square CV (CV_{rms}) is the most appropriate statistical method (Glüer et al. 1995). Another method of

TABLE 3.2

METHODS OF CALCULATING PROPORTIONATE ESTIMATES OF PRECISION[a,b]

Statistical tests which estimate precision[a]	Mathematical equations[b]
Precision error: CV	$=\frac{SD_{meas}}{\overline{X}}(100\%)$
Precision error: CV_{rms}	$=\frac{\sqrt{\sum_{j=1}^{n} d^2/2n}}{\sum_{j=1}^{n}(mean_j)/n} * 100$
Precision: R	= (BMS-EMS / BMS+ (k-1)EMS)* 100

[a] abbreviated variables are described in the text.

[b] where $\overline{X}$ is the grand mean for the repeated measurements, d is the difference between the 2 measurements for each subject, j is the subject index, n is the number of subjects, BMS is the observed mean square for intersubject variability, EMS is the observed mean square for residual variation and k is the number of measurements (ie, 2). BMS and EMS are determined using ANOVA.

estimating proportionate precision is the intraclass correlation reliability coefficient (R). The R-value gives an estimate of the true correlation of the measurements and describes the proportion of the intersubject measurement variance which is error-free within the study population (Shrout and Fleiss 1979).

The precision error of *in vivo* measurements of BD acquired at a standard 4 % site in the radius using pQCT has been reported as CV based on repeated measurements in 6 subjects over 3 days (Hasegawa et al. 1997) and in 19 subjects over 1 to 36 days (Gatti et al. 1996). The CV for measurements of total BD (ToBD) varied from 1.1% to 1.7%; the CV for cortical BD (CoBD) varied from 1.2% to 1.6%; and the CV for trabecular BD (TrBD) varied from 1.1% to 2.1%. Grampp et al. (1995) used the CV_{rms} to calculate short term *in vivo* precision error for measurements of ToBD, CoBD and TrBD. The values were 2.3%, 2.1% and 2.5%, respectively, in 40 subjects measured twice on the same day. Studies using pQCT have reported that normal age-related losses in BD at the distal radius are of the order of 0.5 to 2% per year and that women lose BD at an annual rate of 2 % to 5% soon after menopause (Krølner and Nielsen, 1982; Hansson and Roos 1986). Martin and Reid (1999) found that the rate of bone loss at the distal radius was accelerated for 2 to 3 decades following the menopause. These findings demonstrate the responsiveness of this measurement technique. It is also apparent that the typical annual rate of BD loss in healthy individuals is close to the precision errors determined for the pQCT.

The reproducibility of pQCT measurements of BD has been determined for scans of the nondominant distal radius at the 4% site using a standard scanning procedure which

takes approximately 5 minutes. When pQCT is used to quantify distal radius trabecular bone structure additional projection angles are used to improve spatial resolution (Gordon et al. 1996). Since a longer scanning time is required, it is necessary to evaluate the precision of the pQCT measurements obtained using the modified software.

The purpose of this chapter is to describe the standard protocol for quantifying bone density and trabecular bone structure at the distal radius using pQCT imaging and evaluate the reproducibility of the pQCT-derived measurements. Two potentially important factors which may contribute to variability of the measurements are the repositioning of the subject's forearm in the scanning field and movement of the forearm during the scan. Therefore, the effects of both subject repositioning and forearm movement on reproducibility of the measurements are described here.

3.2 Materials and Methods

3.2.1 *In Vitro* Reproducibility of pQCT

The calibration of the pQCT scanner is factory calibrated to convert the linear attenuation coefficient into mg/cm^3. The assessment of long-term instrument stability is based on the daily measurements of the hydroxyapatite phantom (0.495 cm^{-1}) supplied by the manufacturer.

3.2.2 Subjects

The study was approved by the McMaster University Research Ethics Board. All subjects gave written informed consent prior to participating.

3.2.2 i Short Term In Vivo Reproducibility

Healthy volunteers who participated in a cross-sectional study to determine normal gender and age-related changes in trabecular bone structure at the nondominant distal radius (section 4.2.1) were recruited. In total, 25 subjects (6 men, 19 women) agreed to have two scans of the nondominant forearm performed within a one month period. A subgroup (4 men and 12 women) participated in the protocol to determine the effects of both subject repositioning and controlled forearm movements on the reproducibility of measurements of BD and trabecular bone structure.

3.2.2ii Long Term In Vivo Reproducibility

A subgroup of healthy volunteers who participated in a cross-sectional study to determine typical between-limb differences in trabecular bone structure at the distal radius (section 5.2.1) were recruited to determine the long term *in vivo* reproducibility of the pQCT. In this subgroup (composed of 6 men and 5 women), two sets of bilateral pQCT measurements were performed approximately 1 year apart.

3.2.3 pQCT Equipment and Standard Procedure

Images of the distal radius were acquired using a second generation XCT 960 pQCT scanner (manufactured by Stratec Medizintechnik, Germany and distributed in North America by Norland Corporation, Fort Atkinson, WI, USA). A high resolution image of

the distal forearm is generated by reconstructing 145 projection angles obtained by means of a narrow fan beam emitted from an x-ray tube (38 keV). The high resolution image is acquired in the transverse plane at the standard 4% site which is located automatically by the system software. This scan location is based on the length of the ulna and the location of the most proximal aspect of the radial articular surface determined from an initial scout scan in the coronal plane. The transverse slice thickness is 2.5 mm and the in plane voxel dimension is 0.33 mm^2. The total scanning time for both the scout and the cross-sectional view is approximately 10 minutes. The radiation dose associated with this standard procedure is low (0.2 mSv). The subjects were seated on a non-swivel chair adjusted to the appropriate height and offered the use of a foot stool and cushions to optimize comfort. Care was taken to ensure that the forearm being scanned was well supported and centered appropriately in the imaging field. The same operator acquired images of the distal radius of each subject.

The images were analyzed using the commercial software (version 5.2) to determine values for ToBD, CoBD and TrBD. The images were downloaded onto computer diskettes and transferred to a computer system at Hamilton Health Sciences Corporation (Sun Microsystems, Mountain View, CA, USA) for postprocessing and analysis using in-house developed software (Gordon et al. 1996). Values for indices of trabecular bone structure including connectivity index (CI), maximum hole size (H_M) and mean hole size (H_A) were derived.

3.2.4 Specific Imaging Protocols

3.2.4 i Short Term In Vivo Reproducibility

For all subjects (n = 25), the standard procedure as described in section 3.2.3 was followed to obtain an initial image of the nondominant distal radius and a replicate image within 4 weeks. The subgroup of 16 volunteers who performed controlled movements during the scan were studied under 4 different test conditions. For test condition 1, the standard procedure described above was followed to obtain images of the distal radius in the coronal and transverse planes (Scan 1). Without repositioning the forearm, a second high resolution image was acquired in the transverse plane (Scan 2). Volunteers were instructed to remain motionless during the total scanning time of 15 minutes. One week later, the subjects returned for a second set of scans. The scout scan in the coronal plane and the high resolution scan in the transverse plane (Scan 3) were performed according to the standard procedure. The volunteers were requested to remain motionless during the 10 minute scanning time. Thus, test condition 2 compared scans with repositioning of the forearm between scans. Two subsequent high resolution scans were acquired without repositioning of the forearm to evaluate the effect of controlled movements on the results obtained. Half way through the scan (at 2.5 minutes), the volunteers were instructed to drop their thumb from the hand rest to produce a slight pronation (rotational) movement of the radius (Scan 4). The new position was maintained during the remainder of the scanning time. During the final scan (at 2.5 minutes), the subjects were asked to keep the thumb on the hand rest and shift the elbow slightly forward off the scanner's positioning block producing a small longitudinal movement (Scan 5). Thus the scan with no

movement was compared to the scans involving controlled movements but no repositioning in test condition 3 (comparing Scans 3 and 4) and test condition 4 (comparing Scans 3 and 5).

3.2.4ii Long Term In Vivo Reproducibility

For the 11 volunteers, the standard procedure described in section 3.2.3 was followed to acquire a high resolution image of the dominant and nondominant distal radius at the time of the initial scan and again at the time of repeat scanning (mean [SD] 1.25 [0.24] years later).

3.2.5 Statistical Analyses

In vitro reproducibility was calculated as the coefficient of variation for the daily phantom linear attenuation coefficient and density measurements. For the studies to determine the short and long term *in vivo* reproducibility, descriptive data were calculated for each group of subjects. The precision of the *in vivo* pQCT structure and BD measurements are expressed as the reliability coefficient (R) using the type 3,1 intraclass correlation equation according to the method of Shrout and Fleiss (1979) which is shown in Table 3.2. The critical value to be exceeded in order to detect real change was calculated using the test statistic ($Z_{\alpha/2}\sqrt{2}\,SE_{meas}$). In addition, precision error for measurements of BD is expressed as the CV_{rms} and was calculated using the method described by Glüer et al. (1996) according to the equation shown in Table 3.2.

3.3 Results

3.3.1 *In Vitro* Reproducibility

The mean (SD) values for attenuation (cm^{-1}), density (mg/cm^3) and voxel number determined for 443 measurements of the polyethylene phantom (0.495 cm^{-1}) over a time period of 3.14 years are 0.496 cm^{-1} (0.001), 263.03 mg/cm^3 (1.14) and 1513.7 (3.0), respectively. There is no drift in the values during the whole measurement period and the *in vitro* precision (CV%) is 0.3% for attenuation, 0.4% for density and 0.2% for voxel number determinations.

3.3.2 Short Term *In Vivo* Reproducibility

The mean (SD) age of the 25 volunteers is 35.3 (9.9) years. An average (SD) of 7.7 (5.1) days elapsed between scans. The descriptive data for the repeated measurements of bone structure and density are presented in Table 3.3.

TABLE 3.3

DESCRIPTIVE DATA FOR REPEAT MEASUREMENTS AT THE 4 % SITE OF THE DISTAL RADIUS IN 25 SUBJECTS [a-c]

Structure[a]	Mean (SD); Min., Max.[b]	Density[c]	Mean (SD); Min., Max.[b]
CI	8.23 (8.01); -8.22, 20.14	ToBD	419.9 (55.9); 315.1, 524.0
H_M	57.88 (37.8); 5.45, 143.96	CoBD	753.9 (57.8); 664.1, 858.0
H_A	1.71 (1.28); 0.53, 6.54	TrBD	225.5 (44.5); 141.1, 308.7

[a] CI: connectivity index; H_M: maximum hole size, mm^2; H_A: mean hole size, mm^2.
[b] Min.: minimum value; Max: maximum value.
[c] ToBD: total bone density (mg/cm^3); CoBD: cortical bone density (mg/cm^3); TrBD: trabecular bone density (mg/cm^3).

Table 3.4 shows the measures of precision of pQCT derived indices of trabecular bone structure at the 4% site of the nondominant radius using the reliability coefficient (R) and the 95% limit of agreement. The R-values vary from 83 % to 96 % demonstrating a substantial correlation between repeated measurements of indices of trabecular bone structure. The minimum critical value that must be exceeded in a second measurement of CI, H_M and H_A is approximately 5, 23 mm^2 and 1.5 mm^2 , respectively.

TABLE 3.4

SHORT TERM *IN VIVO* REPRODUCIBILITY OF BONE STRUCTURE MEASUREMENTS AT THE 4% SITE OF THE DISTAL RADIUS IN 25 SUBJECTS[a]

Estimates of Reproducibility[a]	CI	H_M	H_A
R (95 % CI)	94.7 (88.3, 97.6)	95.5 (90.0, 98.0)	83.1(65.4, 92.2)
Bias	-0.26	+0.69 mm^2	-0.10 mm^2
± 95% limit of agreement	± 5.30	± 23.02	± 1.56
SEmeas	1.87	8.14 mm^2	0.55 mm^2
Minimal Detectable Change	5.19	22.57 mm^2	1.53 mm^2

[a] R: reliability coefficient (%); 95% CI: 95% confidence interval; Bias: mean difference; SEmeas: standard error of the measurement; Minimal Detectable Change: test statistic equated to a standard normal critical value; CI: connectivity index; H_M: maximum hole size, mm^2; H_A: mean hole size, mm^2.

The precision of the repeated measurements of BD at the distal radius is shown in Table 3.5. The CV_{rms} is 2.7%, 3.7% and 4.9% for ToBD, CoBD and TrBD, respectively. There are no significant differences between the replicated measurements (determined by F-tests of variance due to time, $p > 0.05$). The R-values, representing the error-free

proportion of the intersubject variability in the measurements of BD, are 95.5% for ToBD, 76.9% for CoBD and 83.1% for TrBD. The R-values show that measurements of ToBD are most reliable. The 95% limit of agreement is 33.8 mg/cm^3. For the measurements of CoBD and TrBD the 95% confidence intervals overlap. Thus, the precision of the latter two measurements are similar. Looking at the 95% limit of agreement, a repeated measure of CoBD may be 82.2 mg/cm^3 below or 84.6 mg/cm^3 above the value of the initial measurement. The absolute difference one can expect for repeated measurements of TrBD is 29.6 mg/cm^3 above or below the first value obtained. Changes of these magnitudes are associated with pQCT measurement error and can not be attributed to biological events.

TABLE 3.5

SHORT TERM REPRODUCIBILITY OF *IN VIVO* BONE DENSITY MEASUREMENTS AT THE 4% SITE OF THE DISTAL RADIUS IN 25 SUBJECTS [a]

Estimates of Reproducibility[a]	ToBD	CoBD	TrBD
R (95 % CI)	95.5 (90.1, 98.0)	76.9 (54.3, 89.1)	83.1 (65.4, 92.2)
Bias ± 95% limit of agreement	+2.53 ± 33.8	+1.22 ± 83.4	+0.01 ± 29.6
SEmeas	11.95 mg/cm^3	29.49 mg/cm^3	10.48 mg/cm^3
Minimal Detectable Change	33.11 mg/cm^3	81.74 mg/cm^3	29.05 mg/cm^3
CV_{rms}	2.7 %	3.7 %	4.9 %

[a] R: reliability coefficient, %; 95% CI: 95% confidence interval; Bias ± 95% limit of agreement: mean difference ± 2(SD), mg/cm^3; SEmeas: standard error of the measurement; Minimal Detectable Change: test statistic equated to a standard normal critical value; CV_{rms}: root mean square coefficient of variation; ToBD: total bone density, mg/cm^3; CoBD: cortical bone density, mg/cm^3; TrBD: trabecular bone density, mg/cm^3.

In Figure 3.1 the mean values of the indices of trabecular bone structure are plotted against the difference between the two measurements for each of the 25 subjects. Figure 1A illustrates that larger differences in measurements of CI are associated with lower mean values. In contrast, differences in measurements of H_M (Figure 3.1B) are not influenced by the magnitude of the mean value for this bone variable. Repeated measurements of H_A are less consistent in individuals with larger mean values for H_A (Figure 3.1C). Significant associations are observed when the absolute difference is regressed on the mean value for each subject for both CI and H_A ($r = -0.57$, $p = 0.003$ and $r = 0.90$, $p < 0.001$, respectively). Differences in repeat measurements of ToBD, CoBD and TrBD (Figure 3.2A-C, respectively) are not influenced by the magnitude of the mean value for these bone variables.

3.3.3 Influence of Repositioning on Short Term *In Vivo* Reproducibility

Two potential factors which may contribute to the measurement error are subject repositioning between scans and movement of the forearm during image acquisition. The computer generated representation of the repeated high resolution images for 2 subjects are shown in Figure 3.3. Figure 3.3A shows that the image acquired during the initial scan of the forearm of one subject has slight irregularities in the continuity of the cortical shell which are not prominent in the image acquired on repeat scanning (Figure 3.3B). This subject has the lowest mean value for CI and the highest mean value for H_A in the group of 25 subjects. The images pictured in Figure 3.3A and 3.3B have the largest differences between repeated measurements of CI and H_A. Figure 3.3C and 3.3D show

Figure 3.1 Difference against the mean of two repeated measurements in 25 volunteers for indices of trabecular bone structure at the 4 % site of the distal radius. The mean difference (—) and 95% confidence intervals (- -) are shown. A: Difference in connectivity index (CI) plotted as a function of the mean CI for each subject. B: Difference in maximum hole size (H_M, mm^2) plotted as a function of the mean H_M for each subject. C: Difference in mean hole size (H_A, mm^2) plotted as a function of the mean H_A for each subject.

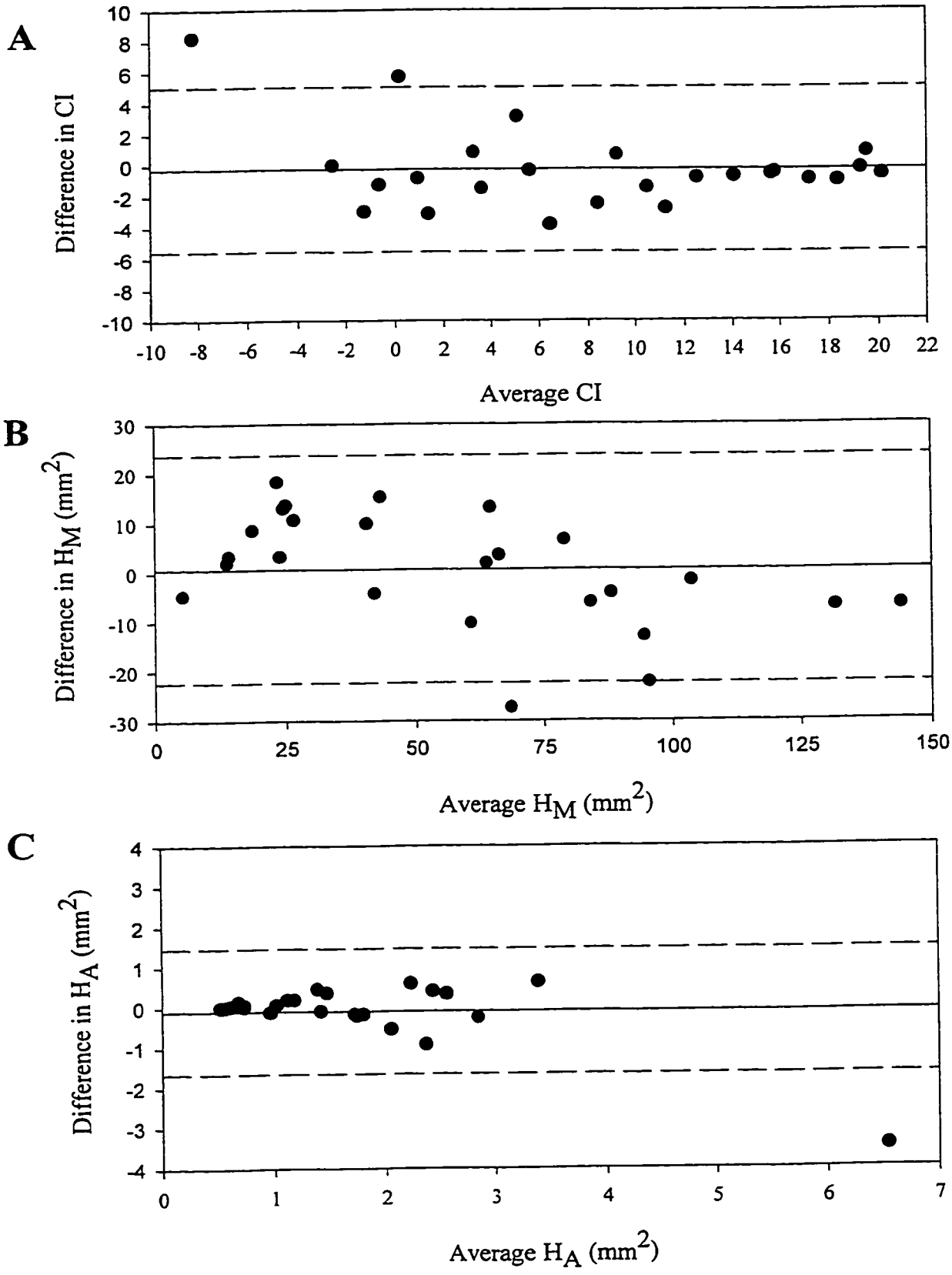
A
Difference in CI
Average CI
B
Difference in H_M (mm^2)
Average H_M (mm^2)
C
Difference in H_A (mm^2)
Average H_A (mm^2)

Figure 3.2 Difference against the mean of two repeated measurements in 25 volunteers for bone density at the 4 % site of the distal radius. The mean difference (—) and 95% confidence intervals (- -) are shown. A: Difference in total bone density (ToBD, mg/cm^3) plotted as a function of the mean ToBD for each subject. B: Difference in cortical bone density (CoBD, mg/cm^3) plotted as a function of the mean CoBD for each subject. C: Difference in trabecular bone density (TrBD, mg/cm^3) plotted as a function of the mean TrBD for each subject.

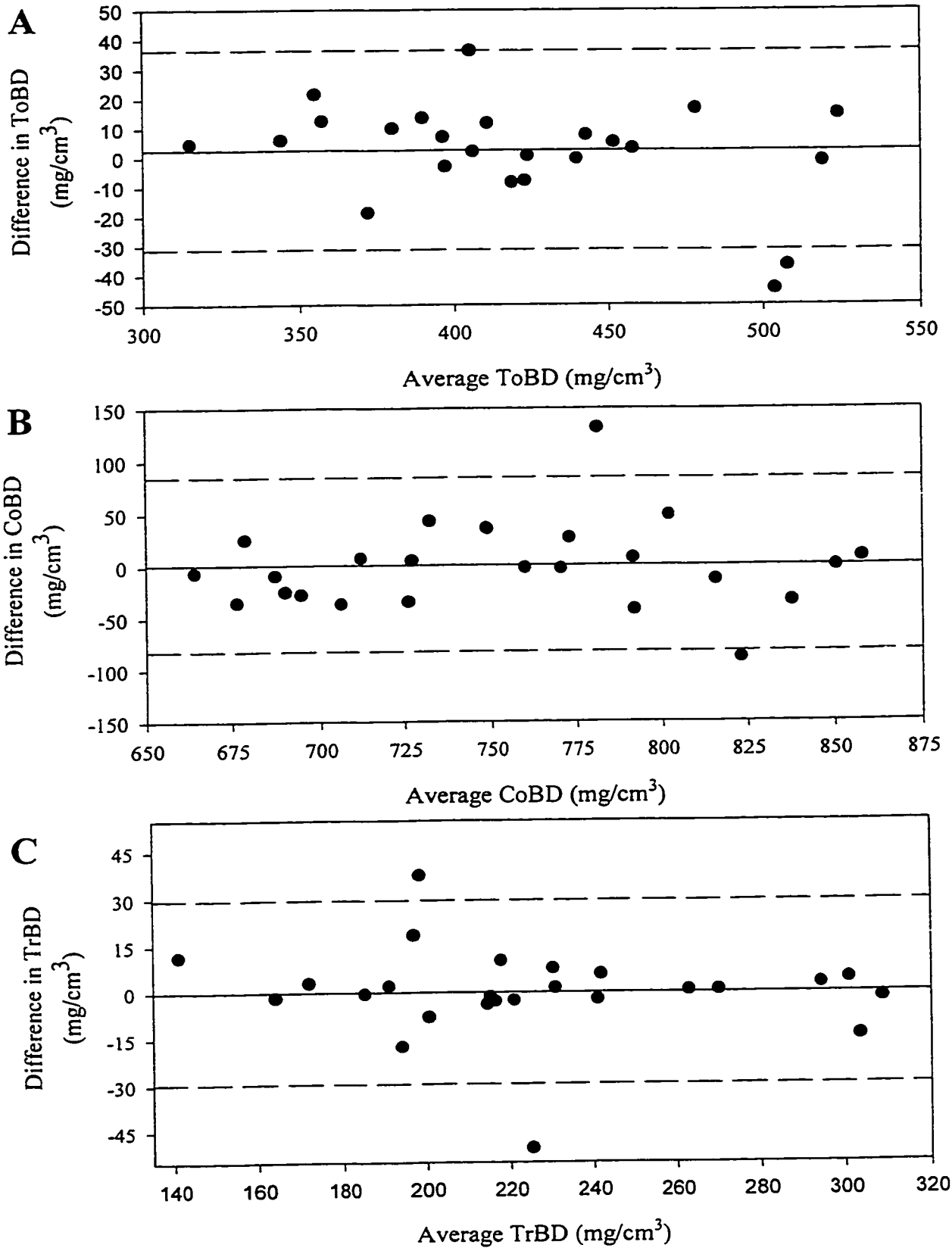
A
Difference in ToBD (mg/cm3)
50
40
30
20
10
0
-10
-20
-30
-40
-50
300
350
400
450
500
550
Average ToBD (mg/cm3)
B
Difference in CoBD (mg/cm3)
150
100
50
0
-50
-100
-150
650
675
700
725
750
775
800
825
850
875
Average CoBD (mg/cm3)
C
Difference in TrBD (mg/cm3)
45
30
15
0
-15
-30
-45
140
160
180
200
220
240
260
280
300
320
Average TrBD (mg/cm3)

Figure 3.3 Images acquired at the 4 % site in the nondominant forearm from an initial pQCT scan and a repeat scan 1 week later for 2 subjects. A and B illustrate the images of the forearm of a 45.4 year old woman. Irregularities in the cortical shell of the radius are observed on the initial scan (A, ↘) but not on the repeat scan (B). C and D illustrate the images of the forearm of a 49.8 year old women. No disruption of the cortical shell is observed in the radius on the initial scan (C) but the cortical ring is disrupted on the repeat scan (D, ↘).

the replicated images with the largest differences in measurements of CoBD, TrBD and H_M. The image in Figure 3.3D clearly shows disruption of the cortical shell compared to the image in Figure 3C. The poorer reproducibility of measurements of these bone variables is not associated with the magnitude of the mean values for bone density and maximum hole size and is probably influenced more by an error in repositioning such that the high resolution cross-sectional image is not acquired at the same site or by movement of the forearm during image acquisition.

To estimate the effect of repositioning of the forearm as a potential source of measurement variability, 16 volunteers underwent repeated pQCT measurements of the distal radius with and without repositioning between scans. This group of subjects was composed of 4 men and 12 premenopausal women between the ages of 23 and 50 years (mean age, 32.7 ± 9.3 years). Scans 1 and 2 were acquired without repositioning while scan 3 was acquired 1 week after the initial visit. Table 3.6 shows the agreement between repeat measurements acquired without repositioning between scans (Condition 1) and the agreement between repeat measurements when repositioning occurs between scans (Condition 2). Comparison of the reliability coefficients for the 2 test conditions show that the reproducibility of the measurements of bone structure fall within overlapping 95% confidence intervals and repositioning has little influence. Similarly, the reliability coefficients for measurements of bone density are within the same range with and without repositioning of the forearm between scans except for ToBD which is adversely affected by repositioning but remains highly reliable (R = 94.8%; Table 3.6).

TABLE 3.6

REPRODUCIBILITY OF REPEAT MEASUREMENTS OF RADIAL BONE STRUCTURE AND DENSITY AT THE 4% SITE IN 16 SUBJECTS WITH AND WITHOUT REPOSITIONING [a-c]

Variable[a]	Condition 1 (Scans 1 & 2)	Condition 2 (Scans 1 & 3)
CI	93.3% (83.5, 97.8) [b]	95.9% (88.7, 98.6) [b]
H_M (mm^2)	93.5% (82.5, 97.7) [b]	91.8% (78.1, 97.0) [b]
H_A (mm^2)	82.0% (55.9, 93.3) [c]	90.1% (74.0, 96.4) [c]
ToBD (mg/cm^3)	98.3% (95.2, 99.4) [b]	94.8% (85.7, 98.1) [b]
CoBD (mg/cm^3)	84.1% (60.4, 94.1) [c]	77.5% (46.8, 91.5)
TrBD (mg/cm^3)	94.3% (84.6, 98.0) [b]	91.1% (76.5, 96.8) [b]

[a] Data expressed as reliability coefficient (95% confidence interval). CI: connectivity index; H_M: maximum hole size; H_A: mean hole size; ToBD: total bone density; CoBD: cortical bone density; TrBD: trabecular bone density; Condition 1: no repositioning of the forearm between scans; Condition 2: replicate scan acquired one week later.
[b] : true reliability coefficient is > 80%, $p \leq 0.01$.
[c]: true reliability coefficient is > 60%, $p < 0.01$.

It has been suggested that a change in the number of voxels present in the pQCT image reflects a difference in scan location and, therefore, should be related to the precision of the measurements. On the initial scan (Scan 1) of the 16 subjects, the mean (SD) voxel number determined in the total, cortical and trabecular compartments is 2516 (430), 940.7 (134.2) and 1575.1 (322.4), respectively. Figure 3.4 shows the difference in ToBD, CoBD and TrBD plotted as a function of the difference in voxel number for scans 1 and 2. For the total bone and cortical bone compartments, 73% of the variance in the difference in density is explained by the variance in the difference in voxel number. The relation between the difference in TrBD and the difference in voxel number is weaker (R^2

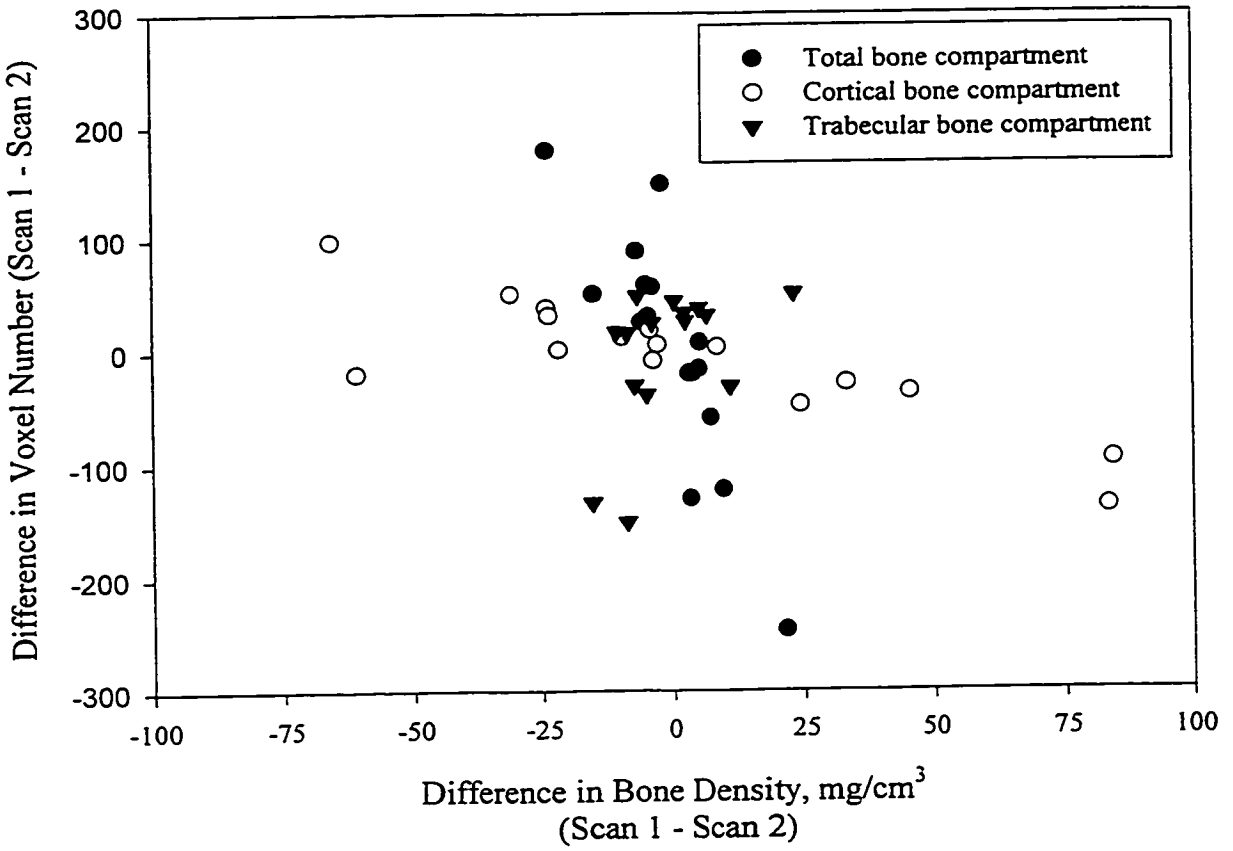

Figure 3.4 The difference in voxel number plotted as a function of the difference in bone density for the total, cortical and trabecular bone compartments at the 4 % site of the distal radius determined from repeat pQCT imaging without repositioning of the forearm between scans.

= 0.50, Figure 3.4). If the difference in voxel number was due to inadvertent changes in position between scans 1 and 2, we would expect to see greater differences when the forearm was repositioned in the scanner 1 week later when repositioning errors would be expected. Consequently, precision error was calculated for voxel number measurements for scans 1 and 2 and compared to the precision error for measurements of voxel number in scans 1 and 3 (Table 3.7). The R-values (95% confidence interval) demonstrate that repositioning does not significantly decrease the reproducibility of measurements of voxel number detected by the software for the total, cortical and trabecular bone compartments.

TABLE 3.7

REPRODUCIBILITY OF VOXEL NUMBER FOR REPEAT MEASUREMENTS IN 16 SUBJECTS WITH AND WITHOUT REPOSITIONING BETWEEN SCANS[a-c]

Estimates of Reproducibility [a]	Condition 1 (Scans 1 and 2)	Condition 2 (Scans 1 and 3)
Total Bone Compartment:		
R (95% CI)	97.1% (91.8,99.0)*	96.1% (89.3,98.6) *
Bias ± 95% level of agreement	+2.6 ± 212.4	-45.2 ± 269.8
CV_{rms}	2.77%	3.93%
Cortical Bone Compartment:		
R (95% CI)	91.6% (77.7,97.0) *	93.7% (82.9, 97.7) *
Bias ± 95% level of agreement	-6.7 ± 112.4	+16.0 ± 96.4
CV_{rms}	3.74%	3.74%
Trabecular Bone Compartment:		
R (95% CI)	97.1% (92.0,99.0) *	93.0% (81.1,97.5) *
Bias ± 95% level of agreement	+9.3 ± 158.2	-61.2 ± 285.6
CV_{rms}	4.92%	5.06%

[a] R: reliability coefficient; 95% CI: 95% confidence interval; Bias: mean difference; CV_{rms}: root mean square coefficient of variation; Condition 1: no repositioning of the forearm between scans; Condition 2: replicate scan acquired one week later.
*: true reliability coefficient is > 80%, $p < 0.05$.

3.3.4 Influence of Controlled Movements on Short Term *In Vivo* Reproducibility

Controlled movements of the forearm were introduced half way through scans 4 and 5. Table 3.8 shows that a rotational movement results in a decrease in the R-value and less confidence (compared with Table 3.6) around those values for all the bone variables. The 95% confidence interval crosses zero for both H_A and CoBD. None of the bone variables have a true reliability coefficient that is greater than 60% with the exception of H_M ($p = 0.03$).

TABLE 3.8

REPRODUCIBILITY OF MEASUREMENTS OF BONE VARIABLES AT THE 4% SITE IN 16 SUBJECTS UNDER CONDITIONS OF CONTROLLED MOVEMENT [a]

Variable[a]	Condition 3 (Scans 3 and 4)	Condition 4 (Scans 3 and 5)
CI	70.8% (34.3, 88.7)	77.6% (47.0, 91.6)
H_M (mm^2)	83.2% (58.4, 93.8) *	84.3% (60.8, 94.2) *
H_A (mm^2)	42.2% (-7.5, 75.1)	71.9% (36.3, 89.2)
ToBD (mg/cm^3)	79.7% (51.1, 92.4)	86.0% (64.5, 94.9) *
CoBD (mg/cm^3)	21.9% (-29.5, 63.4)	33.6% (-17.4, 70.4)
TrBD (mg/cm^3)	65.7% (25.5, 86.5)	52.5% (5.8, 80.4)

[a] Data expressed as reliability coefficient (95% confidence interval). Abbreviations as in Table 3.6. Condition 3: comparison of scans with no intentional movement and scans with controlled rotational movements of the forearm; Condition 4: comparison of scans without intentional movement and scans with controlled longitudinal movement.
*: true reliability coefficient is > 60%, $p < 0.05$.

Condition 4 introduced a controlled longitudinal movement of the forearm half way through the scanning procedure. Again, the R-values for all of the bone variables decrease and the 95% confidence intervals for the reliability coefficient are wide, crossing zero for CoBD and approaching zero for TrBD (Table 3.8). Under this condition, the true correlation coefficient is greater than 60% for only H_M and ToBD ($p = 0.02$ and $p = 0.01$, respectively).

Figure 3.5 illustrates scans 3, 4 and 5 obtained on the second visit for the 3 subjects who demonstrate the largest difference between scans for bone variables. The largest differences in CI, H_A and H_M are seen between Scans 3 and 4 (Condition 3) depicted in Figure 3.5A and Figure 3.5B. For this subject, the difference in CoBD is greater with rotational movement (Figure 3.5B). The largest difference in ToBD is seen between Scans 3 and 5 shown in Figure 3.5A and Figure 3.5C, respectively. Similarly, the difference in TrBD is also greater with longitudinal movement (Figure 3.5C). Figures 3.5D and 3.5F show the images for the subject with the greatest difference in H_M and H_A with longitudinal movement (Scans 3 and 5, respectively). Figures 3.5G-I illustrate the images for the subject with the greatest difference in bone density measurements under these 2 test conditions. This subject has the greatest difference in ToBD, CoBD and TrBD with controlled rotation of the forearm (Figure 3.5H). As well, this subject has the second largest difference in ToBD and the largest difference in CoBD and TrBD with controlled longitudinal movement (Figure 3.5I). The magnitude of the differences in measurements of all the bone variables is greater when the subjects performed controlled movements than with repositioning alone.

Figure 3.5 Images acquired at the 4 % site in the distal radius using pQCT during scanning protocols involving no intentional movement (Scan 3), controlled rotational movement (Scan 4) and controlled longitudinal movement (Scan 5) of the nondominant forearm. A-C: Images obtained from a 49.8 year old woman. D-F: Images obtained from a 35.5 year old woman. G-I: Images obtained from a 45.0 year old woman.

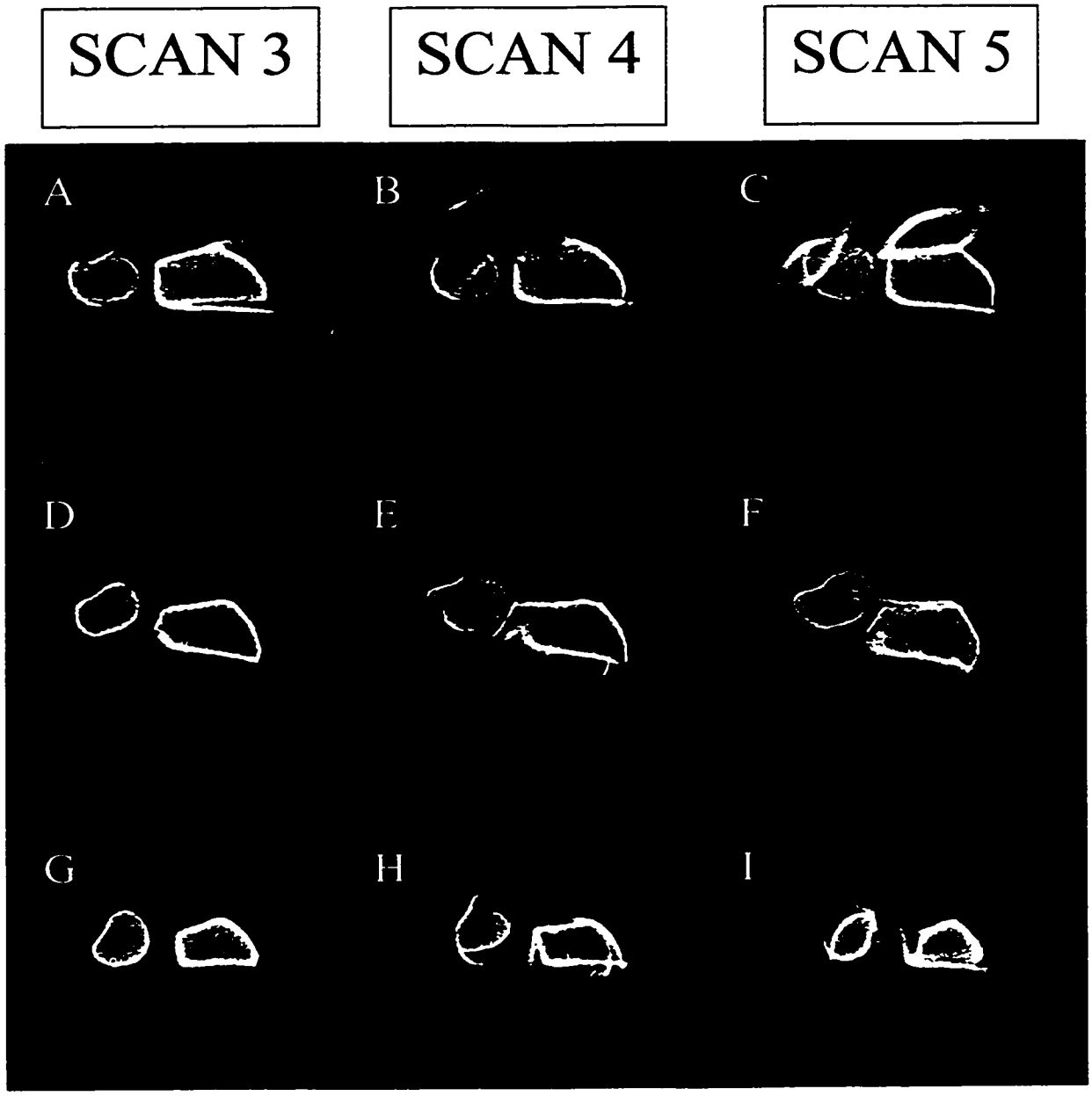
SCAN 3
SCAN 4
SCAN 5
A
B
C
D
E
F
G
H
I

3.3.5 Long Term *In Vivo* Reproducibility

After 1.25 ± 0.24 years, 6 men and 5 women (mean age ± SD: at initial scan = 44.6 ± 19.8 years; at repeat scan = 45.8 ± 19.6 years) returned for repeat scans. Table 3.9 summarizes the precision of *in vivo* measurements of bone structure and density in the dominant and nondominant distal radii for 11 subjects (i.e., duplicate measurements of 22 radii). The reproducibility for all measurements is good; measurements of CI, H_A, ToBD and TrBD are more similar than those of H_M and CoBD when scans are repeated over one year later.

TABLE 3.9

LONG TERM REPRODUCIBILITY OF *IN VIVO* MEASUREMENTS OF BONE STRUCTURE AND DENSITY AT THE 4% SITE OF THE DISTAL RADIUS[a]

Reproducibility[a]	CI	H_M	H_A	ToBD	CoBD	TrBD
R% (95% CI) lower limit: upper limit:	92.5 (82.8, 96.8)[b]	82.9 (63.2, 92.5)[c]	90.7 (79.1, 96.1)[b]	92.7 (83.3, 96.9)[b]	82.4 (62.3, 92.3)[c]	97.4 (93.9, 98.9)[b]
Bias ± 95% limit of agreement	-0.102 ± 6.05	+0.13 ± 35.52	-0.104 ± 0.806	-4.30 ± 37.68	-5.50 ± 91.92	-4.47 ± 21.20
SEmeas	2.14	12.56	0.28	13.32	32.50	7.50
CV_{rms} %	NA	NA	NA	3.47	4.62	3.48

[a] R: reliability coefficient; 95% CI: 95% confidence interval; Bias: mean difference; SEmeas: standard error of the measurement; CV_{rms}: root mean square coefficient of variation; CI: connectivity index; H_M: maximum hole size, (mm^2); H_A: mean hole size, (mm^2); ToBD: total bone density, (mg/cm^3); CoBD: cortical bone density, (mg/cm^3); TrBD: trabecular bone density, (mg/cm^3); NA: not applicable due to the low mean values. Moreover, CI has a distribution of values which crosses zero.
[b]: true reliability coefficient is > 80%, $p < 0.05$.
[c]: true reliability coefficient is > 60%, $p < 0.05$.

3.4 Discussion

This study determines the reproducibility of *in vivo* measurements of bone structure and density in the 4 % site of the distal radius using high resolution pQCT (XCT 960) imaging. If reproducibility is expressed as the reliability coefficient (R) then a value of 100% would mean that there is no variation in the measurement due to error and a value of 0% would indicate that there is no error-free component to the variation in the measurement. The measurements of connectivity and maximum spacing of the trabecular elements were shown to be highly reproducible (R = 94.7% and 95.5%, respectively) and only approximately 5% of the variation in the measurement is due to error. We can be quite confident about these estimates of the true correlations as shown by the narrow 95% confidence intervals (Table 3.4). The proportion of the measurement of H_A which is error-free is 17%. This measurement quantifies the average size of the holes within the trabecular compartment of the cross-sectional image. In the group of healthy subjects who participated in this study, the mean difference between repeated measures was small (Figure 3.1C) and the magnitude of the difference was minimal in individuals with average hole sizes less than 2 mm^2. The reproducibility of the measurement is not affected in a systematic way as the average area of the holes increases although the absolute difference between repeated measurements increases significantly.

A similar pattern in seen in measurements of connectivity such that as connectivity increases, the magnitude of the absolute difference decreases. This suggests that when hole area is small and connectivity is good, the trabecular network is relatively uniform and errors associated with repositioning are less influential. However, when the image

slice is in a slightly different location within a radius which has a poorer spatial arrangement of trabecular bone, as in the case of individuals with osteoporosis, reproducibility is adversely affected.

There is no apparent dependence of the difference between repeated measurements of H_M upon the magnitude of the maximum hole area. The mean difference in maximum hole size is 0.69 mm^2 (Table 3.4). If we assume that the hole is circular then this difference in hole area corresponds to a difference in radius of 0.03 mm for a maximum hole of 58 mm^2 (mean value for this group, Table 3.3). Comparatively, if the largest absolute difference in repeated measurements of maximum hole size (27.69 mm^2) is converted to a difference in radius for the same maximum hole size, the difference increases to 0.94 mm. Errors in repositioning on two measurement occasions or movement during image acquisition could account for these differences.

When the intersubject variability is taken into account, the error-free proportion of *in vivo* measurements of total bone density acquired over a short period of time is 95.5%. The measurements of the cortical and trabecular compartments have lower but similar degrees of reproducibility (76.9% and 83.1%, respectively). Grampp et al. (1995) calculated the CV_{rms} for measurements of ToBD (2.3%), CoBD (2.1%) and TrBD (2.5%) using a pQCT (XCT 960). Such values are better than those determined in the study presented in this chapter (2.7%, 3.7%, and 4.9%, respectively). The study designs may explain these differences since our repeated measurements were obtained within one month while Grampp et al. (1995) obtained both measurements during a single visit, perhaps reducing sources of measurement error due to environment, operator or subject.

Also, the subjects in the current study represented a broader age group which may increase the variability in the measurements given the age-related changes which occur in bone density and structure. However, since the reproducibility of bone density measurements is not dependent upon the value of the bone variable, this should not have affected our results.

It is possible that the additional time required to obtain high resolution images capable of providing information about trabecular bone structure influences the reproducibility of the BD measurements. Recently Sievänen et al. (1998) used the newest version of pQCT scanners (XCT 3000) to measure CoBD and TrBD at the 4 % site of the distal radius in 19 volunteers (12 men and 7 women) varying in age from 23 to 47 yr (mean age [SD], 32 [8] yr) and determined mean (SD) group values of 756.2 (82.7) mg/cm^3 and 237.4 (34.2) mg/cm^3, respectively. The CV_{rms} calculated for CoBD was 6.5% (R = 29.0%) and for TrBD was 2.2% (R = 95.2%). In the present study, the group mean (SD) values for CoBD and TrBD are similar at 753.9 (57.8) mg/cm^3 and 225.5 (44.5) mg/cm^3 while the calculated precision error is lower for CoBD but higher for TrBD (Table 3.3). The present study also shows that the reproducibility of measurements of trabecular bone connectivity and maximum hole size are similar to that of ToBD and repeated measurements of mean hole size are as consistent as those of CoBD and TrBD. The reproducibility of the measurements of bone structure and density obtained using the modified pQCT XCT 960 is similar when compared with proportionate *in vivo* precision error (CV) data for standard pQCT scanners (XCT 900, XCT 960, and XCT 3000).

A change in the number of voxels present in subsequent pQCT images could reflect a difference in location from the site of the initial image slice. This study shows that, under the conditions of these experiments, the difference in voxel number does not increase with repositioning when reasonable efforts are made to locate the same scan site during repeat imaging. With repositioning of the forearm between repeat scans, the error-free proportion of the measurement of voxel number varies from 93.0% in the trabecular bone compartment to 96.1% in the total bone compartment. These values fall within the 95% confidence intervals determined for the error-free proportion of the variation in the measurement when the forearm is not repositioned between scans (Table 3.7). We found that changes in voxel number in the trabecular bone compartment varying between 347 below or 224 above the initial number (mean value of 1575.1) are not indicative of poor precision. Changes in voxel number in the cortical bone compartment varying from less than 80 below to 112.4 above the number determined on the initial scan (mean value of 940.7) are not associated with reduced precision. Similarly, the reproducibility of *in vivo* measurements of CI, H_M, H_A, ToBD and TrBD is not different with and without repositioning (Table 3.6). In contrast, repeat measurements of CoBD appear to be adversely affected by repositioning since the probability that the true reliability coefficient is greater than 60% was observed only when the forearm was not repositioned between scans.

The major source of imprecision in measurements of all bone variables is movement of the forearm during image acquisition (Table 3.8). The controlled movement evaluated in this study was designed to be subtle; it was not possible to detect the movement

visually in some subjects. Subjects determined the magnitude of the movement they felt was required in order to follow the protocol. Thus, there are inconsistencies in the amount of movement which took place. Despite this, the mean differences in the measurements of the six bone variables are more pronounced when controlled movement occurs. With movement, the reliability coefficients for H_A and CoBD could equal zero and only for H_M is there a statistically significant probability that the true correlation is greater than 60%. Based on these results, it is possible to identify artifacts of movement which indicate that the measurements are not reliable. An image acquired during controlled movement (Figure 3.5) has blurring and/or disruption of the cortical shell and pixels outside the cortical ring can be identified as containing moderately dense tissue which is interpreted to be in the range of trabecular bone. These results underline the importance of positioning each subject's forearm appropriately in the imaging field such that no motion occurs during the scanning procedure. If it is not possible to achieve this goal, then the images which contain disrupted cortical shells and 'bone' pixels outside the cortical ring should not be analyzed.

Long term *in vivo* reproducibility of pQCT measurements is slightly poorer although similar to the short term reproducibility with the exception of H_M (Table 3.9). The long term repeat measurements were acquired approximately 1.25 years apart in a group of adults with a mean (SD) age of 45.8 (19.6) years at the time of the second set of scans. The decrease in precision may be influenced by true biological changes in the bone including decreased bone density and connectivity of the trabecular network and

increased spacing between the trabecular elements. Perhaps the measurement of H_M may be more sensitive to age-related changes.

In conclusion, the *in vitro* precision errors associated with pQCT measurements are minimal and confirm that the calibration and instrument reliability has remained stable during the 3.4 year period over which the studies presented in this thesis were completed. The evaluation of short term *in vivo* reproducibility shows that the error-free proportion of pQCT measurements of trabecular bone connectivity, maximum hole size and ToBD is approximately 95%. The error-free proportion of the measurements of H_A, CoBD and TrBD are lower (83.1%, 76.9% and 83.1%, respectively). Reproducibility of measurements of CI and H_A are influenced by the value of these variables and these measurements will be more reliable in individuals with well connected, closely spaced trabecular elements. While careful attention is required when relocating the exact site of a previous scan, movement of the forearm during image acquisition has a pronounced negative effect on reproducibility of all pQCT measurements. Effort is necessary to prevent movement of the forearm during the scanning procedure and images which are affected by movement are not reliable - particularly with respect to H_A and CoBD measurements. It is apparent that the reliability of measurements obtained using pQCT are close to the typical annual rate of BD loss in healthy individuals. However, the long term *in vivo* reproducibility of these measurements suggests that this measurement tool is sensitive to age-related changes in bone structure.

CHAPTER FOUR

GENDER DIFFERENCES IN NORMAL AGE-DEPENDENT PATTERNS OF RADIAL BONE STRUCTURE AND DENSITY: A CROSS-SECTIONAL STUDY USING PERIPHERAL QUANTITATIVE COMPUTED TOMOGRAPHY[1]

4.1 Introduction

The vast majority of fractures of the distal radius (95%) occur within 1.6 and 3.0 cm from the tip of the radial styloid (Eastell et al. 1989). Thus, the bone fails in the region which contains a substantial fraction of trabecular bone (Schlenker and VonSeggen 1976). Given the common occurrence of fracture at this site among postmenopausal women (Cummings et al. 1985), this type of fracture is considered to be one of the earliest clinical manifestations of primary (type I) osteoporosis (Mallmin and Ljunghall 1994; Dai et al. 1998; Earnshaw et al. 1998). This type of primary osteoporosis typically affects estrogen deficient women within 25 years after menopause (Consensus Development Conference 1993). These facts have inspired investigations into gender differences and age-related changes in bone mass.

---

[1] These data have been published in an article by the same title, co-authored by Drs. JD Adachi and CE Webber, in *The Journal of Clinical Densitometry* (1999;2:163-173) and are reprinted here with permission from The Humana Press, Inc. (Appendix 1).

Reduced bone mass predicts increased fracture risk. The relation between areal bone mineral density and fracture risk is clearly demonstrated in large groups of people (Marshall, Johnell, and Wedel 1996). However, it is difficult to predict the fracture risk for a particular individual given that large overlaps in values exist for individuals with and without osteoporotic fractures (Marshall, Johnell, and Wedel 1996; Webber 1998). The distal radius has been studied using peripheral quantitative computed tomography (pQCT) which determines true volumetric bone density (BD) and bone mineral content (BMC) for trabecular and cortical bone compartments separately (Ferretti 1995; Gasser 1995). Some studies have shown that the bone loss in these two compartments is homogeneous in healthy women (Rüegsegger, Durand, and Dambacher 1991; Gatti et al. 1996; Hernández et al. 1997; Wapniarz et al. 1997; Nijs et al. 1998), whereas others report a significant age-dependent loss of cortical BD but not trabecular BD (Boonen et al. 1997). In healthy men, the rate of bone loss is more gradual than in women (Butz et al. 1994). Compared to the normative data, changes in the patterns of bone loss distinguish individuals with altered bone metabolism. The rate of cortical bone loss is accelerated in individuals with surgical menopause (Hernández et al. 1997), while individuals with osteoporosis can be distinguished by the accelerated loss in trabecular BD (Rüegsegger, Durand, and Dambacher 1991; Wapniarz et al. 1997).

Technology that permits separate analysis of volumetric density of trabecular and cortical bone appears to be advantageous in determining the natural history of bone loss in aging men and women. However, Mosekilde, Mosekilde, and Danielsen (1987) have shown that the age-related decrease in vertebral bone strength is much greater than the

observed decrease in bone mass (as measured by ash density). Additionally, Hui, Slemenda, and Johnston (1988) identified both bone mass and age as independent predictors of fracture and stressed the need to identify other relevant age-related factors.

Bone structure is an independent predictor of fracture risk (Kleerekoper et al. 1985). At the distal radius, bone structure has been described in terms of cross-sectional geometry. There is a significant age-related increase in cross-sectional area for the whole bone and for trabecular bone in healthy women, whereas there is a decrease in cortical bone cross-sectional area (Bouxsein et al. 1994; Gatti et al. 1996; Wapniarz et al. 1997). In the shaft of the distal radius, the increases in area are more pronounced in aging men than in aging women (Burr and Martin 1983). Gender differences and age-dependent patterns of trabecular structure have been described for human bone specimens obtained from the iliac crest (Parfitt et al. 1983; Mellish, Garrahan, and Compston 1989) and vertebral bodies (Mosekilde Li 1988, 1989; Vesterby et al. 1989). These structural changes have been associated with a decrease in mechanical competency (Kleerekoper et al. 1985; Mosekilde Li 1989). Similar information regarding connectivity and spacing of trabecular elements is not yet available for the distal radius. Perhaps gender differences in age-related structural adaptations of the radius may explain why fractures of the distal radial metaphysis are seen predominantly in aging women.

In vivo measurements of the distal radius using pQCT permit the separate analysis of trabecular and cortical bone compartments with respect to gross geometry, density and mass (Ferretti 1995). Also, pQCT images can be analyzed to determine indices of bone structure which quantify the intertrabecular connectedness and spacing at the distal radius

(Gordon et al. 1996). The primary purpose of this study is to identify typical gender and age-dependent patterns of trabecular bone structure in the nondominant distal radius using pQCT imaging. In addition, this study characterizes gender and age-dependent patterns for geometry, density and mass of the cortical and trabecular bone compartments at this site. This will provide a normative database for Canadian adults with which to compare individuals with medical conditions affecting bone metabolism.

4.2 Materials and Methods

4.2.1 Subjects

The target population for this cross-sectional study was healthy Canadian men and women, aged 20 to 85 years. Volunteers were recruited from the local community by poster advertisements and word of mouth. As well, members of a random sample recruited for a regional population survey of osteoporosis in the framework of the Canadian Multi-center Osteoporosis (CaMOs) study[2] were invited to participate. In response to these recruitment strategies, 192 individuals expressed an interest in participating in this study between December 1996 and December 1997.

Interested individuals were screened for eligibility and those who were pregnant or reported a history of injuries, menstrual abnormalities, precocious menopause (prior to 45 year of age), diseases or medication usage which might have affected bone metabolism were excluded. Individuals taking multivitamins, vitamin D, calcium, hormone

---

[2] Access to this sample population was provided by Dr. J.D. Adachi, St. Joseph's Hospital, Suite 501, 25 Charlton Ave. E., Hamilton, ON Canada L8N 1YZ.

replacement therapy for menopause-related symptoms unrelated to bone loss or oral contraceptives were eligible to participate and usage was documented. Based on these criteria, 26 volunteers were excluded. Another 14 individuals did not attend for scheduled appointments. Informed consent was obtained from 152 subjects (92 women and 60 men) who met the inclusion criteria. The study was approved by the McMaster University Research Ethics Board.

4.2.2 Procedure

Before performing the pQCT scans, subjects completed a questionnaire to document age, sex, race, height, body weight, hand dominance and a general health/medical history profile. In women, menopausal status was determined by self report and natural menopause was defined as the age at which menses first ceased for a period of 12 months. Height and body weight was recorded to the nearest 0.1 cm and 0.1 kg, respectively. The body mass index (BMI) was calculated as weight / height^2 for each subject. The distance from the olecranon process to the ulnar styloid was measured to the nearest 0.1 cm on the nondominant forearm of each subject. Scans were performed on the nondominant forearm of each subject using the standard imaging procedure as described previously (section 3.2.3).

4.2.3 Equipment

The images were acquired using the Stratec pQCT (XCT 960) scanner and analyzed as described in section 3.2.3. Indices of trabecular bone structure, including connectivity

index (CI), mean hole size (H_A) and maximum hole size (H_M), were determined using in-house developed software (Gordon et al. 1996). In addition, the commercial software (version 5.2, Stratec) calculates total bone area (ToBA, mm^2) and bone area of the cortical and trabecular compartments, CoBA (mm^2) and TrBA (mm^2), respectively. It has been suggested that the cortical bone area index (CoBA index), derived by dividing CoBA by ToBA, provides an estimate of the thickness of the cortical shell (Bouxsein et al. 1994). Thus, the CoBA index was calculated and included in the analyses of gender and age-related changes in radial bone structure.

From determinations of BD for total bone (ToBD, mg/cm^3), cortical bone (CoBD, mg/cm^3) and trabecular bone (TrBD, mg/cm^3) obtained using the commercial analysis software, the bone mineral content (mg) at the 4 % site in the nondominant distal radius (described as ToBMC, CoBMC, and TrBMC) was calculated as the product of bone density and area in each compartment and the thickness of the imaging slice.

Long-term precision of the pQCT over the duration of the study was evaluated by performing daily (n = 238) measurements of the polyethylene phantom (0.495 cm^{-1}). The coefficients of variation for the attenuation coefficient (cm^{-1}) and calibrated bone density (mg/cm^3) are 0.3% and 0.4%, respectively.

4.2.4 Statistical Analyses

Descriptive statistics were calculated for anthropometric measurements of the study subjects and all measured variables of bone structure, geometry, mass, and density. The measured bone variables were regressed on age and values which were more than 3 SD

from the regression were identified as outliers. The data was analyzed with and without outliers. For a conservative evaluation of the associations between bone structure indices and both gender and aging, the results are shown with the outliers excluded from analysis. For men, one value was identified as an outlier for each of the following variables: H_A, CoBA, CoBA index, TrBD and CoBMC. Thus, the results for these variables are calculated for 56 men. For women, regression of H_A on age revealed 3 outliers and the results are given for 85 women (63 premenopausal and 22 postmenopausal). For measurements of H_M, CoBA and TrBD, one outlier was identified for each and the results are shown for 87 women (64 premenopausal and 23 post-menopausal). Outliers were identified when CoBA index and ToBMC were regressed on age; thus, the results are calculated for 87 women (63 premenopausal, 24 post-menopausal). The subjects were grouped according to gender and menopausal status and group differences were determined using one-way ANOVA. Age-dependent patterns were determined using univariate regression analysis. The slope of the linear regression line is reported as the annual rate of change in the independent variables for study subjects grouped by gender and menopausal status. An unpaired two-tailed *t* test was used for intergroup comparisons. The rate of change for each variable was calculated as the slope of the regression line divided by the mean value for gender-matched subjects aged between 20 and 40 years and expressed as a percentage. The statistical results have been calculated using the statistical package, Minitab (release 11). Differences were considered significant for $p < 0.05$.

4.3 Results

4.3.1 Characteristics of the Study Subjects

In 7 of the images obtained from the 152 volunteers, the software was unable to close the cortical ring. These 7 images were acquired from 3 men (mean age [SD], 70.8 [1.6] years) and 4 women (mean age [SD], 69.5 [6.6] years) and were excluded from further analyses.

Table 4.1 summarizes the characteristics of the 145 subjects whose images were studied. No significant gender-related difference in age exists ($p = 0.44$). On average, men have a significantly greater height (cm), weight (kg) and BMI ($p < 0.001$, for each variable) than women. When the group of women are subdivided according to menopausal status, no significant difference is detected between these subgroups with respect to height ($p = 0.90$), weight ($p = 0.57$) or BMI ($p = 0.54$).

Table 4.2 gives the population means and standard deviations for the measured variables of bone structure, geometry, density and mass. With respect to structure, men have a significantly higher mean value for CI compared with the total group of women and the women subgrouped according to menopausal status. Men have a significantly smaller mean value for H_A when compared with the whole group of women and the subgroup of postmenopausal women. No gender-related difference in H_M is observed except when the mean values for men and postmenopausal women are compared, 60.23 mm^2 and 86.07 mm^2 respectively. Postmenopausal women have a significantly lower CI and significantly larger H_A and H_M compared with the subgroup of premenopausal women.

TABLE 4.1

ANTHROPOMETRIC CHARACTERISTICS, HAND DOMINANCE AND MEDICATION USAGE OF THE STUDY SUBJECTS GROUPED ACCORDING TO GENDER AND MENOPAUSAL STATUS [a,b]

	Men	Women		
	Total (n = 57)	Total (n = 88)	Premenopause (n = 64)	Postmenopause (n = 24)
Age (years) [a]	46.6 (16.4)	44.3 (17.5)	35.6 (10.5)	67.6 (8.9)
Height (cm) [a]	178.0 (6.6)*	165.3 (6.3)*	165.3 (6.7)	165.1 (5.4)
Weight (kg) [a]	84.3 (12.2)*	65.9 (12.0)*	66.4 (12.7)	64.7 (10.2)
Body Mass Index (kg/m^2) [a]	26.6 (3.9)*	24.1 (3.5)*	24.2 (3.7)	23.7 (2.9)
Hand Dominance:				
Right	90 %	91 %	89 %	96 %
Left	10 %	9 %	11 %	4 %
Medications:				
Birth control	0 %	32 %	44 %	0 %
HRT[b]	0 %	10 %	2 %	33 %
Vitamin D	2 %	6 %	6 %	4 %
Calcium	7 %	18 %	16 %	25 %
Multivitamins	12 %	24 %	25 %	21 %

[a] Data are expressed as mean (SD); *: Statistically significant differences between genders ($p < 0.001$).
[b] HRT: hormone replacement therapy.

As expected, men have significantly higher mean values for all measurements of cross-sectional bone area compared to those for all women and the subgroups. The CoBA index is larger in men compared to all women and the subgroup of postmenopausal women but not significantly different from the mean value for premenopausal women. No significant difference in bone geometry is observed between premenopausal and postmenopausal women.

TABLE 4.2

PQCT MEASUREMENTS OF INDICES OF BONE STRUCTURE, GEOMETRY, DENSITY AND MASS AT THE 4 % SITE IN STUDY SUBJECTS GROUPED ACCORDING TO GENDER AND MENOPAUSAL STATUS [a-k]

	Men	Women		
Variable	Total	Total [a,b,c]	Pre [d,e,f]	Post [g,h/ i,jk]
Structure:				
CI	9.78 (6.69)	5.12 (8.57)[b]	7.07 (7.11)[f]	-0.08 (10.00)[g, i]
H_A (mm^2)	1.34 (0.66)	2.31 (2.18)[b]	1.77 (1.25)[f]	3.86 (3.31)[g, i]
H_M (mm^2)	60.23 (35.84)	65.18 (35.87)	56.68(31.36)	86.07 (39.91)[h, j]
Geometry:				
ToBA (mm^2)	335.86 (49.37)	262.00 (42.68)[a]	259.68 (43.67)[d]	268.20 (40.16)[g]
CoBA (mm^2)	122.18 (13.29)	90.36 (9.42)[a]	91.35 (9.40)[d]	87.58 (9.12)[g]
TrBA (mm^2)	212.31 (41.50)	171.19 (37.87)[a]	168.33 (38.44)[d]	178.82 (35.97)[g]
CoBA index	36.89 (4.27)	35.04 (4.56)[c]	35.55 (4.44)	33.73 (4.69)[h]
Density:				
ToBD (mg/cm^3)	442.46 (54.61)	395.76 (65.99)[a]	414.19 (48.91)[e]	346.64(80.34)[g,i]
CoBD (mg/cm^3)	785.36 (65.23)	720.20 (104.4)[a]	749.79 (65.35)[e]	641.50(143.7)[g,i]
TrBD (mg/cm^3)	203.98 (36.47)	203.98 (36.47)[a]	212.21 (31.70)[d]	181.06(39.67)[g,i]
Mass:				
ToBMC (mg)	368.16 (49.66)	253.74 (38.08)[a]	263.96 (32.80)[d]	226.93(38.57)[g,i]
CoBMC (mg)	241.28 (40.10)	163.79 (31.27)[a]	171.55 (25.54)[d]	143.10 (36.0)[g, i]
TrBMC (mg)	125.69 (25.78)	84.87 (20.0)[a]	88.17 (19.80)[d]	76.07(18.12)[g, k]

Data are expressed as mean (SD). See text for description of bone variables. Pre: premenopausal women; Post: postmenopausal women. Significant differences between groups are indicated according to the following key:
men vs women - [a] $p < 0.001$, [b] $p < 0.01$, [c] $p < 0.05$;
men vs premenopausal women - [d] $p < 0.001$, [e] $p < 0.01$, [f] $p < 0.05$;
total men/post-menopausal women - [g] $p < 0.001$, [h] $p < 0.01$;
premenopausal women vs postmenopausal women - [i] $p < 0.001$, [j] $p < 0.01$, [k] $p < 0.05$.

Men have significantly greater values for all measurements of bone mass and density than the total group of women and each of the subgroups. Premenopausal women have significantly higher mean values for these variables than postmenopausal women.

4.3.2 Gender-Related Differences in Structure and Geometric Variables with Aging

All cross-sectionally calculated annual rates of change in structure variables are listed in Table 4.3 as slopes, whereas Figure 4.1 shows the individual values with the calculated regression equations and 95% confidence intervals. Figure 4.1A shows the age-dependent decrease in trabecular bone connectivity for both men and women. In men, CI decreases at a rate of 0.8% /yr, while in women the annual rate of decrease is 2.2%. Both of these rates of loss are significantly different from a zero rate ($p = 0.047$ and $p = 0.001$, respectively); however, the rate at which CI decreases in women is significantly greater than in men ($p < 0.001$). When women are categorized according to menopausal status, no significant age-dependent patterns of change in connectivity are identified.

Figure 4.1B shows age-related changes in H_A which increases at a rate of 0.8% /yr in men and 2.2% /yr in women. The increase in H_A is significantly different from a zero rate in women ($p < 0.01$) but not in men ($p = 0.10$). Again, there is no statistically significant age-dependent pattern of change in H_A when women are separated into premenopausal and postmenopausal groups.

Figure 4.1C shows the age-related changes in H_M for men and women. Men have no statistically significant age-related change ($p = 0.06$), while H_M increases in aging women at a rate of 1.1 % /yr ($p = 0.001$). Once more, no statistically significant age-dependent pattern of change is identified for H_M in the subgroups of premenopausal and postmenopausal women.

TABLE 4.3

REGRESSION OF INDICES OF BONE STRUCTURE AND GEOMETRY ON AGE[a]

Variables[a]		Men	Women			Comparisons of group slopes			
		Total	Total	Premenopausal	Postmenopausal	p*	p**	p***	p#
CI:	Slope	-0.11 (0.05)	-0.17 (0.05)	-0.08 (0.09)	+0.02 (0.24)	**<0.001**	0.06	**<0.001**	**0.003**
	p	**0.047**	**0.001**	0.33	0.93				
H_A: (mm_2)	Slope	+0.01 (0.01)	+0.04 (0.01)	-0.01 (0.02)	-0.05 (0.08)	**<0.001**	**<0.001**	**<0.001**	**<0.001**
	p	0.10	**0.005**	0.71	0.51				
H_M: (mm_2)	Slope	+0.54 (0.29)	+0.63 (0.21)	+0.16 (0.38)	-0.08 (0.97)	**0.036**	**<0.001**	**<0.001**	0.09
	p	0.06	**0.004**	0.67	0.94				
ToBA: (mm_2)	Slope	-0.37 (0.40)	+0.32 (0.26)	+0.29 (0.52)	+0.96 (0.94)	**<0.001**	**<0.001**	**<0.001**	**<0.001**
	p	0.36	0.22	0.58	0.32				
CoBA: (mm_2)	Slope	-0.25 (0.10)	-0.11 (0.06)	-0.09 (0.11)	-0.10 (0.24)	**<0.001**	**<0.001**	**<0.001**	0.86
	p	**0.019**	0.06	0.40	0.670				
TrBA: (mm_2)	Slope	-0.14 (0.34)	-0.70 (0.21)	+0.38 (0.46)	+0.67 (0.85)	**<0.001**	**<0.001**	**<0.001**	**0.048**
	p	0.68	0.12	0.41	0.44				
CoBA index:									
	Slope	-0.05 (0.04)	-0.05 (0.03)	-0.06 (0.05)	+0.00 (0.11)	0.07	**<0.042**	**0.008**	**<0.001**
	p	0.21	0.05	0.25	1.00				

[a]Variables as listed in the text. Slopes are reported as regression coefficient (SD). p: The p value gives the significance of the difference between the slope of the regression and a zero rate of change; Differences in the slope of the regression between groups are indicated by: p* men vs women; p** men vs premenopausal women; p*** men and postmenopausal women; p#: premenopausal vs postmenopausal women. Significant p values are shown in **bold**.

Figure 4.1 The individual values for indices of trabecular bone structure as a function of age in men and women. Fits to the linear regression line (—) are shown with 95% confidence intervals (– –). A: Connectivity Index (men, n = 57; women, n = 88). B: Mean Hole Size (men, n = 57; women, n = 85). C: Maximum Hole Size (men, n = 57; women, n = 87).

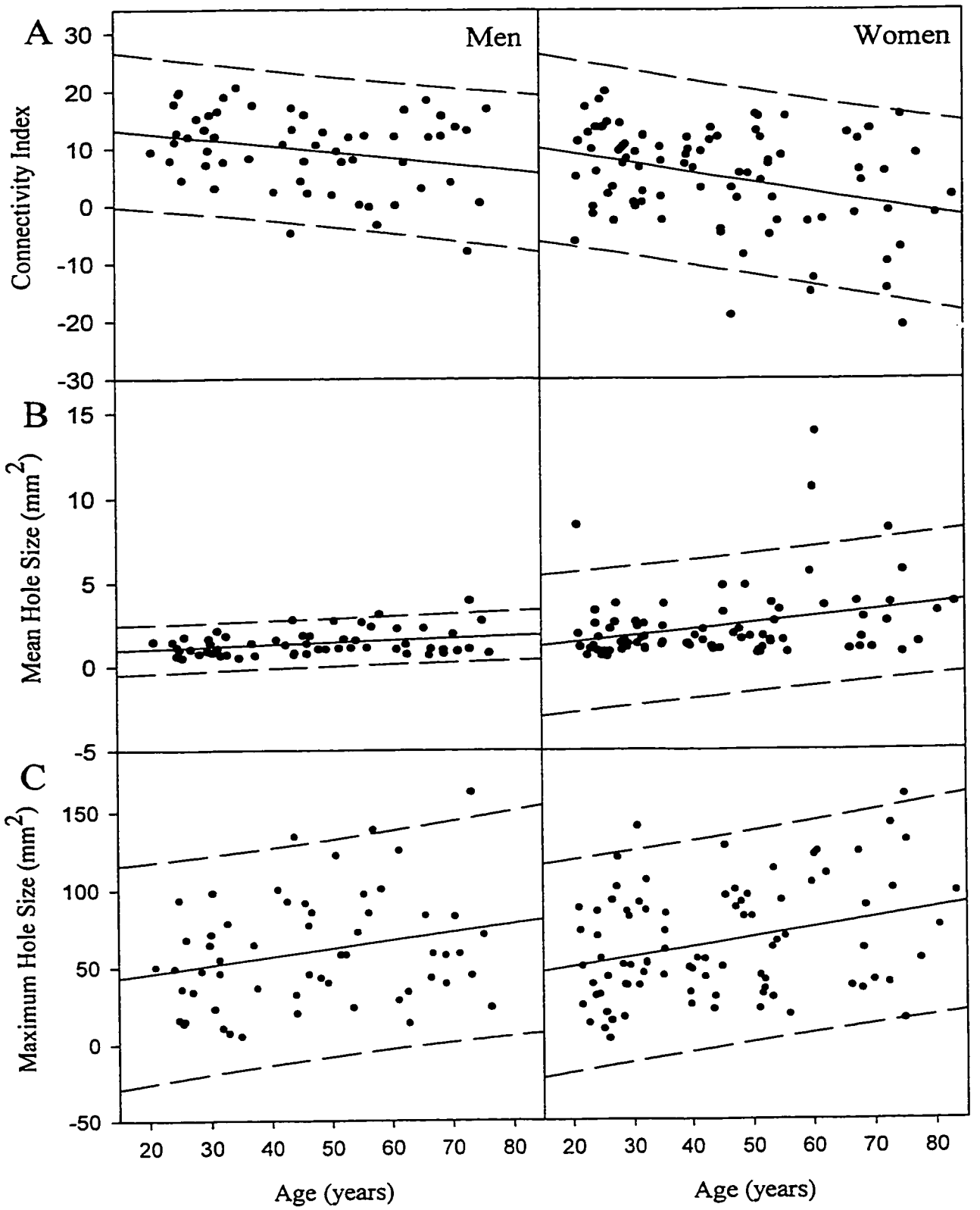
A
Men
Women
Connectivity Index
30
20
10
0
-10
-20
-30
B
Mean Hole Size (mm2)
15
10
5
0
-5
C
Maximum Hole Size (mm2)
150
100
50
0
-50
20
30
40
50
60
70
80
Age (years)
Age (years)

The rates of change for geometric variables are also reported in Table 4.3. In men, CoBA decreases by 0.2% /yr ($p = 0.019$). There are no statistically significant age-related changes in any other bone area variable in men or in women.

4.3.3 Gender-Related Differences in Bone Density and Mass with Aging

The rates of change for BD and BMC are shown in Table 4.4. For total bone, the age-dependent loss of ToBD is not significant for men ($p = 0.12$) but is significant for women (-0.4 % /yr, $p < 0.001$) and the subgroup of postmenopausal women (-1.1 % /yr, $p < 0.05$). For cortical bone, the rate of loss in CoBD is 0.2 % /yr in aging men and 0.4 % /yr in aging women. Both of these rates are significantly different from a zero rate ($p < 0.01$ and $p < 0.001$, respectively) and are significantly different from each other ($p < 0.001$). When the women are grouped according to menopausal status, no significant age-related change is observed in CoBD in premenopausal women. In contrast, CoBD decreases at an annual rate of 1.5 % ($p < 0.001$) in postmenopausal women. This rate of loss is significantly more pronounced than in men and in the group of all women ($p < 0.001$). For trabecular bone, age is not a significant predictor of TrBD in men ($p = 0.09$). In contrast to men, there is a significant annual decrease of 0.3% ($p < 0.01$) in TrBD in women, whereas the rate of loss in TrBD is not significantly different between premenopausal and postmenopausal women. These dramatic differences in rates of change between CoBD and TrBD and between premenoopausal and postmenopausal losses in CoBD are shown in Figure 4.2.

TABLE 4.4

REGRESSION OF INDICES OF BONE DENSITY AND MASS ON AGE[a]

		Men	Women			Comparisons of group slopes			
Variables[a]		Total	Total	Premenopausal	Postmenopausal	p*	p**	p***	p#
ToBD:	Slope	-0.70 (0.44)	-1.77 (0.36)	-0.24 (0.59)	-4.38 (1.69)	**<0.001**	**<0.001**	**<0.001**	**<0.001**
(mg/cm^3)	p	0.12	**<0.001**	0.69	**0.017**				
CoBD:	Slope	-1.58 (0.49)	-2.98 (0.56)	+0.18 (0.79)	-11.2 (2.48)	**<0.001**	**<0.001**	**<0.001**	**<0.001**
(mg/cm^3)	p	**0.002**	**<0.001**	0.82	**<0.001**				
TrBD:	Slope	-0.46 (0.30)	-0.70 (0.21)	-0.20 (0.38)	-0.05 (0.96)	**<0.001**	**<0.001**	**<0.001**	0.08
(mg/cm^3)	p	0.13	**0.002**	0.60	0.96				
ToBMC:	Slope	-0.98 (0.39)	-0.91 (0.21)	+0.11 (0.40)	-2.42 (0.77)	0.17	**<0.001**	**<0.001**	**<0.001**
(mg)	p	**0.014**	**<0.001**	0.78	**0.005**				
CoBMC:	Slope	-0.97 (0.30)	-0.78 (0.17)	-0.11 (0.31)	-2.20 (0.73)	**<0.001**	**<0.001**	**<0.001**	**<0.001**
(mg)	p	**0.002**	**<0.001**	0.71	**0.006**				
TrBMC:	Slope	-0.35 (0.21)	-0.21 (0.12)	+0.19 (0.24)	-0.02 (0.44)	**<0.001**	**<0.001**	**<0.001**	**0.007**
(mg)	p	0.10	0.09	0.44	0.97				

[a] Variables as listed in text. Slopes are reported as regression coefficient (SD). p: The p value gives the significance of the difference between the slope of the regression and a zero rate of change; Differences in the slope of the regression between groups are indicated by: p* men vs women; p** men vs premenopausal women; p*** men and postmenopausal women; p#: premenopausal vs postmenopausal women. Significant p values are shown in **bold**.

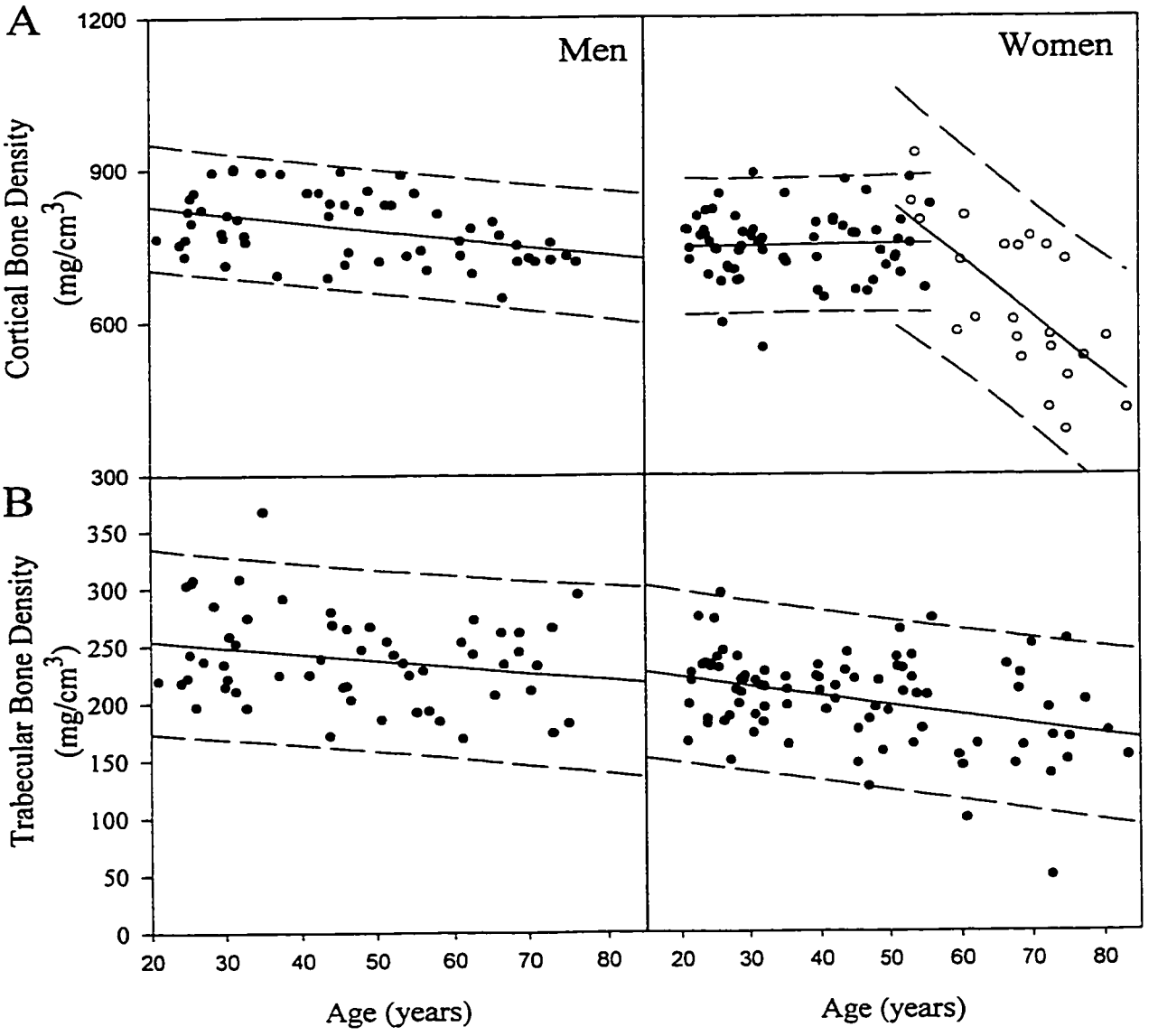

Figure 4.2 The individual values for bone density as a function of age in men and women. Fits to the linear regression line (—) are shown with 95% confidence intervals (– –). A: Cortical bone density (men, n = 57; women: premenopausal, n = 64, postmenopausal, n = 24). B: Trabecular bone density (men, n = 56; women, n = 87).

Both genders experience significant age-related losses in ToBMC (men, 0.3% /yr, $p = 0.01$; women, 0.3% /yr, $p < 0.001$) which are not significantly different from each other. The rate of loss in CoBMC in men is less pronounced than in the total group of women ($p < 0.001$), although the percent change is similar (0.4% /yr, $p < 0.01$ and 0.5% /yr, $p < 0.001$, respectively). In post-menopausal women, the rates of age-related loss in ToBMC (0.9 % /yr, $p < 0.01$) and CoBMC (1.3 % /yr, $p < 0.01$) are significantly more pronounced than in men or premenopausal women ($p < 0.001$, each). Neither gender experiences significant age-related changes in TrBMC (men, $p = 0.10$; women $p = 0.09$) in the nondominant radius.

4.4 Discussion

This is the first report of *in vivo* measurements at the 4 % site of the nondominant radius in Canadian adults using pQCT. The measurements determine the anticipated trends in gender differences and age-dependent patterns of bone structure, geometry, density and mass. The differences in gender-specific rates of loss of bone density are most apparent between men and the subgroup of postmenopausal women. This is consistent with the practice of using BMD values to determine osteoporotic fracture risk in postmenopausal women.

These data suggest that the age-related loss of bone density in the cortical and trabecular bone compartments is heterogeneous in healthy men and homogeneous in healthy women. In men, the age-related loss in CoBD is significant (although less

pronounced than in women), while no age-related decrease in TrBD is observed. In women, significant age-related annual losses in both CoBD and TrBD (0.4% and 0.3%, respectively) are observed. The decrease in TrBD in aging women is not accompanied by a decrease in TrBMC but is observed in association with a decrease in cortical bone mass and density. This supports the concept of trabecularization of the endosteal surface of the cortical bone compartment which has been described by others (Gatti et al. 1996). This phenomenon is not observed for the men in this study.

In both sexes, when expressed as an annual percent change, indices of trabecular bone structure change to a greater extent than indices of bone mass and density. More importantly, the *in vivo* measurements of structure appear biologically sensible when considered in the context of the available literature. *In vivo* measurements of connectivity of trabecular bone at the distal radius demonstrate age-related decreases which are more pronounced in women. This decrease in intertrabecular connectivity may result from an age-related loss of entire structural elements which is consistent with the findings of *ex vivo* studies of biopsied human iliac crest (Parfitt et al. 1983) and cadaver specimens of vertebral body trabeculae (Mellish, Garrahan, and Compston 1989; Vesterby et al. 1989). Also, the CI value may decrease due to the age-related imbalance in bone resorption and formation during remodeling resulting in the perforation of progressively thinning trabeculae as described for necropsied vertebral trabecular bone specimens (Mosekilde 1989). Such perforations would result in an increase in the number of free ends and isolated points without reducing the measured length of the trabecular bone network.

H_A values reflect the mean distance between trabecular struts. The significant age-related increase in H_A observed in 85 women is 2.2% per year, whereas no significant age-related increase is observed in 56 men. This is the only variable for which the results were significantly altered when the outlying values were included in the analysis. In women, the mean (SD) H_A for the 3 outlying values (acquired from 1 premenopausal and 2 postmenopausal women) is 43.39 (6.75) mm^2 as compared to the group mean of 2.31 (2.18) mm^2 when these values are excluded. When these values are included, H_A increases at a rate of 7.2% /yr. In men, one H_A value (3.93 mm^2) was identified as an outlier and the group mean is 1.34 (0.66) when this value is excluded. The inclusion of this value results in a significant age-related increase in H_A in men ($p = 0.028$), although still less pronounced than in women ($p < 0.001$). One of the postmenopausal women with an outlying value for H_A, also had outlying values for H_M and TrBD. These outlying values are clearly different and may reflect the difficulty in identifying a 'normal' population. It may be that the recent onset or the presence of asymptomatic medical conditions may have effected skeletal health. When these values are excluded from the analysis, a conservative estimate of the annual increase in H_A is 2.2% in women and 0% in men. This suggests that there is a significant age-related increase in the distance between trabecular struts in the transverse plane at the 4 % site of the distal wrist in women but not in men.

Mosekilde (1988, 1989) found a steady increase in the distance between horizontally oriented vertebral trabeculae which was slightly more pronounced in aging women than

aging men and an age-related thinning of horizontal trabeculae which was observed in both sexes. As muscle strength declines with aging, the decrease in mechanical loading at the distal radius may be evidenced by a decrease in trabecular thickness which we detect as an increase in H_A.

Alternatively, little change may occur in mean trabecular thickness, as is the case in transiliac biopsies (Parfitt et al. 1983; Mellish, Garrahan, and Compston 1989), and the age-related increase in H_A may reflect the loss of entire trabecular structural elements or perforations of trabecular plates creating some very large holes which result in a small increase in the average hole size observed in the transverse plane. This explanation appears to be supported by the significant age-related increase in H_M observed in women. This may reflect a gender-specific increase in perforations of the trabecular network creating larger marrow spaces. A similar gender difference in perforation rates in horizontally oriented vertebral trabeculae was reported for women over the age of 75 years (Mosekilde 1989). In men, the rate of increase in H_M is not significantly different from a zero rate ($p = 0.06$) but this may be because this study lacked the power to detect a small age-related change.

In aging men, CI and CoBA decrease while no significant changes in H_A, H_M, ToBA, TrBA or CoBA index are detected. Again, a larger sample size may have revealed statistically significant endosteal resorption (evidenced by increased TrBA) or periosteal expansion (as evidenced by increased ToBA). In women, our indices of trabecular bone

structure (CI, H_A and H_M) were responsive to aging, while no age-related changes in gross geometry were detected.

Gatti et al. (1996) used pQCT to measure the cross-sectional bone area at the distal radius in 270 women (241 postmenopausal women aged 45 to 78 years; 29 premenopausal women aged 32 to 40 years) and found a significant age-related increase in TrBA of 0.31 mm^2 /yr but the change in CoBA and ToBA did not reach statistical significance. The ToBA at the distal radius measured in 583 women (aged 40 to 60 years) using pQCT increased significantly with age at a rate of 1.25 mm^2 /yr (Wapniarz et al. 1997). TrBA and CoBA were not reported in the latter study but it is apparent that large numbers of individuals need to be studied in order for the changes in cross-sectional bone area to reach statistical significance. A much larger sample size is required to detect any true compensatory increase in total bone diameter to maintain bone strength, suggesting that this beneficial adaptation is not commonly observed at an individual level. Our study shows that the indices of trabecular bone structure are more sensitive to age-related changes than measurements of bone area or CoBA index for both men and women.

Distal radial fractures occur in women around the time of menopause which suggests that there are changes in bone which are occurring as women are approaching menopause. Indices of trabecular bone structure demonstrate significant age-related changes which occur across the life span in adult women. Connectivity, as determined by CI, decreases at a rate of 2.2% /yr, H_A enlarges at a rate of 2.2 % /yr and H_M increases by 1.1% /yr. In contrast, the percentage of ToBD, CoBD and TrBD lost per year is 0.4%, 0.4% and 0.3%

respectively, with greater annual rates of loss in ToBD and CoBD following menopause. Thus, the assessment of structural indices of trabecular bone structure may improve our ability to identify individuals at risk for fractures of the distal radius, the earliest clinical manifestation of osteoporosis.

CHAPTER FIVE

IMPACT OF DIFFERENTIAL LOADING ASSOCIATED WITH HAND DOMINANCE ON BONE STRUCTURE AND DENSITY[1]

5.1 Introduction

Mechanical loading, by means of muscle activity and anti-gravity weight bearing, is critical to the development and maintenance of strong bones (Garn 1972; Johnston and Slemenda 1993; Kannus, Sievänen, and Vuori 1996; Ferretti et al. 1998). The human skeleton must withstand the repeated and varied loads experienced in normal activities as well as any unexpected impact loads. Habitual loading patterns give rise to adaptations in bone mass and structure to achieve the required bone strength (Biewener et al. 1996; Lanyon 1996).

The positive relation between physical activity and bone mass has been well established in cross-sectional studies (Chilibeck, Sale, and Webber 1995). Additionally,

---

[1] This work has been accepted for publication in the following manuscript: MacIntyre NJ, Adachi JD, Webber CE. Structural differences between dominant and nondominant radii are detected *in vivo* using peripheral quantitative computed tomography. Journal of Clinical Densitometry 1999; 2 (4): in press. The data are reprinted here with permission from The Humana Press, Inc. (Appendix 1).

the influence of physical activity on bone mass has been studied using comparisons between limbs within subjects thus controlling for the confounding effects of genetic, hormonal and nutritional factors encountered in cross-sectional studies (Haapasalo et al. 1994; Kannus et al. 1994; Rico et al. 1994; Alfredson, Nordström, and Lorentzon 1997; Walters et al. 1998). Significant differences in bone mass between the dominant and nondominant arms are seen in athletes who play racquet sports (Haapasalo et al. 1994; Kannus et al. 1994). Also, bone mass of the upper extremities of sedentary, healthy adults are significantly different between arms although the magnitude of the difference is less pronounced (Haapasalo et al. 1994; Kannus et al. 1994; Rico et al. 1994; Alfredson, Nordström, and Lorentzon 1997; Walters et al. 1998). Greater bone mass in the dominant limb may be a natural anthropometric asymmetry or it may represent the long-term influences of greater mechanical loading.

How physical activity affects bone mass is controversial. By measuring areal bone mineral density at various regional sites, some investigators report a homogeneous influence of exercise on cortical and trabecular bone (Pocock et al. 1989; Kannus et al. 1994). Others report the influence of physical activity is heterogeneous with the affected variable being only trabecular bone mass (Colletti et al. 1989; Vico et al. 1995) or only cortical bone mass (Tsuji et al. 1995; Nordström, Nordström, and Lorentzon 1997). Trabecular and cortical bone compartments can be analyzed separately using peripheral quantitative computed tomography (pQCT) imaging (Gasser 1995). With this technique, Rico et al. (1994) report that differential loading of the upper limbs as a function of hand dominance results in significant differences in the cortical bone compartment of the distal

radii, but not in the trabecular bone compartment. Despite differences between limbs, assessment of bone mineral density by x-ray based dual photon absorptiometry in the contralateral hip of individuals with recent hip fractures provided the best discrimination between patients with and without fracture (Augat et al. 1998).

Images of the distal radius obtained using pQCT can be analyzed to determine bone mass and indices of bone structure which quantify the intertrabecular connectivity and spacing (Gordon et al. 1996). These structural indices are significant predictors of bone strength (Gordon, Webber, and Nicholson 1998). Preliminary results indicate that measures of trabecular bone structure in the contralateral distal radius are significantly different from expected values in individuals who have sustained an osteoporotic wrist fracture (Gordon et al. 1996). As a first step, it is important to characterize the typical differences in these bone variables between the dominant and nondominant arms. Therefore, the twofold purpose of this cross-sectional study is:

1) to identify differences in indices of trabecular bone structure related to normal differential use of the dominant upper extremity; and

2) to determine whether measurements of these indices in one limb serve as satisfactory surrogates for the contralateral limb.

5.2 Materials and Methods

5.2.1 Subjects

A subgroup of the men and women, aged 20 to 83 years, who volunteered to participate in the study described in Chapter 4 (section 4.2.1), were invited to participate.

Informed consent was obtained from 114 subjects (43 men and 71 women). The study was approved by the McMaster University Research Ethics Board.

5.2.2 Procedure

Subjects completed a questionnaire to document age, sex, race, height, weight, hand dominance, menopausal status and a general health/medical history profile as previously described (section 4.2.1). The distance from the olecranon process to the ulnar styloid was measured to the nearest 0.1 cm on the dominant and nondominant forearms of each subject. Consecutive scans were performed at the 4 % site of the distal radius for both the dominant and nondominant forearm of each subject within an average of about 15 minutes according to the procedure described in section 3.2.3.

5.2.3 Equipment

Images were acquired using the Stratec XCT-960 pQCT scanner as described in section 3.2.3. The radiation dose associated with the total scanning procedure is low (0.4 mSv).

The images were postprocessed and analyzed using in-house developed software (Gordon et al. 1996) to quantify indices of trabecular bone structure, including connectivity index (CI), maximum hole size (H_M) and mean hole size (H_A). The same images were also analyzed with the commercial software (version 5.2, Stratec) to determine volumetric bone density for total bone (ToBD, mg/cm^3), cortical bone (CoBD, mg/cm^3) and trabecular bone (TrBD, mg/cm^3). In addition, this software calculated total

bone area (ToBA, mm^2) and bone area of the cortical and trabecular compartments, CoBA (mm^2) and TrBA (mm^2) respectively. A cortical bone area index (CoBA index) was derived by dividing CoBA by ToBA. This index provides an estimate of the thickness of the cortical shell (Bouxsein et al. 1994). Bone mineral content (mg) at the 4% site of the distal radius is described for total, cortical and trabecular bone compartments (ToBMC, CoBMC, and TrBMC, respectively) and was calculated as the product of density and area in each bone compartment and image slice thickness.

The software was unable to close the cortical ring in one or both of the images for 8 volunteers (5 men and 3 women) between the ages of 63.6 and 72.4 years (mean age [SD], 68.9 [2.8] years); therefore, these pairs of images were excluded from further analyses.

5.2.4 Statistical Analyses

Descriptive statistics were calculated for anthropometric measurements of the study subjects and all measured variables of bone structure, geometry, mass and density. The mean difference between the dominant and nondominant radius was calculated for each variable. Results which were more than 3 SD from the mean were identified as outliers. The data was analyzed with and without outliers. The results are shown with the outliers excluded from analysis. No outlying values were identified for H_M, ToBA, ToBD and CoBD. For six subjects, the between-limb difference was more than 3 SD from the total group mean difference for one or more (maximum of 4) bone variables. Thus, the between-limb difference in CI, CoBA, TrBA, CoBA index, ToBMC and TrBD is

reported for 105 subjects. The comparison between limbs for H_A and CoBMC is reported for 104 subjects and the between-limb difference in TrBMC is reported for 103 subjects. The side-to-side measurements of bone variables were compared using the two - tailed paired t-test. The strength of association between the side-to-side measurements was calculated using the Pearson Product Moment Correlation for parametric data and the Spearman Rank Order Correlation for nonparametric data. The statistical results have been calculated using the statistical package, Minitab (release 11). Differences were considered significant when $p < 0.05$.

5.3 Results

5.3.1 Subject Characteristics

Bilateral images of the distal radii of 106 volunteers were considered to be satisfactory for analysis and the characteristics of these subjects are summarized in Table 5.1.

TABLE 5.1

CHARACTERISTICS OF SUBJECTS

Variables	Participants (n = 106)
Age (years) [a]	44.3 ± 17.5 (21.0, 83.33)
Height (cm) [a]	170.3 ± 9.0 (151.0, 190.5)
Weight (kg) [a]	72.1 ± 14.0 (47.7, 109.0)
Body Mass Index (kg/m^2) [a]	24.7 ± 3.4 (18.2, 36.0)
Right Handed	91 %
Female	64 %
Postmenopausal	20 %

[a] Data are expressed as mean ± SD (minimum, maximum).

5.3.2 Between-Limb Differences in Bone Structure and Geometry

Table 5.2 summarizes the side-to-side differences at the 4% site of the distal radii with respect to bone structure and geometry. For all subjects, H_M is significantly smaller in the dominant radius ($p < 0.01$). No other structure or geometry variable demonstrates a significant between-limb difference for the total study group. For the subgroup of right handed subjects, connectivity is greater and maximum hole diameter is smaller in the

TABLE 5.2

BETWEEN-LIMB DIFFERENCES IN BONE VARIABLES[a,b]

Bone Variables[a]	Mean Difference (p value)[b]		
	Total Group (n = 106)	Right Handed Subjects (n = 96)	Left Handed Subjects (n = 10)
Structure:			
CI	+0.80 (0.06)	+1.03 **(0.02)**	-1.42 (0.43)
H_M (mm^2)	-5.44 **(0.006)**	-5.85 **(0.005)**	-1.57 (0.78)
H_A (mm^2)	+0.03 (0.87)	-0.05 (0.79)	+0.70 (0.28)
Geometry:			
ToBA (mm^2)	+0.55 (0.79)	+0.93 (0.68)	-3.04 (0.56)
CoBA (mm^2)	+0.48 (0.60)	+0.51 (0.60)	+0.26 (0.94)
TrBA (mm^2)	-1.31 (0.46)	-1.10 (0.57)	-3.32 (0.38)
CoBA index	+0.0005 (0.88)	+0.0002 (0.95)	+0.003 (0.79)
Mass:			
ToBMC (mg)	+4.64 **(0.004)**	+5.44 **(0.001)**	-2.96 (0.57)
CoBMC (mg)	+3.18 **(0.024)**	+3.50 **(0.017)**	+0.22 (0.97)
TrBMC (mg)	+0.32 (0.79)	+0.70 (0.58)	-3.18 (0.42)
Density:			
ToBD (mg/cm^3)	+5.56 **(0.04)**	+5.86 (0.05)	+2.68 (0.59)
CoBD (mg/cm^3)	+9.70 (0.08)	+10.35 (0.07)	+3.44 (0.86)
TrBD (mg/cm^3)	+4.64 (0.47)	+1.92 (0.29)	-5.07 (0.45)

[a] See text for explanation of abbreviations.
[b] Significant p values shown in **bold**.

dominant radius ($p < 0.05$ and $p < 0.01$, respectively). There is no significant difference between limbs for the average hole size or bone geometry. For the subgroup of left handed subjects, there were no statistically significant differences between limbs.

5.3.3 Between-Limb Differences in Bone Mass and Density

Table 5.2 also summarizes the comparison between limbs with respect to radial bone mass and density. For the total group, the dominant limb has a greater mass (ToBMC, $p < 0.01$ and CoBMC, $p < 0.05$), and a greater volumetric density (ToBD, $p < 0.05$). Similarly, in the dominant limb of right handed subjects there is a greater mass (ToBMC, $p < 0.01$ and CoBMC, $p < 0.05$), and ToBD tends to be greater ($p = 0.05$). Again, there are no statistically significant differences between limbs for the group of left handed subjects.

Figure 5.1 illustrates the greater association between side-to-side differences in ToBD and CoBD ($r = 0.77$; 95% CI: 0.69 to 0.85) than between side-to-side differences in ToBD and TrBD ($r = 0.37$; 95% CI : 0.20 to 0.54). Therefore, the between-limb difference in ToBD reflects the difference in the cortical bone compartment more than the difference in the trabecular bone compartment.

5.3.4 Impact of Aging on Between-Limb Differences in Bone Variables

To determine whether the duration of differential loading of the arms has any influence, the variables which are significantly different between limbs were examined as a function of age. Figure 5.2A shows that connectivity in the group of right handed

subjects is greater in the dominant limb and this difference does not increase with age ($r = 0.15$, $p = 0.14$). Figure 5.2B shows that the maximum marrow pore size is smaller in the dominant distal radius for the total group of subjects and this between-limb difference is more pronounced with age ($r = -0.17$, $p = 0.03$). Figure 5.3A and 5.3B show that both total and cortical bone mass are greater in the dominant limb and this difference is not associated with aging ($r = +0.016$, $p = 0.88$ and $r = +0.025$, $p = 0.81$, respectively). Likewise, Figure 5.4 shows that total bone density is greater in the dominant limb and this difference also shows no dependence on age ($r = +0.062$, $p = 0.53$).

5.3.5 Association of Mean Values for Bone Variables and the Between-Limb Difference

Table 5.3 shows the relations of both the differences (dominant - nondominant) between and the absolute differences (| dominant - nondominant |) between limbs as a function of the mean values for each variable. None of the between-limb differences showed a significant association with the mean values. For the structural variables, as mean connectivity increases, the absolute between-limb difference in connectivity decreases significantly ($p < 0.01$). The absolute difference in H_M has no significant association with mean H_M ($p = 0.12$). As mean H_A increases the absolute difference in H_A increases ($p < 0.01$). Similarly, subjects with higher mean ToBA, TrBA and CoBA index have greater absolute between-limb differences in these variables ($p = 0.01$, $p < 0.01$ and $p = 0.03$, respectively). No relation is observed between mean CoBA and the absolute difference in CoBA ($p = 0.22$).

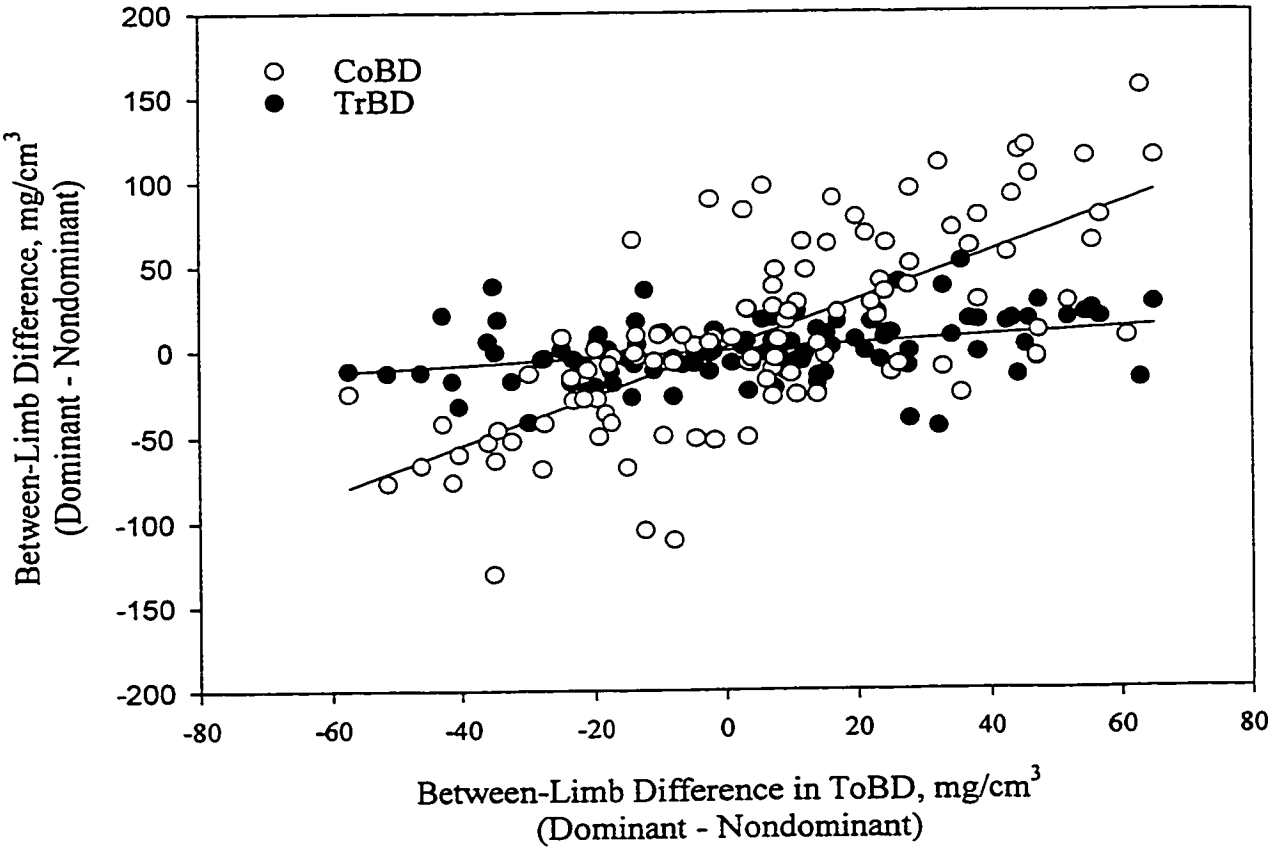

Figure 5.1 Linear regression analysis of the relation of both the between-limb difference in cortical bone density (o , CoBD) and the between-limb difference in trabecular bone density (• , TrBD) with the between-limb difference in total bone density (ToBD). The straight lines (—) represent the fits to linear regression equations.

Figure 5.2 Linear regression analysis of the individual between-limb differences (dominant - nondominant) in indices of bone structure as a function of age. Fits to regression equations are shown (—). A: Between-limb difference in Connectivity Index (CI) for right handed subjects (n = 95). B: Between-limb difference in Maximum Hole Size (H_M) for all subjects (n = 106).

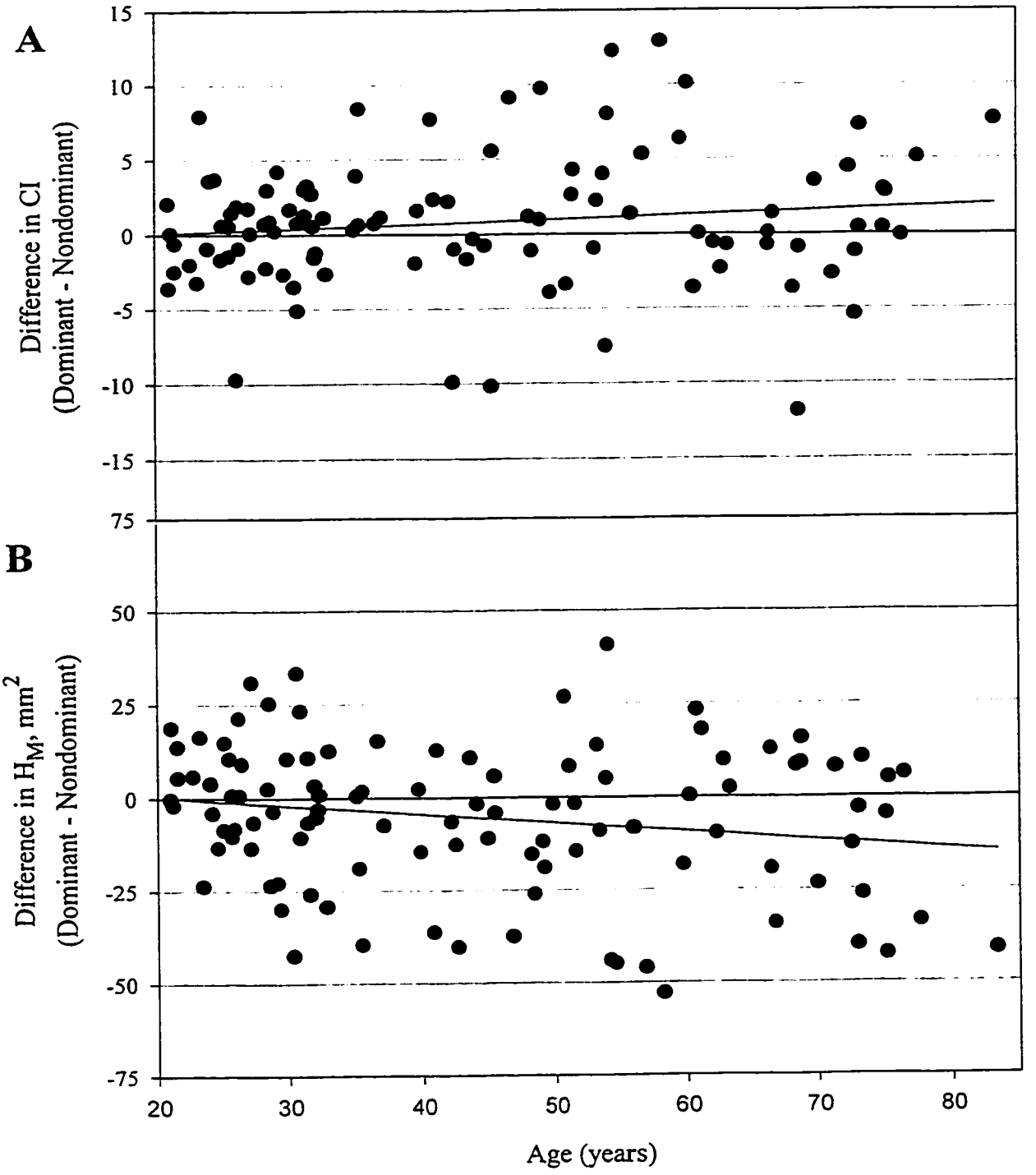
A
B
Difference in CI
(Dominant - Nondominant)
Difference in H_M, mm^2
(Dominant - Nondominant)
15
10
5
0
-5
-10
-15
75
50
25
0
-25
-50
-75
20
30
40
50
60
70
80
Age (years)

Figure 5.3 Linear regression analysis of the individual between-limb differences (dominant - nondominant) in bone mass as a function of age. Fits to regression equations are shown (—). A: Between-limb difference in total bone mineral content (ToBMC) for all subjects (n = 105). B: Between-limb difference in cortical bone mineral content (CoBMC) for all subjects (n = 104).

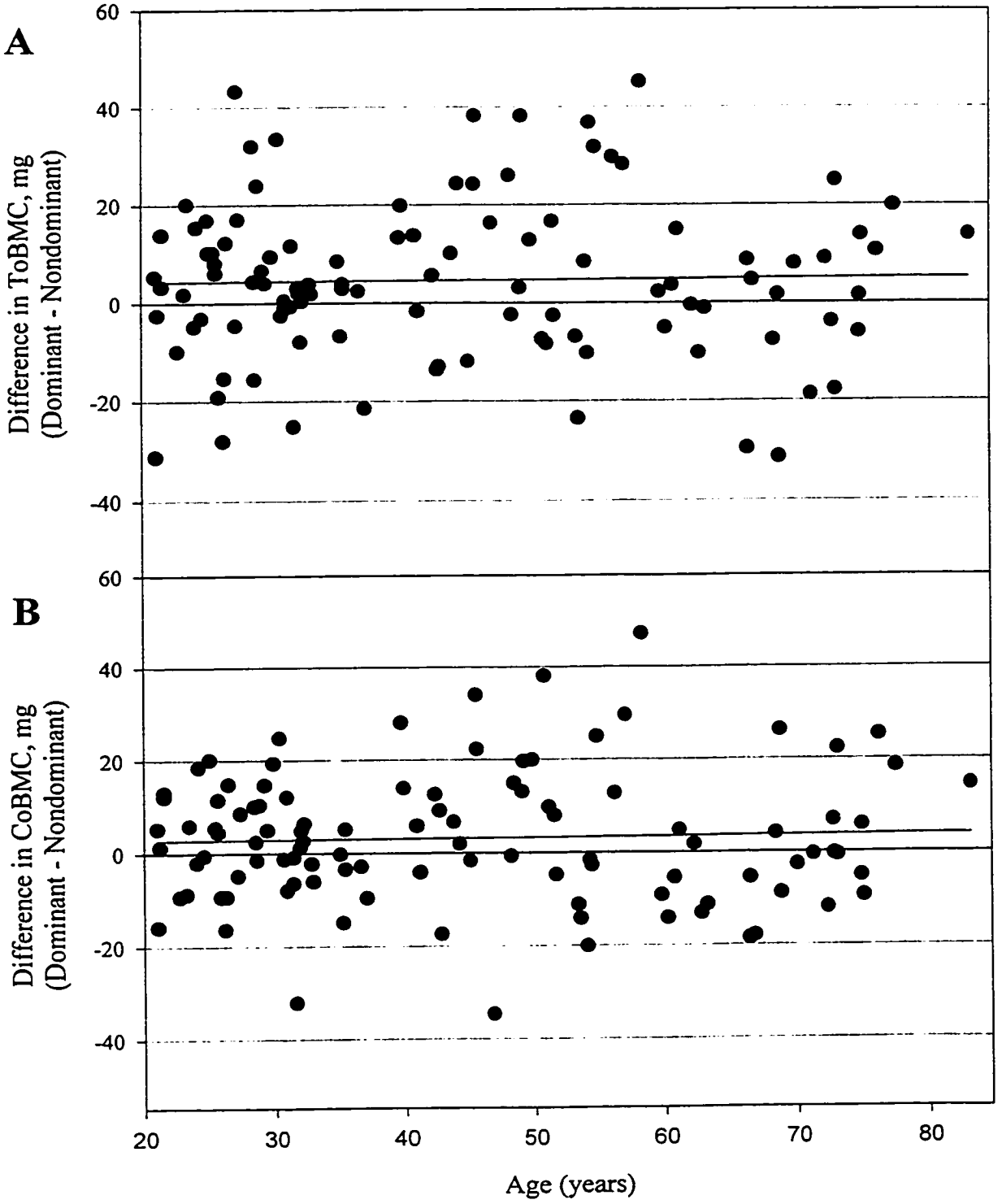
A
Difference in ToBMC, mg
(Dominant - Nondominant)
60
40
20
0
-20
-40
B
Difference in CoBMC, mg
(Dominant - Nondominant)
60
40
20
0
-20
-40
20
30
40
50
60
70
80
Age (years)

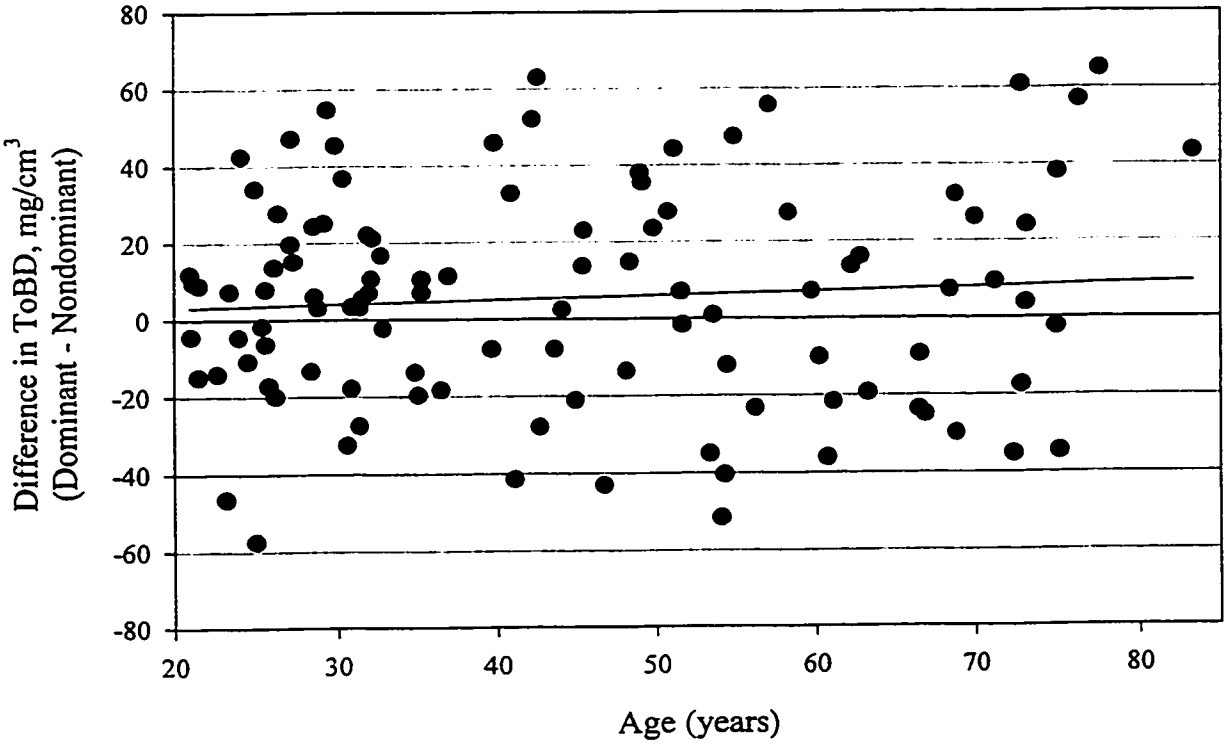

Figure 5.4 Linear regression analysis of the individual between-limb differences (dominant - nondominant) in total bone density (ToBD) as a function of age for all subjects (n = 106). The straight line (—) represents the fits to the linear regression equation.

TABLE 5.3

CORRELATION COEFFICIENTS FOR THE ASSOCIATION OF MEAN VALUES FOR BONE VARIABLES WITH THE ACTUAL AND WITH THE ABSOLUTE BETWEEN-LIMB DIFFERENCES[a-d]

	Correlation with Mean Value[b], r[c] (p value)[d]	
Bone Variables[a]	Difference	Absolute Difference
Structure:		
CI	+ 0.040 (0.68)	- 0.269 **(0.006)**
H_M (mm^2)	- 0.027 (0.78)	+0.151 (0.12)
H_A (mm^2)	- 0.005 (0.96)	+0.721 **(<0.001)**
Geometry:		
ToBA (mm^2)	+ 0.007 (0.94)	+0.238 **(0.01)**
CoBA (mm^2)	+ 0.093 (0.34)	+0.121 (0.22)
TrBA (mm^2)	- 0.037 (0.70)	+0.303 **(0.002)**
CoBA index	- 0.057 (0.56)	+0.213 **(0.03)**
Mass:		
ToBMC (mg)	+ 0.158 (0.11)	+ 0.262 **(0.007)**
CoBMC (mg)	+ 0.014 (0.89)	+0.029 (0.77)
TrBMC (mg)	+ 0.095 (0.34)	+ 0.055 (0.58)
Density:		
ToBD (mg/cm^3)	- 0.125 (0.20)	- 0.173 (0.08)
CoBD (mg/cm^3)	- 0.105 (0.28)	- 0.173 (0.08)
TrBD (mg/cm^3)	+ 0.146 (0.14)	- 0.089 (0.37)

[a] See text for description of bone variables
[b] mean value = (value for the dominant radius + value for the nondominant radius)/2.
[c] correlation coefficient calculated using the Spearman Rank Order Correlation for variables with residuals which are not normally distributed and/or have non-constant variances. The Pearson Product Moment Correlation was computed for the rest of the variables.
[d] Significant p values are shown in **bold**.

Subjects with higher mean ToBMC have greater absolute between-limb differences in ToBMC ($p < 0.01$). In contrast, absolute between-limb differences in bone mass in the cortical and trabecular bone compartments are not associated with mean CoBMC and

mean TrBMC values ($p = 0.77$ and $p = 0.58$, respectively). The absolute between-limb difference in bone density has no significant association with mean bone density values.

5.3.6 Measurements of Bone Variables as Surrogates for Assessing the Contralateral Limb

The correlation coefficients describing the association between variables measured in the dominant and nondominant limb are shown in Table 5.4. As expected, significant associations exist for side-to-side measurements of bone structure and geometry ($p < 0.001$). The variance of indices of trabecular bone structure in one radius explains 72% (H_M) to 76% (H_A) of the variance of the measurements at the 4% site in the contralateral limb. Geometric bone variables measured in one limb explain between 44% (CoBA index) to 86% (ToBA) of the variation in the same geometric measurement in the contralateral limb. As well, the variables describing bone mass and density in the dominant and nondominant distal radius are significantly associated ($p < 0.001$).Values for BMC are strongly associated and measurements in one arm explain between 87% (TrBMC) to 95% (ToBMC) of the variance in the measurements of bone mass in the other arm. Similarly, the variance in measurements of ToBD, CoBD and TrBD in one radius explain large fractions of the variance in the measurements for the other radius (81%, 54% and 85% respectively).

TABLE 5.4

CORRELATION OF SIDE-TO-SIDE MEASUREMENTS OF BONE STRUCTURE, GEOMETRY, MASS AND DENSITY AT THE 4% SITE OF THE DISTAL RADIUS[a,b]

Bone Variables[a]	r [b] (95% Confidence Interval)
Structure:	
CI	+0.86 (0.82, 0.91)
H_M (mm^2)	+0.85 (0.79, 0.90)
H_A (mm^2)	+0.87 (0.82, 0.92)
Geometry:	
ToBA (mm^2)	+0.93 (0.91, 0.95)
CoBA (mm^2)	+0.82 (0.75, 0.88)
TrBA (mm^2)	+0.91 (0.87, 0.95)
CoBA index	+0.66 (0.54, 0.78)
Mass:	
ToBMC (mg)	+0.98 (0.97, 0.99)
CoBMC (mg)	+0.95 (0.93, 0.97)
TrBMC (mg)	+0.93 (0.91, 0.95)
Density:	
ToBD (mg/cm^3)	+0.90 (0.86, 0.94)
CoBD (mg/cm^3)	+0.73 (0.64, 0.82)
TrBD (mg/cm^3)	+0.92 (0.90, 0.94)

[a] See text for description of bone variables.

[b] Correlation coefficient calculated using the Spearman Rank Order Correlation for variables with residuals which are not normally distributed and/or have non-constant variances (CI, H_M, H_A, CoBA, CoBD). The Pearson Product Moment Correlation was computed for the rest of the variables. All correlation coefficients are statistically significant at $p < 0.001$.

5.4 Discussion

This study identifies differences in indices of trabecular bone structure which may be related to normal differential use of the dominant upper extremity. The maximum spacing of the trabecular elements is smaller and the connectivity is better (in right handed subjects at least) in the dominant distal radius. The age-dependency of the between-limb difference in maximum hole size (Figure 5.2B) suggests that H_M becomes

progressively greater in the nondominant radius with aging. This is consistent with the age-related increase in H_M observed in women in the study presented in Chapter 4. The significant increase in the magnitude of the difference between limbs with respect to maximum hole size suggests that the differential pattern of habitual use of the dominant arm preserves bone structure. Thus the structural integrity is preserved in the dominant limb, although the geometry, amount and density of mineralized bone in the trabecular compartment of the radius is similar in both limbs.

The significantly greater bone mass in the total and cortical bone compartments in the dominant radius observed in this study (Table 5.2) is consistent with the findings of others (Haapasalo et al. 1994; Kannus et al. 1994; Rico et al. 1994; Alfredson, Nordström, and Lorentzon 1997; Walters et al. 1998). The side-to-side difference in BMC in the distal radius of athletes is greater than the difference in bone density suggesting that physical loading results in increased bone size (Haapasalo et al. 1994; Kannus et al. 1994). Walters et al. (1998) used x-ray based dual photon absorptiometry to investigate the effect of hand dominance on bone mass in 213 healthy sedentary young women and found significantly higher BMC in the dominant distal radius but no between-limb difference in BMD (total region: $p = 0.099$). Rico et al. (1994) used pQCT to evaluate between-limb differences in bone density and determined that the dominant distal radius has a greater volumetric bone density in the cortical bone compartment but is not different from the nondominant distal radius in the trabecular compartment at the 4% site. Similarly, the data presented in this chapter shows that the radius in the dominant limb has a greater ToBD and this most likely reflects differences in the cortical bone

compartment given the stronger association between differences in ToBD and CoBD than between differences in ToBD and TrBD (Figure 5.1). Also, the total bone mass was greater in the dominant limb and this difference was present in the cortical bone compartment. Investigators measuring areal bone mineral density at various regional sites have reported conflicting findings regarding the type of bone affected by physical loading (Colletti et al. 1989; Pocock et al. 1989; Kannus et al. 1994 Tsusi et al. 1995; Vico et al. 1995; Nordström, Nordström, and Lorentzon 1997) and this may be a limitation of the technique since it is not possible to examine the two bone compartments separately. While the results reported here show no significant differences in trabecular bone density and mass between the dominant and the nondominant limbs at the distal radius, structural differences in the trabecular bone network suggest that bone strength is better preserved in the dominant limb.

The mean marrow pore size is not significantly different between limbs (Table 5.2). In fact, the values are very similar between limbs and among the entire group of healthy study subjects. The variability of the values increases as the mean hole size increases but the actual between-limb differences which were measured were not affected in any systematic way (Table 5.3). The relation between each subject's mean H_A value and the absolute difference in H_A between limbs is significant. Eleven out of 104 subjects had a mean H_A of 4 mm^2 or more (4.01 to 12.08 mm^2) and the absolute differences between limbs varied from 0.49 mm^2 to 7.72 mm^2 (data not shown). If we assume that the holes are circular and the maximum absolute difference in H_A (7.72 mm^2) is associated with a maximum hole area in the dominant limb of 13.5 mm^2 then the difference in hole

radii between limbs will be only 0.71 mm. Therefore, a small difference in hole radius produces a difference of 7.72 mm^2 and the relatively few individuals with mean H_A values greater than 4 mm^2 have a large influence on the absolute difference between limbs in H_A. This measure of trabecular bone structure may be more discriminating in individuals with bone disorders.

The absolute between-limb differences are associated with the mean value for structure (CI for right handed subjects and H_A), geometry (ToBA, TrBA, CoBA index) and mass (ToBMC) variables (Table 5.3). Individuals with poor trabecular connectivity and large average marrow pore sizes will have greater absolute between-limb differences. The data in Chapter 4 shows that connectivity in the trabecular bone at the 4 % site in the nondominant distal radius in men and women decreases with age and both H_M and H_A demonstrate an age-related increase at this site in women. One might speculate that the difference between limbs would be more apparent with age and could reflect a measurement bias given this association between absolute differences and mean values. However, any age-related decrease in CI is not associated with an increase in the magnitude of the difference in connectivity between limbs (Figure 5.2A). Age is associated with an increase in H_M and an increase in the magnitude of the between-limb difference (Figure 5.2B). However, the magnitude of the absolute difference in H_M between limbs is not associated with the subject's mean value for H_M (Table 5.3). The significant age-dependent increase in H_M may reflect the influence of increased differential loading of the dominant limb throughout the lifespan as discussed above. No significant between-limb differences were observed for H_A; therefore, the positive

association between absolute side-to-side differences and mean values for H_A does not influence the findings. The other variables which demonstrate an association between absolute differences and mean values are either not significantly different between limbs (ToBA, TrBA, CoBA index) or do not show an age-dependent increase in the magnitude of the between-limb differences (ToBMC).

Left handed subjects had no significant differences between limbs for any of the bone variables measured. It is tempting to speculate that this is due to similar habitual loading of the dominant and nondominant limbs. However, this cross-sectional study included only a small number of left-handed subjects (n = 10) limiting the power to detect a true difference. Moreover, a causal relation between habitual loading and bone characteristics was not investigated directly.

Despite significant between-limb differences in connectivity (in right handed subjects), maximum hole size, ToBMC, CoBMC and ToBD, the bilateral measurements are highly correlated in each subject (Table 5.4). While CoBA index and CoBD in the dominant radius are not significantly different from that in the nondominant arm, these measurements are only moderately correlated (r = 0.66 and r = 0.73, respectively). With the exception of these 2 variables, our assessment of bone structure, geometry, mass and density in one radius provides acceptable surrogate measurements for the contralateral radius. The indices of trabecular bone structure are significant predictors of compressive strength of the distal radius *ex vivo* (Gordon, Webber, and Nicholson 1998). *In vivo* assessment of trabecular bone structure may improve the ability to identify individuals at risk for osteoporotic wrist fracture.

CHAPTER SIX

RESPONSE OF HEALTHY NONWEIGHTBEARING BONE TO ALTERATIONS IN MECHANICAL LOADING

6.1 Introduction

Changes in habitual loading patterns experienced by the human skeleton give rise to adaptations in bone mass and structure to achieve the required bone strength (Biewener et al. 1996; Lanyon 1996). Bone strength adapts to changes in the strain environment as determined by a negative feedback (Frost 1996). Since strong correlations between skeletal mass and whole body lean mass are observed (Ferretti et al. 1998) and the largest bone strains are experienced as a result of loading by the musculature (Kannus et al. 1996), muscle strength and habitual physical activity have a significant influence on bone strength.

Dramatic decreases in mass have been demonstrated in response to disuse in weightbearing bone (Bagi and Miller 1994; Lane et al. 1996). Little is known about the changes in bone strength and structure associated with these changes in mass. Young, Niklowitz and Steele (1983) restrained 8 male adult monkeys for 6 months and observed a decrease in BMD (ranging from 23% to 31%) and bending stiffness (ranging from 36% to 40%) in the tibia. Young et al. (1986) also characterized changes in trabecular bone

structure in the proximal tibia of the adult primate and reported that 10 weeks of restraint caused a thinning and loss of trabeculae. In the young adult dog, trabecular thinning and increased intertrabecular spacing was induced by immobilizing the forelimb for 16 weeks (Lane et al. 1996). Bourrin et al. (1995) found that bone mass and trabecular thickness decreased in response to 2 weeks of tail suspension in young rats. In humans, immobilization due to reduced activity, bedrest, weightlessness, casting and spinal cord injury is associated with the loss of varying amounts of cortical and trabecular bone primarily from weightbearing bones (Hangartner 1995; Bloomfield 1997). Few human studies have examined the relation between immobilization and alterations in bone architecture (Palle et al. 1992) and even less is known about the effects of immobilization on the mass and structure of nonweightbearing upper limb bone.

Studies in animals and humans have suggested that the recovery of bone mass following a period of immobilization is slow and may require greater than normal activity (Maeda et al. 1993; Kannus et al. 1994; Sievänen et al. 1994; Bourrin et al. 1995; Lane et al. 1996). The optimal parameters for remobilization in order to restore bone mass and structure are not known. The literature suggests that the most effective loading modality is one which results in high peak forces, preferably produced at high rates and with novel distributions (Kannus et al. 1996). Animal models of disuse suggest that recovery may take at least twice as long as the duration of immobilization. After 6 months of immobilization, a recovery period of 8.5 months was required to restore tibial bending stiffness whereas bone mass remained depressed 15 months post immobilization in middle aged monkeys (Young, Niklowitz, and Steele 1983). Similarly, after 10 weeks of

restraint mature primates recovered tibial bone mass after 6 months of reambulation but recovery of trabecular elements did not occur within a 15 month follow up period (Young et al. 1986). In contrast, Lane et al. (1996) showed that trabecular thinning and increased intertrabecular spacing induced by immobilizing the forelimb of young adult dogs for 16 weeks recovered in 32 weeks when the post immobilization period included 16 weeks of graded treadmill exercise. Bourrin et al. (1995) found that bone mass and trabecular thickness decreased in response to 2 weeks of tail suspension in young rats; controlled physical activity was required during the 4 week recovery period to restore trabecular alterations, whereas bone mass recovered with normal weightbearing. Further studies are required to determine the critical factors which optimize recovery of immobilization-induced changes in bone mass and structure.

The purpose of this study is to determine the changes in mass and structure of the radius following alterations in habitual loading patterns. The response to a period of immobilization will be determined in normal nonweightbearing bone and musculature. Also, the effect of a subsequent exercise program imposing a high magnitude strain on the bone will be determined.

6.2 Materials and Methods

6.2.1 Subjects

The target population was young adult female Caucasians with healthy bones and a sedentary lifestyle. In response to posters and newspaper advertisements, 57 individuals (54 women) expressed an interest in participating in the study. All interested individuals

received further explanation regarding the purpose and requirements of the study and the compensation ($400) for participating was detailed. Of the 57 individuals, 36 declined to participate. The inclusion requirements pertaining to gender and age were broadened. Interested individuals were questioned to determine eligibility (young adult Caucasian, sedentary lifestyle, adequate daily calcium intake, not pregnant and no history of skeletal pathology, previous fracture or nerve injury of the upper extremity, bedrest for more than 1 month, menstrual/hormonal abnormalities, or use of medications which affect bone metabolism). Based on the questionnaire, 6 individuals did not meet the inclusion criteria. Informed consent was obtained from 15 subjects (12 women). All methods and procedures for the study were approved by the McMaster University Research Ethics Board.

6.2.2 Study Design

The design is a 2 group prospective randomized trial with repeated measures on all dependent variables at baseline, 1.5 months, 4.5 months, 7.5 months and 13.5 months. The same operator acquired all the measurements. The subjects were randomly assigned to a post immobilization control or a post immobilization exercise group using a table of random numbers.

6.2.3 Interventions

The dominant arm served as the within subject control. All subjects had the nondominant (experimental) forearm lined with a webril padding and a well molded

plaster cast[1] was applied extending from the metacarpals to the proximal 1/3rd of the forearm. The subjects were instructed to wear the cast and sling for 1.5 months at which time the immobilization intervention ended and the subjects assumed the post immobilization group assignment. To monitor the influence of habitual physical activity levels on any between-group differences in the outcome measures, each subject wore an activity monitor (TriTrac-R3D Ergometer; Hemokinetics Inc, Madison, WI) on the experimental arm for 3 continuous days during waking hours at 3 different time points throughout the study. The short term *in vivo* reliability for the TriTrac-R3D is R = 0.81 (Kochersberger et al. 1997).

6.2.3 i Control Group

The control group was instructed to resume activities of daily living post immobilization of the experimental wrist.

6.2.3ii Exercise Group

The exercise group was instructed in a daily home exercise program for the experimental (nondominant) forearm following removal of the cast using a user-friendly resistive exercise device developed for this study. The device (Appendix 2) was constructed of a shaft secured in two polymer pillow blocks mounted on a plywood base which is clamped to a desktop. Rubber tubing provides resistance to movement. The

---

[1] The casts were applied, monitored and removed by Dr. Mohit Bhandari, Department of Orthopaedic Surgery, McMaster University.

duration of this exercise intervention was 12 months. The sessions included resisted flexion and extension of the wrist and resisted forearm supination and pronation. When the subjects could complete 3 sets of 10 repetitions of forearm pronation, the load was increased for all exercises by increasing the number of rubber elastics used for resistance. Flowsheets were completed daily by the subjects in order to monitor compliance.

6.2.4 Outcomes Measured

6.2.4 i Anthropometry

For all subjects, height and body weight were recorded to the nearest 0.1 cm and 0.1 kg, respectively, using a balance scale standiometer (Continental Scale Corporation, Chicago, Illinois). Body mass index (BMI = kg/m^2) was calculated for each subject.

6.2.4 ii Trabecular Bone Structure

Bilateral measurements of the length of the ulna from the olecranon process to the ulnar styloid were obtained to the nearest 0.1 cm using a tape measure. Peripheral quantitative computed tomographic images of both forearms were acquired using a second generation Stratec XCT-960 pQCT scanner as described in Chapter 3 (section 3.2.3). The images were postprocessed and analyzed to quantify indices of trabecular bone structure, including connectivity index (CI), maximum hole size (H_M) and mean hole size (H_A), using in-house developed software (Gordon et al. 1996).

6.2.4iii Bone Density and Mass

The same pQCT images were also analyzed using the commercial software (version 5.2, Stratec Medizintechnik, Germany) to determine volumetric bone mineral density (ToBD, mg/cm^3; CoBD, mg/cm^3; TrBD, mg/cm^3), bone mineral content (ToBMC, mg; CoBMC, mg; TrBMC, mg), bone cross-sectional area (ToBA, mm^2; CoBA, mm^2; TrBA, mm^2) and cortical shell thickness (CoBA index) according to the methods described in Chapter 4 (section 4.2.3).

Long term precision of the pQCT over the duration of the study was evaluated by performing daily (n = 143) measurements of a polyethylene phantom (0.495 cm^{-1}). The coefficients of variation (CV) for the attenuation coefficient (cm^{-1}) and calibrated bone density (mg/cm^3) are 0.3% and 0.5%, respectively.

Dual-energy X-ray absorptiometry (DXA; model QDR 4500A; Hologic, Waltham, MA, USA) was used to scan both forearms of all subjects. BMC, areal bone mineral density (BMD) and bone surface area were calculated for the total region of interest, the ultra distal region, the middle region and the distal 1/3 region of the forearm on the basis of the subject's attenuation of the fan-beam in comparison with the internal reference standard. (Refer to Figure 2.2 for an illustration of these regions of interest.)

Long term precision of the DXA over the duration of the study was evaluated by performing daily (n = 332) measurements of the spine phantom (#2603) provided by the manufacturer. The *in vitro* CV for BMD (g/cm^2) and BMC (g) is 0.5% and 0.6% respectively.

The short term *in vivo* precision for the DXA measurements of BMD and BMC in the regions of interest in the radius was determined in 2 men and 5 women (with a mean age [SD] of 25.3 [1.3] years) by scanning the nondominant forearm 3 times over 5.8 (SD: 3.1) days to calculate the root mean square CV (CV_{rms}) . For BMD in the total region of interest, the ultra distal region, the middle region, and the 1/3 region, the CV_{rms} is 1.9%, 2.4%, 2.0% and 1.8%, respectively. For BMC in the total region of interest, the ultra distal region, the middle region and the distal 1/3 region, the CV_{rms} is 1.6%, 1.5%, 1.8% and 1.9%, respectively.

6.2.4 iv Joint Mobility

Range of motion (ROM) of the distal radio-ulnar and wrist joints of both arms was measured with a universal full-circle pocket goniometer (Sammons Preston, Mississauga, ON) using a standard published protocol (Norkin and White 1995). Measurements of the wrist obtained by the same operator are reported to be highly reproducible ($R > 0.90$) for all active and passive motions (Horger 1990). Differences in range of wrist motion which exceed 5° are considered true differences (Boone et al. 1978).

6.2.4 v Muscle Strength

Maximum grip strength was assessed bilaterally using the adjustable handle Jamar hand dynamometer (Jackson, MI) according to a standardized published protocol (Mathiowetz et al. 1984). The dynamometer was factory calibrated. The second or third

handle position (of the five positions available) was used, depending on the position at which the maximum grip strength was recorded, and the same position was used for both hands on all visits. The dynamometer was reset to zero prior to each reading of grip strength, and it was read to the nearest 1.0 kg increment. The short term reproducibility, reported as the Pearson Product Moment correlation coefficient describing the association between two separate observations of both left and right grip strength ($r = 0.88$ and $r = 0.93$, respectively), is good (Mathiowetz et al. 1984).

Lean tissue mass of the forearms was determined using DXA to acquire whole body scans. Chilibeck et al. (1994) report that the reproducibility (CV) for *in vivo* measurements of lean tissue mass in the right and left arm is 6.6% and 5.7%, respectively.

Endurance of the forearm pronator muscles was assessed bilaterally in each subject with the resistive exercise device described above (section 6.2.3 ii). The subject turned a D-handle through 90°, pronating the forearm from 90° of supination to 0°, thus moving the shaft against the resistance of rubber elastics which spanned from the plywood platform to the shaft. The resisted pronation was repeated as many times as possible until the subject could not maintain good form and complete another repetition. The resistance provided by this exercise device was calibrated using an in-line torque transducer and each elastic required 0.2 Nm of torque to complete one repetition. An estimate of endurance for the pronator muscles was calculated as the product of the number of elastics, the number of repetitions and 0.2 Nm for the dominant and nondominant forearm for each subject.

6.2.5 Statistical Analyses

All outcome measures were analyzed using Analysis of Variance (ANOVA) to determine main effects for time, group (control versus exercise) and the interaction of group and to determine the main effects for subject and time. Additionally, planned comparisons were made using Bonferroni simultaneous tests to identify significant differences between baseline and each of the 4 post immobilization time points for both the control and experimental limbs. Statistical significance was set at $p < 0.05$ for all tests. All data are expressed as mean (standard error of the mean [SEM]) and were analyzed using the statistical package, Minitab (release 12).

6.3 Results

6.3.1 Group Characteristics

Within 3 weeks of immobilization of the experimental (nondominant) wrist in 15 subjects, 5 subjects removed their cast (4 cited personal reasons and 1 experienced a change in medical status) and withdrew from the study. After the 7.5 month time point, one subject, randomized to the exercise group, moved to China and was lost to follow up. Table 6.1 shows that there was no significant difference between groups at baseline for age, BMI, physical activity level, gender or hand dominance.

TABLE 6.1

SUBJECT CHARACTERISTICS [a,b]

	Baseline	
	Control Group (n = 5)	Exercise Group (n = 5)
Age (years) a	25.56 (2.57)	23.61 (0.82)
Body Mass Index (kg/m2) [a]	23.66 (1.77)	23.18 (1.16)
Physical Activity Level [a,b]	548.4 (166)	536.0 (50.1)
% Female	80 %	100 %
% Right Handed	80 %	80 %

[a] Data expressed as mean (SEM)
[b] Group average of vector magnitude measured with the activity monitor.

Table 6.2 shows the baseline measurements of all the dependent variables determined for the 10 subjects who completed the immobilization period and were randomly assigned to either the post immobilization control group or post immobilization exercise group. There was no significant difference between groups at baseline for indices of bone structure, BMD (distal 1/3 region and TrBD), BMC (cortical), active range of motion (flexion, extension and radial deviation), passive range of motion (flexion and extension) and muscle strength (grip and pronator muscle endurance). The remaining variables (identified in Table 6.2) demonstrate a consistent difference between groups at all time points.

6.3.2 Adherence to Group Assignment

At 7.5 months, the exercise group (n = 5) completed the forearm exercises an average of 4.3 days / week over the 6 month remobilization period (subject adherence

TABLE 6.2

MEAN (SEM) BASELINE VALUES FOR ALL GROUP OUTCOMES MEASURED[a,b]

	Control Arm[a]		Experimental Arm[a]	
Variable	CG (n = 5)	EG (n = 5)	CG (n = 5)	EG (n = 5)
Structure				
Connectivity Index	7.49 (1.22)	8.42 (4.83)	8.89 (1.18)	8.35 (5.08)
Maximum Hole Size (mm^2)	55.2 (5.51)	47.2 (14.1)	52.9 (10.2)	40.1 (16.2)
Mean Hole Size (mm^2)	1.57 (0.17)	1.99 (0.76)	1.47 (0.17)	2.76 (1.50)
Volumetric Bone Density				
Total Compartment (mg/cm^3)	427.1 (14.1)	458.4 (18.8) *	422.3 (15.6)	471.6 (24.6) *
Cortical Compartment (mg/cm^3)	771.9 (34.3)	813.3 (20.0) *	781.7 (29.5)	793.6 (14.5)
Trabecular Compartment (mg/cm^3)	208.0 (3.81)	217.6 (20.1)	211.9 (5.99)	227.0 (22.7)
Bone Mass (mg)				
Total Compartment	280.7 (14.9)	258.6 (10.1) *	277.3 (17.2)	256.4 (8.00)
Cortical Compartment	196.4 (11.3)	184.7 (6.87)	189.1 (13.1)	187.2 (7.48)
Trabecular Compartment	84.37 (7.52)	73.90 (9.08) *	88.19 (6.65)	69.11 (4.66) *
Areal Bone Mineral Density				
Total Region (g/cm^2)	0.55 (0.01)	0.59 (0.02) *	0.56 (0.02)	0.59 (0.02) *
Ultra distal Region (g/cm^2)	0.43 (0.02)	0.46 (0.02) *	0.43 (0.02)	0.46 (0.02) *
Middle Region (g/cm^2)	0.58 (0.01)	0.63 (0.02) *	0.59 (0.02)	0.61 (0.02) *
Distal 1/3 Region (g/cm^2)	0.67 (0.02)	0.68 (0.02)	0.69 (0.01)	0.68 (0.02)
Bone Mineral Content (mg)				
Total Region	7.69 (0.49)	6.79 (0.27) *	7.82 (0.68)	6.70 (0.21) *
Ultra distal Region	1.57 (0.12)	1.42 (0.06) *	1.63 (0.17)	1.43 (0.07) *
Middle Region	4.34 (0.35)	3.65 (0.19) *	4.38 (0.44)	3.59 (0.15) *
Distal 1/3 Region	1.78 (0.04)	1.71 (0.06) *	1.80 (0.08)	1.68 (0.03) *
Active Wrist ROM[b] (degrees)				
Flexion	80.2 (12.9)	80.2 (7.92)	79.6 (6.19)	84.0 (8.34)
Extension	71.4 (9.32)	72.4 (6.80)	74.6 (9.94)	72.6 (5.73)
Ulnar Deviation	48.4 (5.59)	50.6 (6.27) *	49.2 (9.65)	51.4 (8.35)
Radial Deviation	21.0 (6.56)	24.0 (6.96)	17.8 (5.26)	25.0 (9.06) *
Passive Wrist ROM[a] (degrees)				
Flexion	96.8 (15.4)	94.6 (10.2)	91.4 (12.4)	97.2 (7.69)
Extension	83.0 (10.2)	86.0 (7.04)	84.0 (12.3)	86.8 (5.76) *
Ulnar Deviation	53.2 (7.29)	55.2 (5.40) *	52.6 (10.6)	55.4 (6.88)
Radial Deviation	22.2 (6.61)	27.2 (6.61) *	19.6 (6.07)	28.2 (6.50) *
Forearm Muscle Strength				
Grip (kg)	30.9 (8.26)	28.2 (4.81)	30.2 (9.44)	25.5 (4.32)
Lean Tissue Mass	1950.4 (77.9)	2321 (271) *	1936.6 (128)	2150 (576) *
Endurance (Nm)	68.9 (18.6)	45.1 (7.34)	83.4 (25.0)	54.8 (12.0)

[a] CG = control group; EG = exercise group; * Significant effect due to group ($p < 0.05$).
[b] ROM: range of motion.

varied from 2.3 days / week to 6.6 days / week). During the final 6 months of the study, 1 subject in the exercise group withdrew from the study. The adherence for the remaining 4 subjects was poor; the exercises were completed an average of 2.8 days / week varying from 0 to 6.0 days / week. There was no significant difference between groups with respect to physical activity level as measured by the TriTrac-R3D Ergometer ($p = 0.57$).

6.3.3 Effect of Exercise on Outcomes Measured

There was no significant interaction between group and time at any point during the study for the outcomes measured ($p > 0.05$).

6.3.4 Effect of Immobilization on Outcomes Measured

Since the response to the exercise intervention did not differ between groups, the results for the response to immobilization are shown with the two groups combined.

6.3.4 i Trabecular Bone Structure

Table 6.3 shows the mean (SEM) values for CI, H_M and H_A for the total study population ($n = 10$) in the control limb and the experimental limb at baseline and at 1.5, 4.5, 7.5 and 13.5 months. Figure 6.1 shows the mean difference (SEM) from baseline at each time point. There is no significant change in the control limb throughout the study (Table 6.3, Figure 6.1A-C). In the ultra distal radius of the experimental limb, there is a significant effect due to time in CI ($p = 0.049$). However, CI is not significantly different from baseline at any single time point (Figure 6.1A). There is a significant increase in H_M

Figure 6.1 Mean difference (SEM) from baseline values (at 0 months) in indices of radial bone structure at the 4% site in the control (●) and casted (○) limbs of 10 subjects immediately after the cast removal (1.5 months), at 4.5 months, 7.5 months and 13.5 months. A: Changes in connectivity index (CI). B: Changes in maximum hole size (H_M, mm^2). C: Changes in mean hole size (H_A, mm^2).

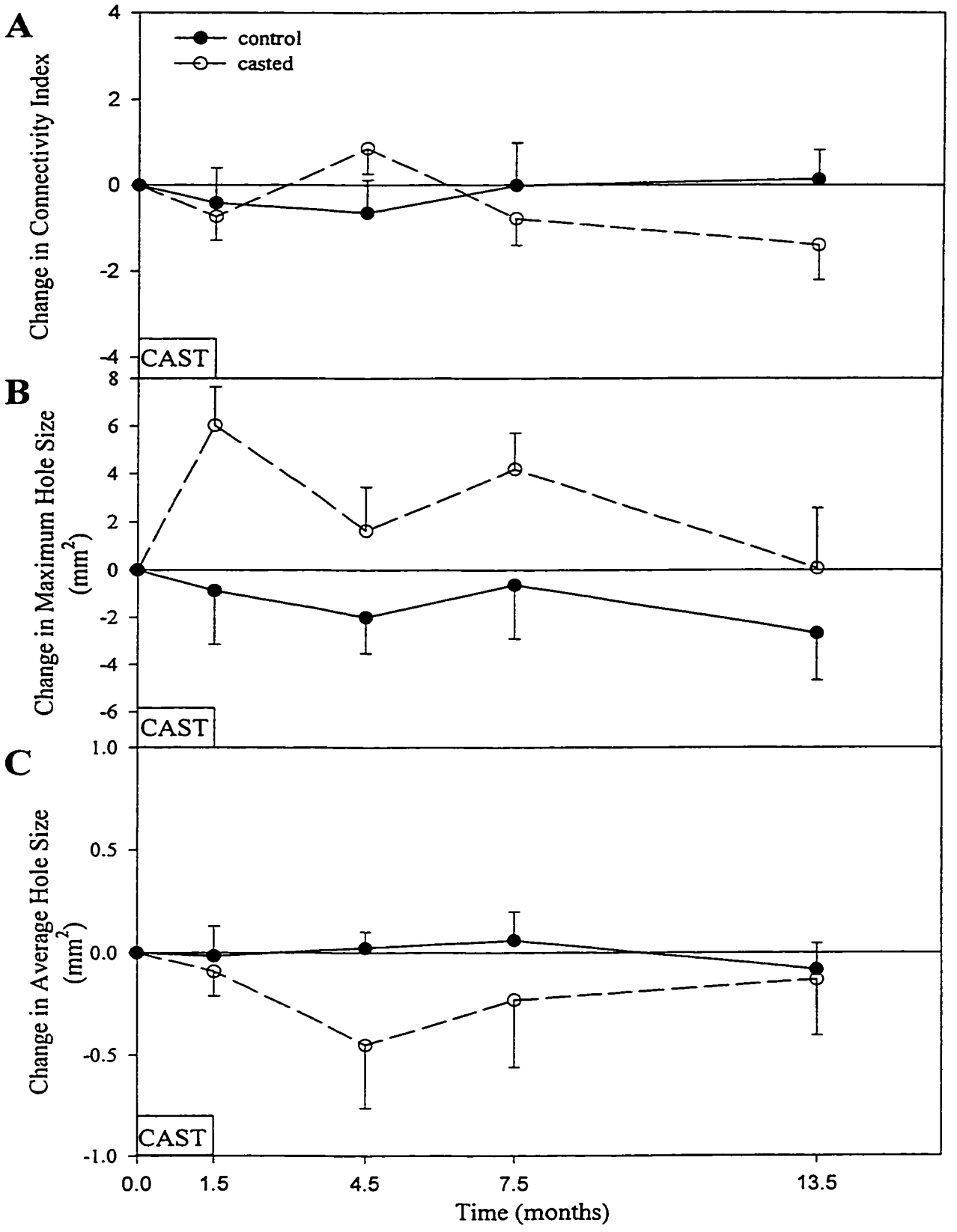
A
control
casted
Change in Connectivity Index
4
2
0
-2
-4
CAST
B
Change in Maximum Hole Size (mm²)
8
6
4
2
0
-2
-4
-6
CAST
C
Change in Average Hole Size (mm²)
1.0
0.5
0.0
-0.5
-1.0
CAST
0.0
1.5
4.5
7.5
13.5
Time (months)

immediately post immobilization (p = 0.043) which returns to the baseline value 3 months post immobilization (Table 6.3, Figure 6.1B). Figure 6.1C shows that, as in the control limb, there is no significant change in H_A in the experimental limb throughout the study.

TABLE 6.3

MEASUREMENTS OF RADIAL BONE TRABECULAR STRUCTURE IN THE CONTROL AND CASTED ARMS FOR ALL SUBJECTS [a-c]

Variable [a]	Baseline	1.5 months	4.5 months	7.5 months	13.5 months
CI					
Control	7.96 (2.35)	7.51 (2.64)	7.31 (2.79)	7.94 (2.89)	9.24 (2.19)
Casted [b]	8.62 (2.46)	7.89 (2.46)	9.49 (2.31)	7.84 (2.67)	8.34 (3.00)
H_M (mm^2)					
Control	51.19 (7.25)	50.32 (7.89)	49.18 (6.93)	50.57 (8.94)	45.98 (7.52)
Casted [b]	46.53 (9.28)	52.57 (8.75) [c]	47.88 (9.41)	50.73 (9.34)	44.01 (9.88)
H_A (mm^2)					
Control	1.78 (0.38)	1.77 (0.40)	1.80 (0.42)	1.84 (0.43)	1.53 (0.30)
Casted	2.12 (0.74)	2.03 (0.63)	1.66 (0.44)	1.89 (0.47)	1.85 (0.58)

[a] Data expressed as mean (SEM). CI: connectivity index; H_M: maximum hole size, mm^2; H_A: mean hole size (mm^2).
[b] Significant variance in the measurement due to time ($p < 0.05$).
[c] Significantly different from baseline value ($p < 0.05$).

6.3.4 ii Bone Density

Table 6.4 shows the mean (SEM) values for volumetric bone density (ToBD, CoBD, and TrBD) at the 4% site in the distal radius of the control limb and the experimental

limb at baseline and at 1.5, 4.5, 7.5 and 13.5 months. There is no significant change in volumetric bone density in either the control or cast immobilized radius.

TABLE 6.4

MEAN (SEM) VALUES FOR VOLUMETRIC BONE DENSITY AT THE 4 % SITE (PQCT) AND AREAL BONE MINERAL DENSITY (DXA) OF THE DISTAL RADIUS IN THE CONTROL AND CASTED LIMBS [a]

Variable [a]	Baseline	1.5 months	4.5 months	7.5 months	13.5 months
pQCT:					
ToBD					
Control	442.8 (12.3)	444.8 (12.2)	445.1 (11.7)	441.6 (13.7)	452.2 (15.2)
Casted	447.0 (16.0)	445.0 (15.9)	444.7 (14.0)	449.7 (17.3)	461.7 (20.1)
CoBD					
Control	792.6 (20.0)	783.7 (16.5)	788.7 (16.5)	782.4 (19.5)	789.3 (20.5)
Casted	787.6 (15.6)	789.6 (20.8)	790.0 (9.73)	795.8 (20.8)	809.7 (18.3)
TrBD					
Control	212.8 (9.77)	217.9 (9.97)	214.9 (9.73)	216.6 (10.2)	224.2 (10.0)
Casted	219.4 (11.4)	219.6 (11.8)	216.9 (10.9)	218.0 (11.5)	222.2 (12.9)
DXA regions:					
Total					
Control [b]	0.57 (0.01)	0.57 (0.01)	0.57 (0.01)	0.57 (0.01)	0.58(0.01)
Casted	0.57 (0.01)	0.57 (0.01)	0.57 (0.01)	0.57 (0.01)	0.58(0.02
Ultra distal					
Control	0.44 (0.02)	0.44 (0.01)	0.44 (0.01)	0.44 (0.01)	0.45 (0.01)
Casted	0.44 (0.02)	0.44 (0.02)	0.43 (0.01)	0.43 (0.02)	0.45 (0.02)
Middle					
Control	0.60 (0.01)	0.60 (0.01)	0.60 (0.01)	0.60 (0.02)	0.61 (0.02)
Casted	0.60 (0.01)	0.60 (0.01)	0.60 (0.01)	0.60 (0.01)	0.61 (0.02)
Distal 1/3					
Control [b]	0.68 (0.01)	0.68 (0.01)	0.68 (0.01)	0.69 (0.01)	0.69 (0.01)
Casted	0.69 (0.01)	0.68 (0.01)	0.68 (0.01)	0.68 (0.01)	0.69 (0.01)

[a] Data expressed as mean (SEM). pQCT derived measurements (mg/cm^3). DXA derived measurements, (g/cm^2).

[b] Significant variance in the measurement due to time ($p < 0.05$).

Table 6.4 also shows the mean (SEM) values for areal bone mineral density in the control and experimental limbs at baseline and at 1.5, 4.5, 7.5 and 13.5 months. Figure 6.2 illustrates the mean differences (SEM) in BMD (in the total region, ultra distal, middle and distal 1/3 regions) from baseline at each time point. There is a significant effect due to time in the total and distal 1/3 regions of the control radius ($p = 0.046$ and $p = 0.047$, respectively). However, no statistically significant difference from baseline was observed in BMD in the total region (Figure 6.2A) or in the distal 1/3 region (Figure 6.2D) of the control limb at any single time point. No significant change occurs in the ultra distal or middle regions of the distal radius in the control limb (Figure 6.2B and 6.2C). Similarly, no significant change in BMD occurs in the casted radius (Figure 6.2A-D).

6.3.4iii Bone Mass and Geometry

Table 6.5 summarizes the mean (SEM) values for bone mass determined from pQCT images and DXA. Figure 6.3 shows the mean (SEM) differences from baseline at all time points for measurements determined using pQCT imaging. There is a significant increase in ToBMC at the 4% site in the control radius measured using pQCT ($p = 0.028$). Figure 6.3A illustrates the significant increase in total bone mass in the control limb radius at the 13.5 month time point ($p = 0.0074$). In contrast, there is no change in CoBMC or TrBMC at this site in the control limb. In the experimental limb, there is no change in ToBMC at the 4% site in the distal radius whereas CoBMC varies significantly over time ($p = 0.035$) but does not differ from baseline values at any single time point (Figure 6.3B). As

Figure 6.2 Mean difference (SEM) from baseline values (at 0 months) in areal bone mineral density (BMD) in regions of the distal radius in the control (●) and casted (○) limbs of 10 subjects immediately after the cast removal (1.5 months), at 4.5 months, 7.5 months and 13.5 months. A: Changes in total region BMD (g/cm^2). B: Changes in ultradistal region BMD (g/cm^2). C: Changes in middle region BMD (g/cm^2). D: Changes in distal 1/3 region BMD (g/cm^2).

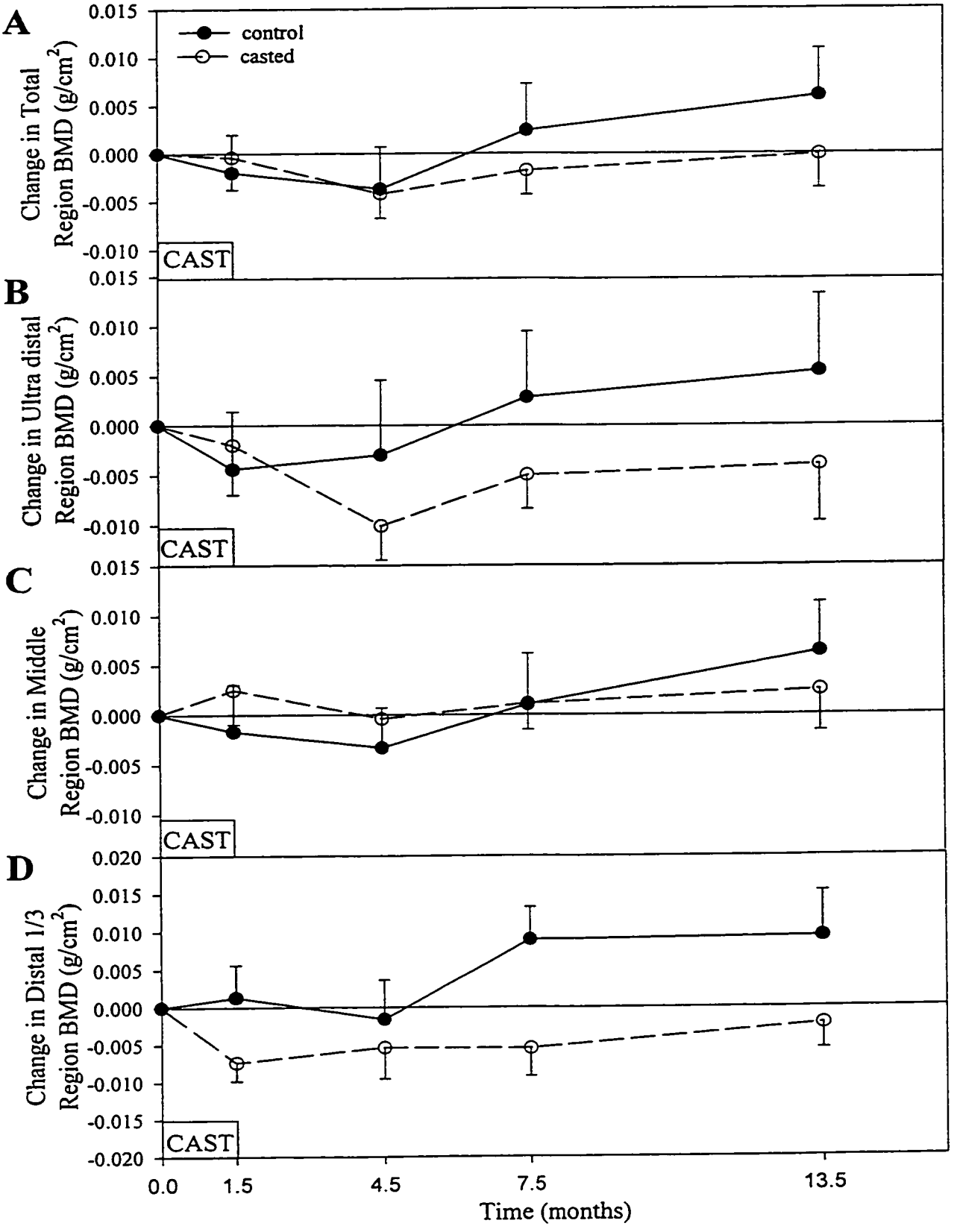
A
B
C
D
control
casted
CAST
Change in Total Region BMD (g/cm²)
Change in Ultra distal Region BMD (g/cm²)
Change in Middle Region BMD (g/cm²)
Change in Distal 1/3 Region BMD (g/cm²)
0.015
0.010
0.005
0.000
-0.005
-0.010
0.020
-0.015
-0.020
0.0
1.5
4.5
7.5
13.5
Time (months)

in the control limb, the amount of bone in the trabecular compartment does not change with immobilization (Figure 6.3C).

TABLE 6.5

MEASUREMENTS OF BONE MASS AT THE 4% SITE (PQCT) AND PROJECTED BONE MASS (DXA) IN THE CONTROL AND CASTED LIMBS [a-c]

Variable [a]	Baseline	1.5 months	4.5 months	7.5 months	13.5 months
pQCT:					
ToBMC					
Control[b]	269.7 (9.26)	273.6 (10.8)	272.1 (9.94)	273.9 (10.4)	279.7 (12.2)[c]
Casted	266.8 (9.61)	267.4 (10.1)	266.4 (10.4)	267.3 (10.9)	269.7 (11.2)
CoBMC					
Control	190.5 (6.53)	192.2 (6.65)	192.5 (6.64)	191.8 (7.61)	194.3 (7.61)
Casted [b]	188.2 (7.12)	186.9 (7.13)	188.1 (7.13)	189.0 (7.41)	192.3 (7.72)
TrBMC					
Control	79.13 (5.83)	81.36 (6.37)	79.63 (6.12)	82.12 (6.40)	85.40 (8.57)
Casted	78.65 (4.98)	80.48 (5.43)	78.32 (4.71)	78.36 (5.62)	77.39 (6.38)
DXA regions:					
Total					
Control	7.24 (0.30)	7.30 (0.34)	7.25 (0.35)	7.34 (0.36)	7.50 (0.37)
Casted [b]	7.26 (0.38)	7.17 (0.38)	7.17 (0.37)	7.15 (0.37)[c]	7.29 (0.39)
Ultra distal					
Control [b]	1.50 (0.07)	1.52 (0.08)	1.53 (0.08)	1.55 (0.08)[c]	1.58 (0.09)[c]
Casted	1.53 (0.09)	1.52 (0.08)	1.50 (0.09)	1.50 (0.09)	1.53 (0.09)
Middle					
Control	3.99 (0.22)	4.03 (0.24)	4.00 (0.24)	4.04 (0.25)	4.13 (0.26)
Casted [b]	4.28 (0.36)	3.94 (0.26)	3.94 (0.25)	3.92 (0.25)[c]	4.01 (0.27)
Distal 1/3					
Control	1.75 (0.04)	1.74 (0.04)	1.73 (0.04)	1.76 (0.04)	1.79 (0.04)
Casted	1.74 (0.04)	1.72 (0.05)	1.73 (0.04)	1.73 (0.04)	1.74 (0.04)

[a] Data expressed as mean (SEM). pQCT derived measurements (mg). DXA derived measurements, (g).
[b] Significant variance in the measurement due to time ($p < 0.05$).
[c] Significantly different from baseline value ($p < 0.05$).

Figure 6.3 Mean difference (SEM) from baseline values (at 0 months) in bone mineral content at the 4 % site for the distal radius in the control (●) and casted (O) limbs of 10 subjects immediately after the cast removal (1.5 months), at 4.5 months, 7.5 months and 13.5 months. A: Changes in bone mineral content in the total bone compartment (ToBMC, mg). B: Changes in bone mineral content in the cortical bone compartment (CoBMC, mg). C: Changes in bone mineral content in the trabecular bone compartment (TrBMC, mg).

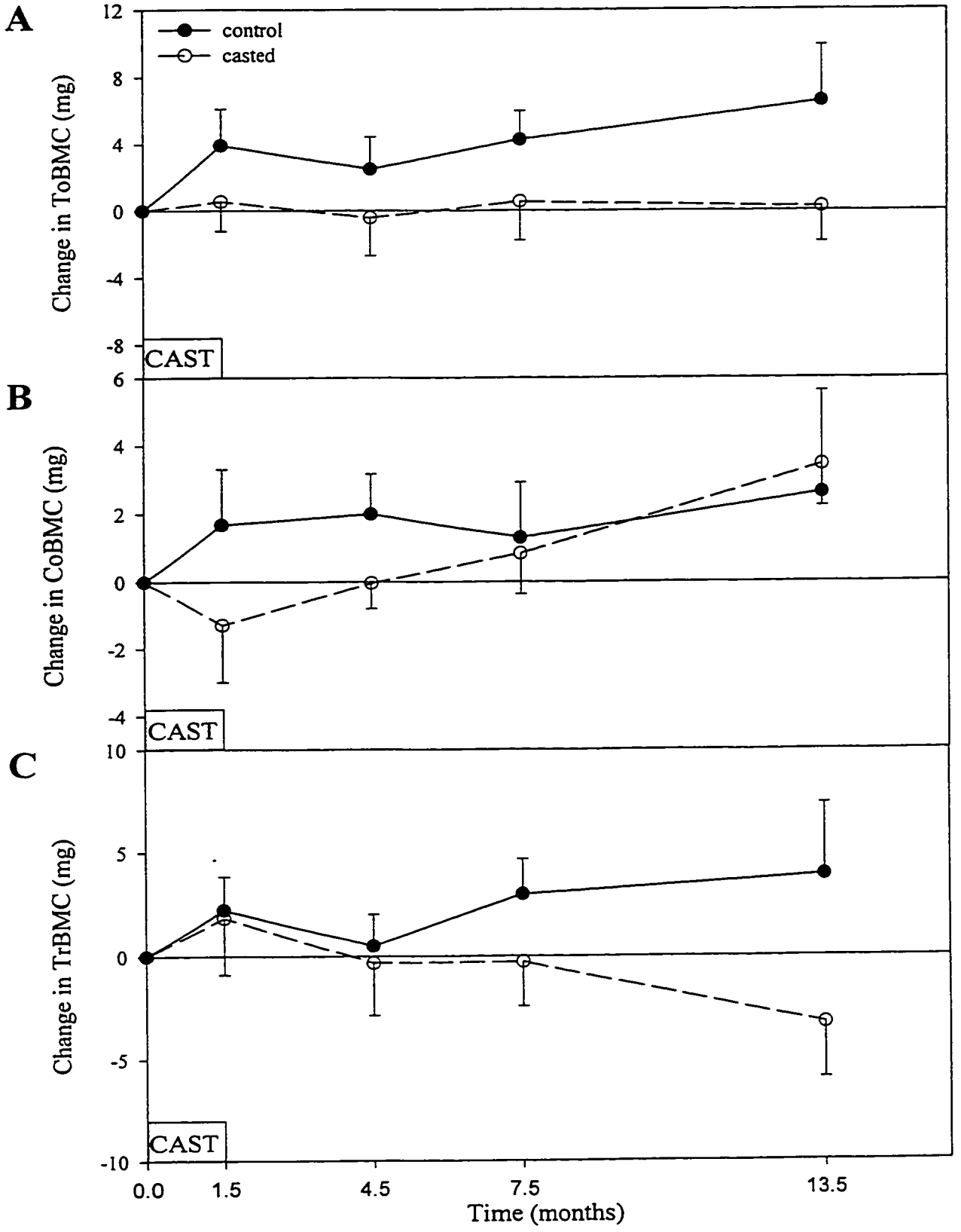
A
B
C
control
casted
Change in ToBMC (mg)
Change in CoBMC (mg)
Change in TrBMC (mg)
CAST
CAST
CAST
12
8
4
0
-4
-8
6
4
2
0
-2
-4
10
5
0
-5
-10
0.0
1.5
4.5
7.5
13.5
Time (months)

Table 6.5 summarizes the mean (SEM) values for BMC determined from DXA based measurements and Figure 6.4 shows the mean (SEM) differences from baseline at all time points. BMC does not change significantly in the total region, middle region or distal 1/3 region of the distal radius in the control limb (Figure 6.4A,C,D). Figure 6.4B shows that there is a significant increase in BMC in the ultra distal region of the control radius at 7.5 months ($p = 0.01$) and 13.5 months ($p = 0.0046$). In the casted limb, radial BMC decreases significantly at 7.5 months in the total region ($p = 0.019$) and middle region ($p = 0.0076$) (Figure 6.4A,C). The decrease in BMC in the ultra distal and distal 1/3 regions is not significant (Table 6.5, Figure 6.4B,D).

Table 6.6 summarizes the mean (SEM) values for measurements of bone geometry. There is no change in cross-sectional bone area at the ultra distal radius nor in DXA based measurements of radial bone geometry in the control and experimental limbs throughout the study.

6.3.4 iv Joint Mobility

Table 6.7 shows the mean (SEM) values for active range of motion of the wrist measured in the control and casted limbs. Figure 6.5 illustrates the mean (SEM) difference from baseline values at 1.5, 4.5, 7.5 and 13.5 months. Joint mobility differs less than 5° for all active movements of the wrist in the control limb (Figure 6.5A-D). In the immobilized limb, active wrist flexion, extension and ulnar deviation decrease immediately post immobilization ($p < 0.001$) and return to within 5° of baseline values 3

Figure 6.4 Mean difference (SEM) from baseline values (at 0 months) in bone mineral content (BMC) determined from projection imaging of the distal radius in the control (●) and casted (○) limbs of 10 subjects immediately after the cast removal (1.5 months), at 4.5 months, 7.5 months and 13.5 months. A: Changes in BMC in the total region (g). B: Changes in BMC in the ultra distal region (g). C: Changes in BMC in the middle region (g). D: Changes in BMC in the distal 1/3 region (g).

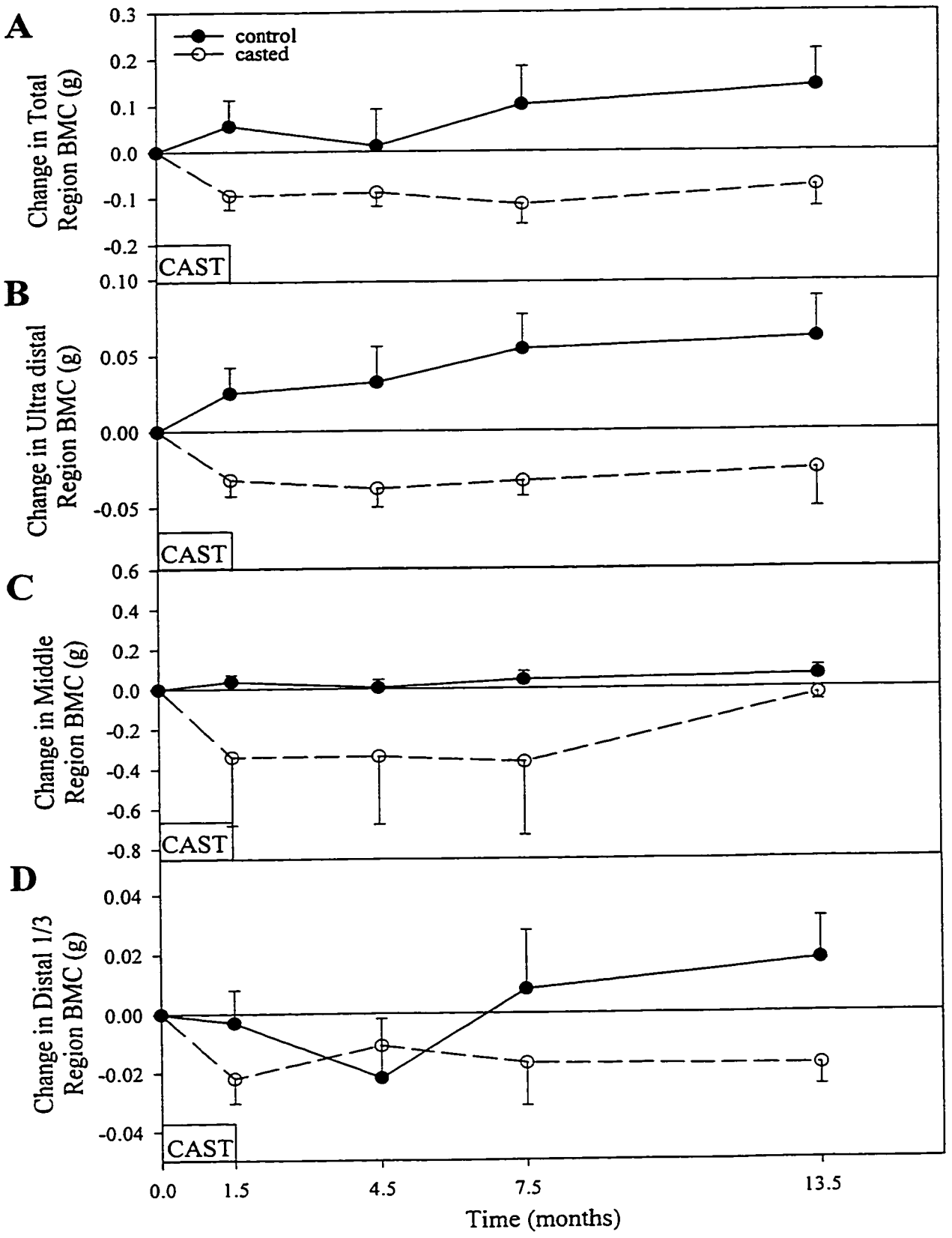
A
B
C
D
control
casted
Change in Total Region BMC (g)
Change in Ultra distal Region BMC (g)
Change in Middle Region BMC (g)
Change in Distal 1/3 Region BMC (g)
CAST
0.3
0.2
0.1
0.0
-0.1
-0.2
0.10
0.05
0.00
-0.05
0.6
0.4
0.2
0.0
-0.2
-0.4
-0.6
-0.8
0.04
0.02
0.00
-0.02
-0.04
0.0
1.5
4.5
7.5
13.5
Time (months)

TABLE 6.6

MEASUREMENTS OF BONE CROSS-SECTIONAL AREA (PQCT) AND BONE SURFACE AREA (DXA) IN THE CONTROL AND CASTED LIMBS [a]

Variable [a]	Baseline	1.5months	4.5 months	7.5 months	13.5 months
pQCT:					
ToBA					
Control	245.4 (11.1)	248.5 (13.8)	246.7 (12.5)	250.7 (13.3)	251.1 (17.0)
Casted	241.7 (13.0)	243.5 (13.7)	241.8 (12.5)	241.3 (14.5)	237.7 (15.5)
CoBA					
Control	96.23 (2.57)	98.35 (3.69)	97.63 (2.71)	98.42 (4.30)	98.69 (3.77)
Casted	95.47 (2.90)	94.95 (3.72)	95.13 (2.78)	95.12 (3.37)	94.96 (3.18)
TrBA					
Control	149.2 (9.07)	150.1 (10.5)	149.0 (10.3)	152.3 (10.0)	152.4 (13.7)
Casted	146.2 (11.0)	148.5 (10.3)	146.7 (10.1)	146.2 (11.4)	142.7 (12.8)
CoBA Index					
Control	0.40 (0.01)	0.40 (0.01)	0.40 (0.01)	0.40 (0.01)	0.40 (0.02)
Casted	0.40 (0.02)	0.39 (0.01)	0.40 (0.01)	0.40 (0.01)	0.41 (0.02)
DXA regions:					
Total					
Control	12.7 (0.67)	12.9 (0.49)	12.8 (0.73)	12.8 (0.75)	13.0 (0.79)
Casted	12.7 (0.77)	12.6 (0.76)	12.7 (0.75)	12.6 (0.76)	12.7 (0.80)
Ultra distal					
Control	3.44 (0.20)	3.50 (0.20)	3.51 (0.20)	3.51 (0.21)	3.53 (0.23)
Casted	3.49 (0.23)	3.43 (0.23)	3.47 (0.22)	3.46 (0.23)	3.47 (0.22)
Middle					
Control	6.70 (0.44)	6.78 (0.48)	6.76 (0.48)	6.77 (0.49)	6.86 (0.52)
Casted	6.68 (0.49)	6.58 (0.48)	6.63 (0.49)	6.56 (0.48) [c]	6.68 (0.53)
Distal 1/3					
Control	2.58 (0.06)	2.57 (0.06)	2.56 (0.07)	2.56 (0.07)	2.60 (0.06)
Casted	2.55 (0.06)	2.54 (0.06)	2.55 (0.06)	2.55 (0.07)	2.54 (0.06)

[a] Data expressed as mean (SEM) in mm^2.

TABLE 6.7

MEAN (SEM) VALUES FOR WRIST RANGE OF MOTION IN THE CONTROL AND CASTED LIMBS [a-c]

Variable [a]	Baseline	1.5 months	4.5 months	7.5 months	13.5 months
Active:					
Flexion					
Control	80.2 (3.19)	79.6 (3.31)	81.0 (2.62)	81.1 (3.13)	79.3 (3.14)
Casted [b]	81.8 (2.31)	64.6 (3.98) [c]	81.3 (2.96)	81.3 (2.73)	81.9 (2.90)
Extension					
Control	71.9 (2.44)	74.5 (1.96)	74.6 (2.06)	74.0 (1.95)	73.6 (2.38)
Casted [b]	73.6 (2.44)	61.9 (3.12) [c]	74.8 (2.37)	75.0 (2.30)	75.1 (2.52)
Ulnar Dev.					
Control	49.5 (1.81)	51.4 (2.11)	50.8 (1.67)	49.1 (1.57)	50.2 (1.82)
Casted [b]	50.3 (2.72)	43.2 (2.74) [c]	53.0 (2.26)	51.0 (2.19)	51.6 (1.92)
Radial Dev.					
Control	22.5 (2.08)	21.7 (1.84)	21.8 (2.00)	22.0 (1.63)	23.1 (1.81)
Casted	21.4 (2.51)	20.1 (2.61)	22.0 (2.02)	21.6 (2.10)	21.3 (2.27)
Passive:					
Flexion					
Control	95.7 (3.90)	94.9 (3.85)	97.1 (3.13)	96.3 (2.92)	95.8 (3.41)
Casted [b]	94.3 (3.23)	78.1 (4.27) [c]	96.1 (2.90)	95.9 (3.11)	96.9 (3.54)
Extension					
Control [b]	84.5 (2.66)	85.5 (2.77)	86.5 (1.88)	87.1 (2.01)	87.6 (2.35)
Casted [b]	85.4 (2.99)	78.0 (3.49) [c]	88.0 (1.81)	87.6 (1.63)	88.1 (1.75)
Ulnar Dev.					
Control	54.2 (1.94)	54.5 (2.11)	56.1 (1.77)	54.9 (1.54)	55.0 (1.52)
Casted [b]	54.0 (2.70)	48.0 (2.69) [c]	54.9 (2.07)	54.9 (2.15)	55.2 (2.15)
Radial Dev.					
Control	24.7 (2.14)	24.1 (1.92)	24.2 (1.88)	24.2 (1.93)	25.1 (2.08)
Casted	23.9 (2.36)	23.1 (2.54)	24.1 (2.28)	24.3 (2.28)	23.1 (2.28)

[a] Data measured in degrees. Ulnar Dev.: ulnar deviation. Radial Dev.: radial deviation.
[b] Significant variance in the measurement due to time ($p < 0.05$).
[c] Only differences of more than 5° are considered to be true biological changes and reported as significantly different from the baseline value ($p < 0.05$).

Figure 6.5 Mean difference (SEM) from baseline values (at 0 months) in active wrist range of motion in the control (●) and casted (○) limbs of 10 subjects immediately after the cast removal (1.5 months), at 4.5 months, 7.5 months and 13.5 months. A: Changes in active wrist flexion (degrees). B: Changes in active wrist extension (degrees). C: Changes in active wrist ulnar deviation (degrees). D: Changes in active wrist radial deviation (degrees).

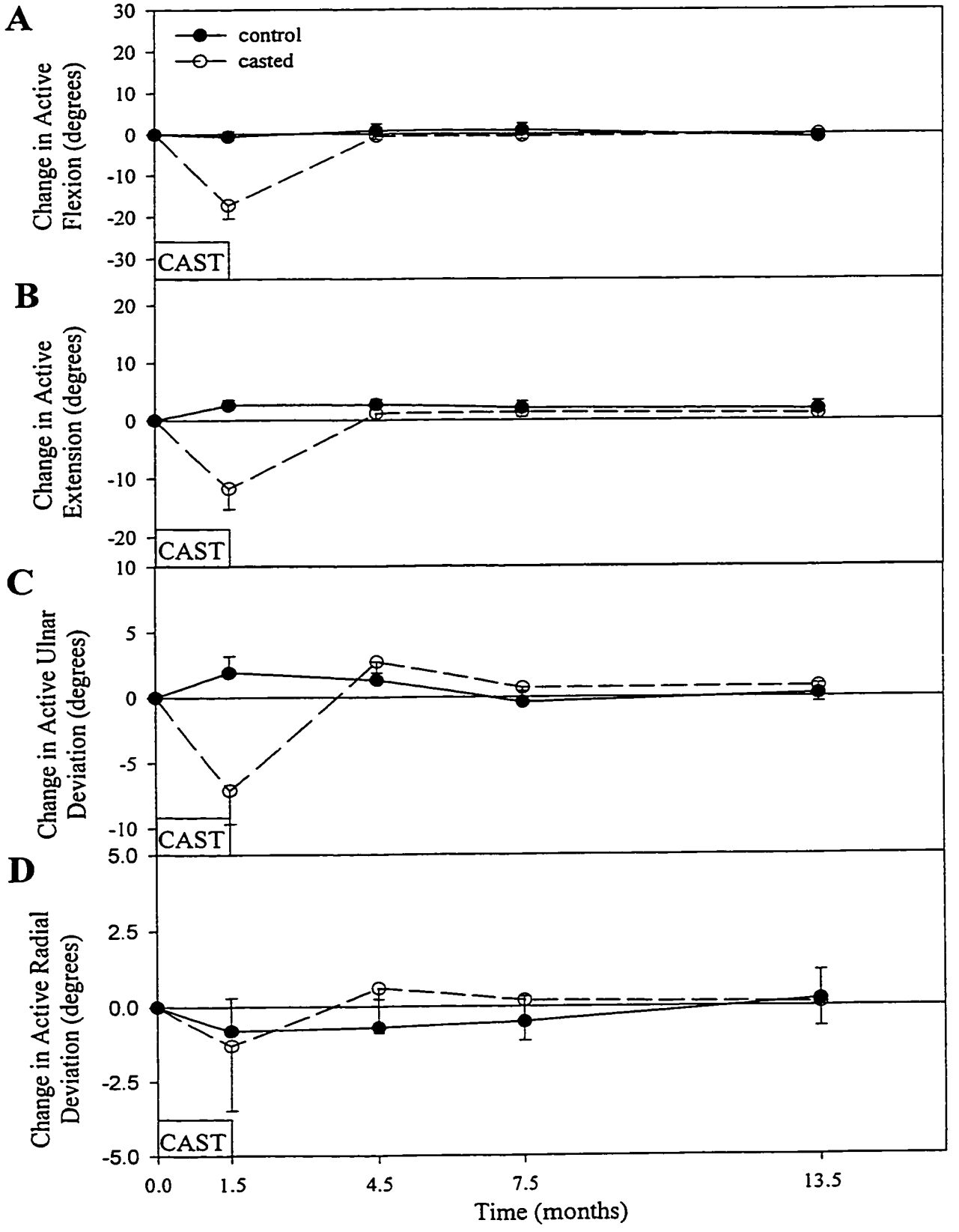
A
B
C
D
control
casted
Change in Active Flexion (degrees)
Change in Active Extension (degrees)
Change in Active Ulnar Deviation (degrees)
Change in Active Radial Deviation (degrees)
CAST
30
20
10
0
-10
-20
-30
5
-5
2.5
0.0
-2.5
-5.0
0.0
1.5
4.5
7.5
13.5
Time (months)

months post remobilizaton (Table 6.7, Figure 6.5A-C). There is no significant change in active wrist radial deviation in response to immobilization (Figure 6.5D).

Table 6.7 also shows the mean (SEM) values for passive range of motion of the wrist measured in the control and casted limb and the mean (SEM) differences from baseline values at 1.5, 4.5, 7.5 and 13.5 months are depicted in Figure 6.6. No significant change in passive wrist mobility occurs in the control limb (Figure 6.6A-D). In contrast, passive wrist flexion, extension and ulnar deviation decrease by 16.2° ($p < 0.0001$), 7.4° ($p = 0.0065$) and 6° ($p = 0.0019$), respectively, in the casted limb immediately post immobilization and recover to within 5° of baseline values by 4.5 months (Figure 6.6A-C). No significant change occurs in passive wrist radial deviation with immobilization (Figure 6.6D).

6.3.4 v Muscle Strength

Table 6.8 summarizes the mean (SEM) values for indices of muscle strength and Figure 6.7 illustrates the mean (SEM) difference from baseline values at 1.5, 4.5, 7.5 and 13.5 months in the control and casted limb. There is no change in grip strength in the control limb during the study (Figure 6.7A). Lean tissue mass and muscle endurance varied with time ($p = 0.039$ and $p = 0.04$, respectively) but were not significantly different from baseline at any single time point (Figure 6.7B and 6.7C, respectively).

In the casted arm, grip strength decreases immediately post immobilization ($p = 0.013$) and returns to baseline levels within 3 months of remobilization (Figure 6.7A).

Figure 6.6 Mean difference (SEM) from baseline values (at 0 months) in passive wrist range of motion in the control (●) and casted (○) limbs of 10 subjects immediately after the cast removal (1.5 months), at 4.5 months, 7.5 months and 13.5 months. A: Changes in passive wrist flexion (degrees). B: Changes in passive wrist extension (degrees). C: Changes in passive wrist ulnar deviation (degrees). D: Changes in passive wrist radial deviation (degrees).

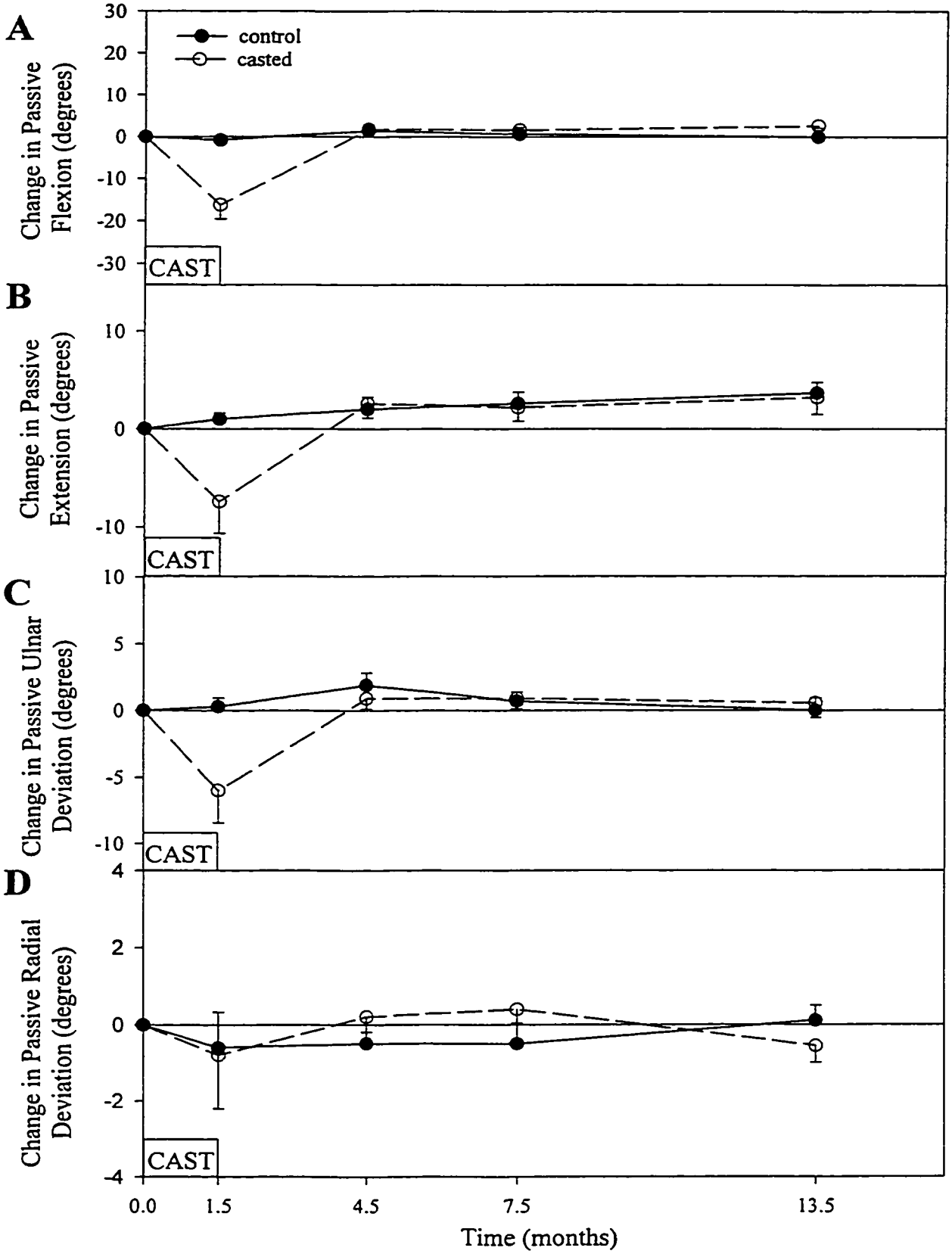
A
B
C
D
control
casted
Change in Passive Flexion (degrees)
Change in Passive Extension (degrees)
Change in Passive Ulnar Deviation (degrees)
Change in Passive Radial Deviation (degrees)
CAST
30
20
10
0
-10
-20
-30
5
-5
4
2
-2
-4
0.0
1.5
4.5
7.5
13.5
Time (months)

The lean tissue mass determined in the immobilized forearm does not change from baseline values during the study (Figure 6.7B). There is a significant decrease in muscle endurance in the casted arm immediately post immobilization ($p = 0.0053$) which returns to baseline values 3 months after remobilization (Figure 6.7C).

TABLE 6.8

FOREARM MUSCLE STRENGTH IN THE CONTROL AND CASTED LIMBS [a-e]

Variable [a]	Baseline	1.5 months	4.5 months	7.5 months	13.5 months
Grip (kg)					
Control	29.6 (2.07)	29.1 (2.02)	30.1 (2.12)	30.5 (1.90)	29.1 (2.04)
Casted [b]	27.9 (2.32)	25.2 (1.97) [c]	27.9 (1.92)	28.7 (2.34)	27.1 (2.07)
LTM (g) [d]					
Control	2136 (147)	2183 (163)	2252 (147)	2260 (131)	2121 (155)
Casted	2043 (129)	2043 (140)	2124 (131)	2135 (128)	2033 (129)
Endurance (Nm)[e]					
Control	57.0 (10.2)	53.8 (6.44)	56.8 (7.05)	53.5 (6.66)	77.3 (9.96)
Casted [b]	69.1 (13.9)	30.4 (6.38) [c]	51.5 (6.05)	63.5 (8.79)	73.6 (11.1)

[a] Data expressed as mean (SEM).
[b] Significant variance in the measurement due to time ($p < 0.05$).
[c] Significantly different from baseline value ($p < 0.05$).
[d] LTM: Lean tissue mass.
[e] Determined for forearm pronator muscles.

Figure 6.7 Mean difference (SEM) from baseline values (at 0 months) in muscle strength in the control (●) and casted (○) arms of 10 subjects immediately after the cast removal (1.5 months), at 4.5 months, 7.5 months and 13.5 months. A: Changes in grip strength (kg). B: Changes in lean tissue mass (g). C: Changes in endurance of forearm pronator muscles (Nm).

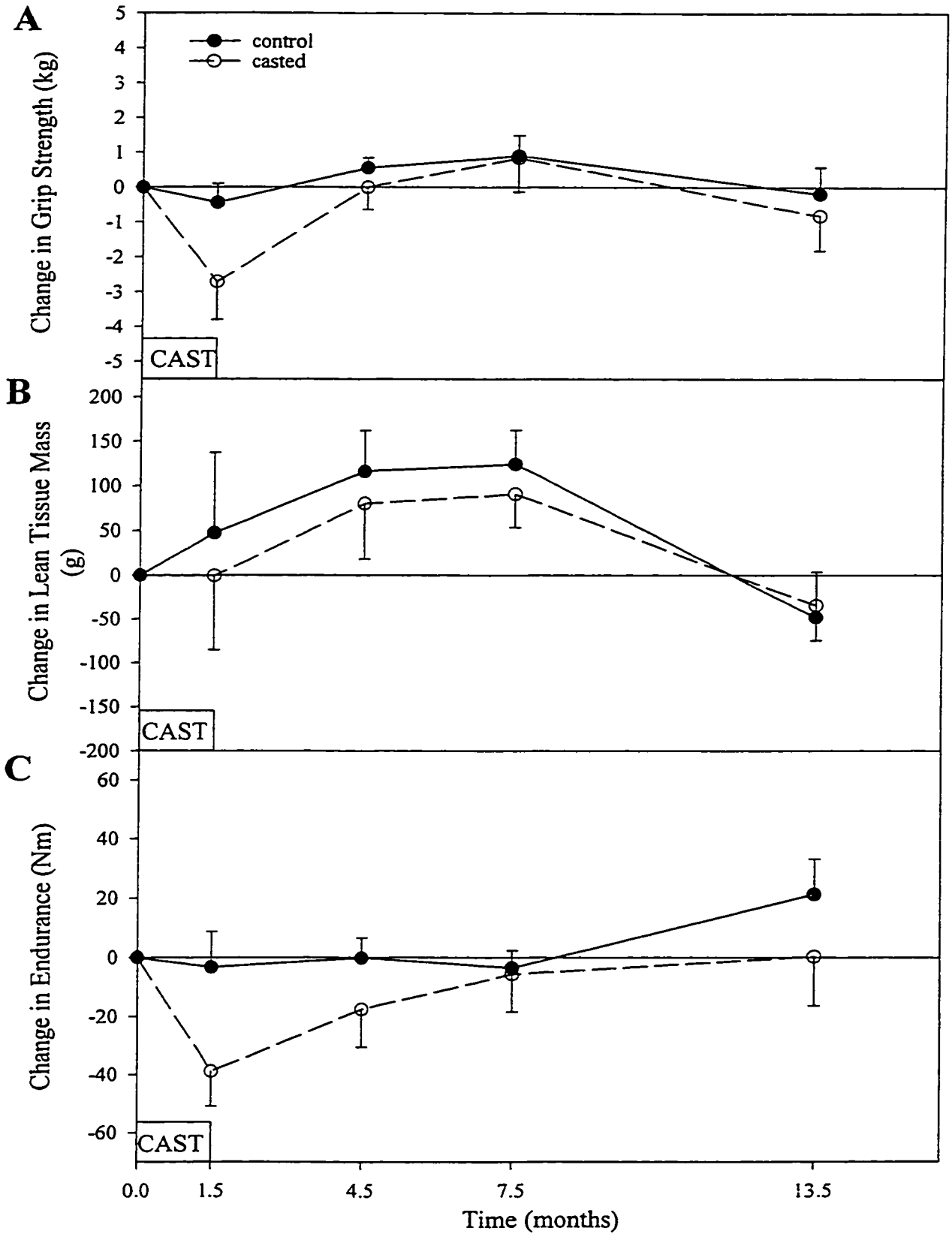
A
control
casted
Change in Grip Strength (kg)
5
4
3
2
1
0
-1
-2
-3
-4
-5
CAST
B
Change in Lean Tissue Mass (g)
200
150
100
50
0
-50
-100
-150
-200
CAST
C
Change in Endurance (Nm)
60
40
20
0
-20
-40
-60
CAST
0.0
1.5
4.5
7.5
13.5
Time (months)

6.4 Discussion

The main finding in this study is that plaster cast immobilization of healthy, young adult, nonweightbearing bone for 6 weeks induces a loss in bone mass and an increase in intertrabecular spacing. Recovery occurs with habitual levels of physical activity; trabecular structure is restored within 3 months whereas bone mass recovers within 1 year. In the mature skeleton, disuse causes an increase in the activation frequency of remodeling sites and a decrease in bone formation (LeBlanc et al. 1987; Jee et al. 1990; Maeda et al. 1993). The increase in maximum pore size in the trabecular network at the ultra distal radius probably is observed due to reduction in trabecular thickness as osteoclastic acitivity increases in concert with a suppression of osteoblastic activity (Maeda et al. 1993). If the dimensions of the thinned trabeculae fall below the resolution of the pQCT scanner, the bone may not be detectable and a larger maximum intertrabecular space may be observed. During the remobilization period, there is increased bone turnover and refilling of bone remodelling units (Young et al. 1986) which restores trabecular thickness to baseline values within 3 months. Young et al. (1986) showed that after a 15 month recovery period following an immobilization period of 6 months, primate weightbearing trabecular bone was not replaced. Likely a 6 week period of cast immobilization of nonweightbearing bone does not cause the loss of entire trabecular elements. Recovery in trabecular bone structure was observed during a period which was about twice the duration of the immobilization period. This observation is further supported by the fact that the structural indices describing the connectivity and

mean hole size of the trabecular network did not change in response to decreased mechanical loading.

In this study, 6 weeks of immobilization did not adversely affect radial bone density but BMC was lost in the total and middle region of the distal radius. Work by others has shown that bone mass is more responsive to physical loading than bone density suggesting that mechanical loading influences bone size (Kannus et al. 1994; Alfredson, Nordström and Lorentzon 1997). The BMC at the distal radius is determined using DXA which is unable to distinguish between cortical and trabecular bone components within the projected image. The middle region of the distal radius contains a smaller fraction of trabecular bone than the ultra distal region (Schlenker and Von Seggan 1976) and no change in response to immobilization was detected at the latter site with DXA nor with pQCT imaging techniques. The extent of immobilization-induced bone loss varies among sites within a given bone (Bourrin et al. 1995; Lane et al. 1996). In the current study the loss of diaphyseal cortical bone is more pronounced than the loss of metaphyseal trabecular bone. However, the changes in trabecular network structure suggest that bone material is lost from both bone compartments in nonweightbearing limbs.

The skeletal changes observed in this study of healthy young adults may be potentiated in individuals who are immobilized post trauma because pain will limit further the use of the arm. In the present study, the elbow joint was not immobilized in order to avoid joint dysfunction. Subjects were instructed to suspend the immobilized limb in a sling during waking hours in order to minimize the loading on the radius due to muscle contraction. Compliance with this was poor and the subjects reported that the arm

was used for some functional tasks such as driving and carrying items. Thus the muscle pull on the radius may have deformed the bone sufficiently such that the strain fell within the normal physiological range. Despite this possibility, immobilization had an adverse effect on mass and structure in healthy nonweightbearing bone. If function was reduced further, larger changes may have been observed.

Normal levels of activity were sufficient for skeletal recovery after 6 weeks of cast immobilization of the nondominant wrist. A number of investigators have reported that the rate of recovery following periods of disuse is positively influenced by physical training (Maeda et al. 1993; Kannus et al. 1994; Sievänen et al. 1994; Bourrin et al. 1995; Lane et al. 1996). In 5 week old rats, controlled physical activity during a 4 week period was required for the recovery of trabecular bone architecture whereas bone mass recovered with normal weightbearing following 2 weeks of hindlimb unloading (Bourrin et al. 1995). Similarly, trabecular thinning and increased intertrabecular spacing in young adult dogs following 16 weeks of forelimb immobilization were reversed during a 32 week remobilization period which involved physical training (Lane et al. 1996). In contrast, 15 months of normal activity was not sufficient for tibial trabecular bone recovery in middle aged primates after a 10 week period of restraint (Young et al. 1986). Discrepancy in the potential for recovery may result from the fact that the extent of bone loss experienced in the nonweightbearing bone of young adults in response to 6 weeks of cast immobilization is small enough that exercise provides no advantage. This seems unlikely, however, since the loss in bone mass was substantial enough to require a long recovery period (almost 9-fold longer than the immobilization period). Alternatively, the

age of the animals studied may explain the differences in the potential for recovery post immobilization. Increased age is associated with bone loss and an increase in the depth of the resorption pits formed on the bone surfaces which is sufficient to perforate trabeculae thereby removing entire structural elements (Young et al. 1986; Mosekilde 1989). Conversely, in the younger skeleton the immobilization-induced bone loss is reversible if the uncoupling of the osteoclasts and osteoblasts causes a thinning of the trabeculae but not perforations.

A number of factors may explain why increased mechanical loading did not accelerate the rate of musculoskeletal recovery in the present study. It is possible that any benefits which may have occurred were undetected in this study due to the small sample size and the poor adherence to the home exercise program. Animal studies suggest that externally loading the adult skeleton 3 to 4 times per week is as effective as daily loading in the stimulation of periosteal bone formation and mineral apposition rate (Raab-Cullen et al. 1994). The subjects in the exercise group in this current study were instructed to perform daily exercises and they reportedly completed the exercise protocol an average of 4.3 days / week. Four of the 5 subjects performed the home program a minimum of 3 times / week during the first 6 months. While this may be sufficient to elicit a skeletal response, the sample size was quite small and no significant group difference was detected. The outcomes were measured immediately following the removal of the cast and then after a recovery period which was twice as long as the immobilization period. In light of the studies of young adult animals described previously, the restoration of bone mass is observed with or without increased physical activity and a positive influence of

exercise on the recovery of bone structure is observed when the remobilization period is equivalent to the period of immobilization. Potentially, the increased physical loading may have had an effect on the rate of recovery which was no longer observed after 3 months of remobilization.

Alternatively, given that remodeling takes 4 to 6 months to complete one cycle, the effect of exercise on rate of bone recovery may not be evident in the first 6 months. It is possible that increased physical loading may have had an effect on the rate of recovery between 6 and 12 months of remobilization. The positive influence of increased mechanical loading is observed in the radius of the control limb. Bone mass is increased in the ultra distal radius 7.5 and 13.5 months after the contralateral limb was immobilized (Figure 6.4B). This pattern probably reflects the influence of increased loading at least during the 6 week immobilization period since this would increase osteoblast activity. About 6 months subsequently the bone would become mineralized and be detectable. Similar changes in the contralateral limb in response to immobilization of weightbearing bones have been observed by others (Lane et al. 1996).

Few studies have investigated the effect of immobilization on muscle function in the upper limb. In the study presented here, an immediate decrease in wrist joint mobility and muscle strength was found post immobilization which recovered rapidly (within 3 months of remobilization). No change in lean tissue mass was associated with disuse. Miles et al. (1994) measured changes in muscle function after 9 days of immobilization of the nondominant upper limb in 12 young adult women and also found that the decrease in muscle strength exceeded the decrease in lean tissue mass (as determined by cross-

sectional area of the forearm muscles). Moreover , isometric muscle strength recovered to within 90% of pre-immobilization values 6 days after resuming habitual activities. It is suggested that the loss of muscle function may be related to neural adaptations during the immobilization period in addition to the loss of contractile proteins. Sale et al. (1982) immobilized the upper limb in 11 healthy young adults for 5 weeks in order to study the neuromuscular response and concluded that neural adaptation contributed to the observed decrease in voluntary muscle strength. Resistive training prior to immobilization (n = 6) attenuated the neuromuscular changes whereas resistive training post immobilization (n = 5) was not as beneficial. These investigations support the findings in the current study where muscle strength was decreased in the immobilized forearm but lean tissue mass was not significantly altered.

The study presented here is one of few which look at musculoskeletal changes due to immobilization of the upper limb. These data demonstrate that 6 weeks of plaster cast immobilization causes an increase in maximum hole size and a loss of bone tissue, joint mobility and muscle strength in healthy nonweightbearing limbs. Normal activity levels are sufficient for complete recovery of bone mass but this requires a remobilization period of 1 year. In contrast, bone structure, joint mobility and muscle strength recover within 3 months of normal activity. Since the recovery of bone mass lags behind that of muscle strength, this study suggests that mechanical loading of the weakened bone may increase the risk of fracture for up to 1 year following a period of disuse.

CHAPTER SEVEN

IN VIVO MEASUREMENTS OF RADIAL BONE STRUCTURE IN INDIVIDUALS WITH LOW BONE DENSITY DISCRIMINATE INDIVIDUALS WITH RECENT WRIST FRACTURES FROM THOSE WITHOUT FRACTURE

7.1 Introduction

When the strength of a bone is insufficient to withstand the forces acting upon it, fracture occurs. Fracture of the distal radius is typically the earliest clinical manifestation of osteoporosis (Owen et al. 1982; Mallmin and Ljunghall 1994). Indeed, fracture of the distal forearm is the most common fracture among women under the age of 75 years (Owen et al. 1982). A number of studies have shown that individuals with distal forearm fractures have significantly lower bone mass compared to normal controls (Jensen et al. 1983; Hesp, Klenerman, and Page 1984; Harma and Karjalaminen 1986; Crilly et al. 1987; Smith et al. 1990; Ooms et al. 1993; Mallmin and Ljunghall 1994; Eastell 1996). On a population basis, fracture risk can be determined by measuring bone mineral density (BMD) at fracture prone sites; however, it is not possible to predict which individual with low BMD will experience a fracture (Marshall, Johnell, and Wedel 1996).

Trabecular bone structure is another determinant of bone strength (Kleerekoper et al. 1985; Mosekilde 1986) and *ex vivo* work has demonstrated that indices of structure at the distal radius significantly predict bone strength on compression loading (Gordon,

Webber, and Nicholson 1998). The purpose of this study is to determine if indices of trabecular structure in the distal radius discriminate individuals who have sustained a low energy fracture of the distal radius from matched controls with no history of fracture.

7.2 Materials and Methods

7.2.1 Subjects

Individuals who attended the St. Joseph's Hospital Fracture Clinic with a recent (< 6 weeks) low energy fracture of the distal radius were recruited for this study. Volunteers (4 men , 32 women) who expressed an interest were contacted for further screening and to arrange an appointment. In 2 volunteers, the fractures resulted from falls from higher than a standing height, the fractured wrist of 1 volunteer was no longer immobilized and 6 others did not attend for the scheduled appointment. Informed consent was obtained from 1 man and 26 women. A control group matched for gender, menopausal status, age (range ± 5 years), trabecular bone density and total bone density was selected from the database of 71 healthy women recruited from the same community to participate in the study of between-limb differences in trabecular bone structure (described in section 5.2.1). The matched control had no history of fracture. All methods and procedures for the study were approved by the McMaster University Research Ethics Board.

7.2.2 Procedure

Before performing the peripheral quantitated computed tomography (pQCT) scans, subjects completed a questionnaire to document age, sex, race, height, weight, hand

dominance and a general health/medical history profile. Menopausal status was determined by self report and natural menopause was defined as the age at which menses first ceased for a period of 12 months. Height and weight were recorded to the nearest 0.1 cm and 0.1 kg, respectively. Body mass index (BMI) was calculated for each subject as the ratio of weight to height in kilograms per meter squared. In the nonfractured forearm, the length of the ulna from the olecranon process to the ulnar syloid was measured to the nearest 0.1 cm using a tape measure.

Scans were performed on the nonfractured forearm of each subject. Care was taken to ensure that the forearm being measured was well supported and positioned appropriately in the imaging field. Volunteers were instructed to remain motionless throughout the scanning procedure which has been described elsewhere (section 3.2.3).

7.2.3 Equipment

The images were acquired at the 4% site of the distal forearm using the Stratec pQCT (XCT 960) scanner as described previously (section 3.2.3) and analyzed to determine measurements of trabecular bone structure (connectivity index, CI; maximum hole size, H_M; mean hole size, H_A), bone density (total compartment, ToBD; cortical compartment, CoBD; trabecular compartment, TrBD), mass (total, ToBMC; cortical, CoBMC; trabecular, TrBMC) and geometry (total, ToBA; cortical, CoBA; trabecular, TrBA; cortical bone area index, CoBA index) as described in Chapter 4 (section 4.2.3).

7.2.4 Statistical Analyses

Descriptive statistics were calculated for anthropometric measurements of the study subjects and all measured variables of bone structure, geometry, mass and density. Comparisons between the group with low energy wrist fractures and the matched control group were made using one way ANOVA and differences were considered significant when $p < 0.05$. The odds ratio was calculated using binary logistic regression to assess the strength of the association between bone structure and fracture risk; in this case, if a decline in bone structure is associated with fracture, the odds ratio rises above 1. The statistical results have been calculated using the statistical package, Minitab (release 11).

7.3 Results

In 3 images, the software was unable to close the cortical ring; therefore, these scans were excluded from further analyses. Two volunteers reported a history of a previous fracture in the currently nonfractured wrist. Figure 7.1A illustrates a typical pQCT image acquired at the 4 % site in the nonfractured distal forearm from a 79 year old woman, whereas Figure 7.1B shows the image acquired at the same site from a 78 year old woman with a previous history of wrist fracture. The previous fracture occurred within the same region as the imaging site, thus the images from the 2 volunteers with previous wrist fractures were discarded. Images of the nonfractured distal radius for 22 volunteers were considered to be satisfactory for analyses and are included in this study.

Figure 7.1 Images acquired at the 4% site using pQCT in the contralateral forearm of 2 women with recent wrist fractures. A: The image of the forearm of a 79 year old woman with no prior wrist fracture. B: The image of the forearm of a 78 year old woman with a prior wrist fracture.

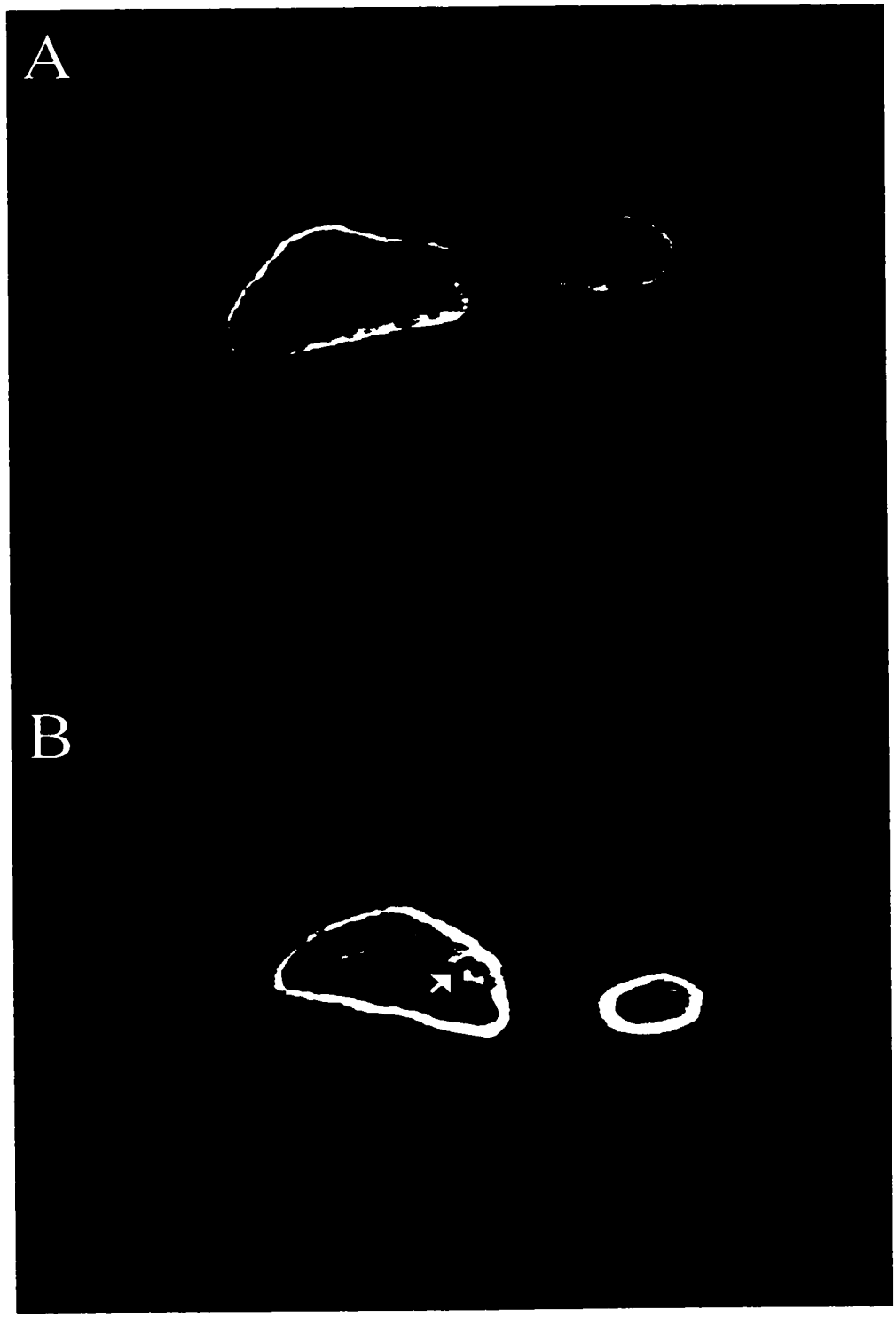
A
B

Table 7.1 summarizes the baseline characteristics of the group of women with recent wrist fractures and the matched control group. No significant difference between groups is observed.

TABLE 7.1

BASELINE CHARACTERISTICS OF THE WOMEN WITH AND WITHOUT A FRACTURE OF THE DISTAL RADIUS [a-d]

Variable	Fracture Group (n = 22)	Control Group (n = 22)
Age (years) [a]	58.69 (2.63)[b]	59.92 (2.61)
BMI (kg • m^2) [a]	26.28 (1.04) [b]	24.66 (0.76)
Right Handed [c]	86% (19)[b]	86% (19)
Postmenopausal [c]	64% (14) [b]	64% (14)
Medication Usage: [c]		
Birth Control Pills	9% (2)	23% (5) [d]
Hormone Replacement Therapy	9% (2)	18% (4) [d]
Didrocal	14 %(3)	0% (0)
Thyroid hormone	18% (4)	0% (0)
Dilantin	5% (1)	0% (0)
Multivitamin	27% (6)	32% (7)
Vitamin D	18% (4)	9% (2)
Calcium	36% (8)	18% (4)
Past Medical History: [c]		
Premature Menopause [e]	18% (4)	0% (0)
Hypothyroidism	14% (3)	0% (0)
Hyperthyroidism	5% (1)	0% (0)
Prior low energy fracture	27% (6)	0% (0)
Family history of osteoporosis	27% (6)	0% (0)
Cancer treated with chemotherapy	9% (2)	0% (0)
Alcohol abuse	5% (1)	0% (0)

[a] Data expressed as mean (SEM)
[b] No significant difference between groups
[c] Data expressed as % (n).
[d] Taken for reasons unrelated to bone loss.
[e] Before the age of 45 years.

Table 7.2 shows the mean (SEM) for each group with respect to bone density, mass and geometry and the p-values for the comparison between groups. There is no statistically significant difference between the two groups.

TABLE 7.2

PQCT MEASUREMENTS OF BONE DENSITY, MASS AND GEOMETRY IN WOMEN WITH AND WITHOUT A FRACTURE OF THE DISTAL RADIUS [a,b]

Variable [a]	Fracture Group (n = 22)	Control Group (n = 22)	p-value [b]
Density (mg/cm^3):			
ToBD	340.5 (15.3)	363.9 (12.5)	0.24
CoBD	633.6 (23.2)	677.3 (23.0)	0.19
TrBD	166.8 (8.06)	187.2 (7.01)	0.06
Mass (mg):			
ToBMC	223.7 (7.82)	244.7 (8.49)	0.08
CoBMC	152.3 (5.84)	164.0 (5.94)	0.17
TrBMC	71.40 (4.55)	80.70 (3.44)	0.11
Geometry (mm^2):			
ToBA	271.5 (12.7)	270.9 (6.89)	0.97
CoBA	97.03 (2.97)	96.99 (1.66)	0.99
TrBA	174.5 (10.7)	173.9 (5.82)	0.97
CoBA Index	0.366 (0.01)	0.360 (0.01)	0.68

[a] Data expressed as mean (SEM)
[b] p-value for 2 sample t-test to compare groups.

Figure 7.2 shows the group mean (SEM) for each of the indices of bone structure. CI and H_M do not differ between groups ($p = 0.17$ and $p = 0.23$, respectively). In contrast, the H_A in the group of women with fracture is larger than in the control group ($p = 0.048$).

Table 7.3 shows the concordance and discordance of the matched pairs with respect to the association between $H_A \geq 6mm^2$ at the 4% site in the distal radius and fracture.

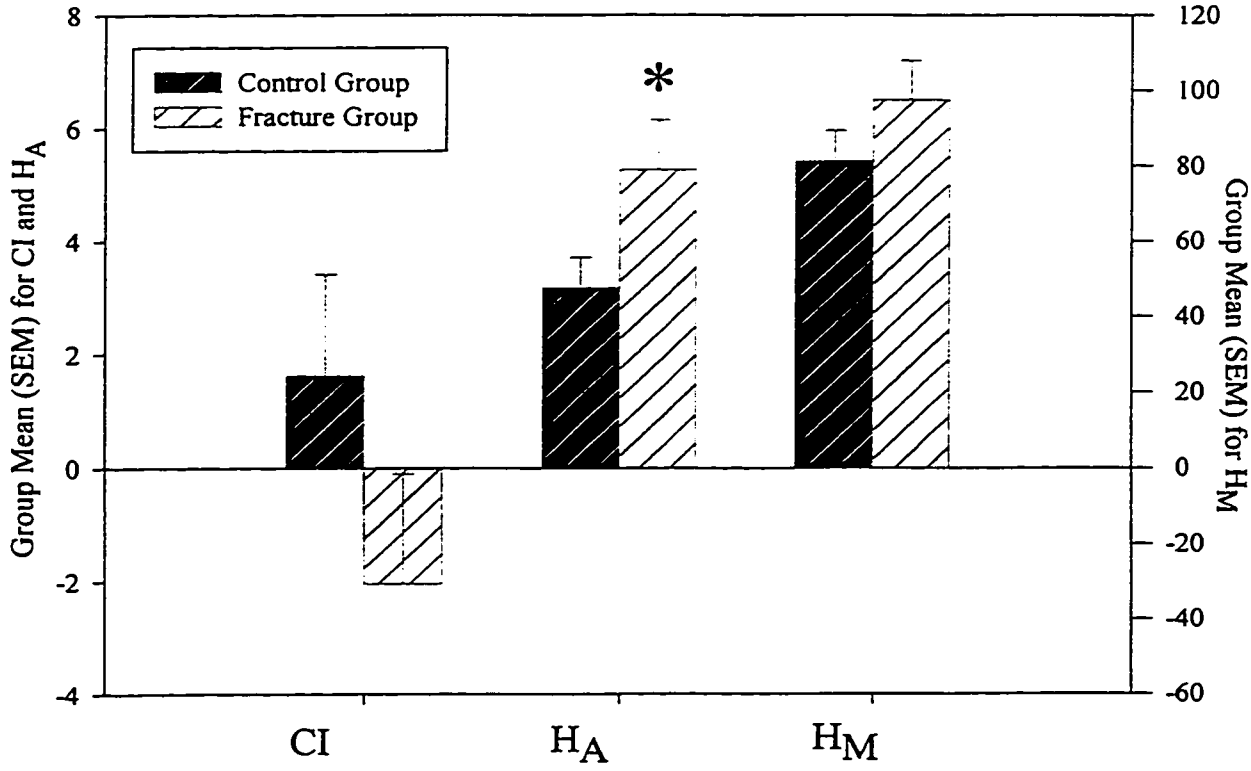

Figure 7.2 Indices of trabecular bone structure at the 4% site of the distal radius in the nonfractured forearm for matched groups of control women (n = 22) and women with recent wrist fractures (n = 22). The left axis displays the values for the group means (SEM) for connectivity index (CI) and mean hole size (H_A). The right axis displays the values for the group means for maximum hole size (H_M). * H_A is significantly greater in the fracture group.

There are 15 concordant pairs; for 13 pairs, both the woman with a wrist fracture and the matched control have $H_A < 6$ mm^2 and for 2 pairs, both the woman with a wrist fracture and the matched control have $H_A \geq 6$ mm^2. There are 7 discordant pairs; for all 7, the woman with the wrist fracture has a $H_A \geq 6$mm^2 and the matched control has a $H_A < 6$ mm^2. There is no discordant pair in which the woman with the wrist fracture has a $H_A < 6$ mm^2 and the matched control has a $H_A \geq 6$mm^2. The odds ratio is 6.9 (95% CI: 1.3 to 37.3), which suggests a significant association between large hole sizes (≥ 6mm^2) and low energy fracture of the distal forearm ($p = 0.02$).

TABLE 7.3

THE ASSOCIATION BETWEEN AVERAGE HOLE SIZE AT THE 4 % SITE OF THE RADIUS AND FRACTURE OF THE DISTAL FOREARM FOR THE MATCHED PAIRS OF SUBJECTS [a]

		Control Group		
		$H_A \geq 6$mm^2	$H_A < 6$mm^2	Total
Fracture Group	$H_A \geq 6$mm^2	2	7	9
	$H_A < 6$mm^2	0	13	13
	Total	2	20	22

[a] H_A : average hole size (mm^2); cut point of ≥ 6mm^2 selected based on sensitivity (41%) and specificity (91%) for discriminating individuals with fractures of the distal forearm.

7.4 Discussion

In individuals with low bone density, the noninvasive measurement of mean hole size in the trabecular network at the 4% site of the distal radius discriminates individuals with recent fractures of the contralateral wrist from individuals with no history of

fracture. Previously, it has been shown that a decrease of 1 SD in BMD as compared to matched young adult mean values is associated with a relative risk for fracture of 1.5 (95% CI: 1.4 to 1.6) (Marshall, Johnell, and Wedel 1996). Currently, the ability to predict who among those with low BMD will experience the potentially severe consequences of fracture is limited. This data suggests that a large average hole size ($\geq$ 6mm^2) is associated with a low energy fracture of the distal forearm with an odds ratio of 6.9 (95% CI: 1.3 to 37.3). Therefore, measurements of bone structure at the 4% site of the radius may facilitate the identification of individuals at risk for fracture of the distal forearm.

The case-control study design used in this investigation has inherent limitations which should be considered when interpreting the results. The results are based on a small number of individuals who attended the fracture clinic with a recent wrist fracture and agreed to return for a subsequent visit in order to participate in this study. First, it is not known how these volunteers differ from the other individuals with recent nontraumatic fracture who did not volunteer to participate in this study. Those who did volunteer may be more mobile and active than those who did not or they may have a particular interest in issues related to health and osteoporosis. If this is the case, the measurements of bone structure may be representative of a more active group of individuals with recent nontraumatic wrist fractures and the trabecular bone structure may be superior to what might be expected in a less active, less health conscious individual. Similarly, the control group of volunteers may not be representative of the general population and may be particularly health conscious and concerned about osteoporosis. Both the control and fracture groups may be composed of individuals who are more

mobile and aware of health issues, yet this study shows that H_A discriminates between the two groups.

There is no significant between-limb difference in measurements of H_A (Table 5.2) and the bilateral measurements of H_A are highly correlated within subjects ($r = 0.87$, Table 5.4). Thus, the evaluation of mean hole size in the nonfractured limb provides a satisfactory estimate of the trabecular bone structure in the fractured limb. This permits early measurement post injury thus avoiding the confounding influences that the fracture and subsequent changes in mechanical usage may introduce. When compared with a control group matched for bone density, the group of individuals with recent wrist fracture have a larger H_A. Since other indices of trabecular bone structure do not discriminate between the groups, it appears that the individuals who sustain low energy fractures have thinner trabeculae. Mosekilde (1988, 1989) identified age-related increases in both intertrabecular spacing and thinning of the horizontally oriented vertebral trabeculae. In addition, an age-related increase in perforations of the trabecular elements was noted in the vertebrae of women over the age of 75 years (Mosekilde 1989). If perforations of the trabecular struts occurred in the fracture group, it is likely that this would be observed as a decrease in connectivity and an increase in maximum hole size as compared to the control group. Such a gender-specific pattern is seen as a function of aging (Table 4.3), but these differences are not observed between the control and fracture groups (Figure 7.2). *Ex vivo*, it has been shown that radial bones with larger intertrabecular spacing fail under lower compressive loading forces (Gordon, Webber, and Nicholson 1998). These data suggest that a generalized thinning of trabeculae is

associated with a decrease in bone strength. The noninvasive assessment of intertrabecular spacing at the distal radius in individuals with low bone mass may improve the diagnostic ability to identify individuals at risk for fractures of the distal forearm.

CHAPTER EIGHT
CONCLUSIONS AND FUTURE DIRECTIONS

The most striking finding of this study is that *in vivo* measurements of trabecular bone structure derived from pQCT imaging at the 4% site of the distal radius discriminate between fracture cases and control subjects with similar bone density. The data from the cross-sectional matched pairs case-control study presented in Chapter 7 shows that when the average diameter of the pQCT-imaged marrow spaces exceeds 6 mm^2, the relative odds that the measurement associated with a fracture at the distal radius is 6.9 (95% CI: 1.3 to 37.3). Currently, fracture risk is predicted using DXA-based measurements of BMD but the predictive power for a particular individual is low since a large overlap in values exists for those with and without osteoporotic fractures (Webber 1998). The amount of mineralized bone (measured as BMD) is one determinant of bone strength and is associated with the amount of compressive force which the bone can withstand before failing.

Others have found that predictive power increased when a combination of factors related to bone quality (i.e., estimates of bone material properties and geometry) are integrated into a single index (bone strength index) compared to measures reflecting material quality alone at the 4% site of the distal radius (Ferretti et al. 1998). The same study also showed that the best predictor of forearm fracture risk was the amount of

mineralized tissue in the trabecular bone compartment (Ferretti et al. 1998). Whereas the *in vivo* assessment of a combination of variables which quantify bone strength may improve the ability to estimate an individual's risk for fracture, the optimal combination has not been identified. Potentially, the combination of BMD and H_A measurements may aid in the early identification of individuals at risk for fracture at the distal forearm, the earliest clinical manifestation of osteoporosis among women.

In vivo measurements of H_A demonstrate the anticipated trends with respect to gender and aging. That is, the average spaces between trabecular elements at the distal radius are larger in women than in men (Table 4.2) and there is a gender-specific increase in mean hole size among aging women (Table 4.3). This is consistent with the fact that most fractures at the distal forearm occur in women around the time of menopause. Interestingly, in the cross-sectional study designed to characterize normal age-related patterns in trabecular bone structure (Chapter 4), four individuals, varying in age from 47 to 75 years, had values for H_A which were identified as statistical outliers which significantly influenced the results. The selection of subjects for generating the normative database was based on self report with respect to skeletal health. Thus, those with outlying values may have asymptomatic, unreported or recent onset medical conditions affecting skeletal health detectable by measurements of H_A.

It would further the understanding of the discriminatory ability of H_A if this work was extended by contacting those individuals with outlying values for H_A and following up on the clinical outcome of fracture and comparing this to the outcome for individuals whose values were included in the normative database. However, the number of subjects

indentified as having outlying values for H_A was very small. Preferably, a random sample of middle aged women categorized as osteopenic and osteoporotic according to BMD values acquired at the spine and radius would be recruited for a prospective study in which *in vivo* measurements of trabecular bone structure would be acquired and the women would be followed for a period of 10 years to determine the prevalence of distal forearm fracture.

The study presented in Chapter 4 is the first to determine normative *in vivo* values for trabecular bone structure at the distal radius. The indices of structure are biologically sensible as evidenced by the expected trends with respect to gender and aging. Men have higher values for CI and lower values for H_M and H_A reflecting a better connected trabecular network at the distal radius compared to women (Table 4.2). The age-related changes in these structural indices also demonstrate a gender difference. The annual rate of decrease in CI is more pronounced for women than for men and the age-related increase in intertrabecular spacing (quantified by H_A and H_M) is significant for women but not for men (Table 4.3). For women, these changes in indices of bone structure occur across the life span as is the case for loss of trabecular bone density, whereas the changes in bone density in the cortical compartment were most pronounced in postmenopausal women. The peak incidence for forearm fracture is among women between the ages of 60 and 70 years (Owen et al. 1982). Thus, trabecular bone structure may be a preferable marker for risk of fracture at the distal radius.

Chapter 5 presents the first study to determine whether pQCT measurements of bone variables in one radius serve as acceptable surrogates for the contralateral radius. Table

5.4 shows that the correlation of side-to-side measurements is satisfactory for all bone variables evaluated with the exception of cortical bone area index and cortical bone density. The findings regarding between-limb differences suggest that trabecular structure is better in the dominant limb than in the nondominant limb. However, it is recommended that follow up measurements for a particular individual be repeated on the same limb since considerable individual variation is observed (Figures 5.2 to 5.4).

This is the first study to investigate the *in vivo* changes in healthy nonweightbearing bone following a 6 week period of cast immobilization. Measurements of bone variables obtained using pQCT were equally sensitive to changes as the bone variable measurements obtained using DXA for comparable regions of the radius. One of the indices of trabecular bone structure (H_M) was sensitive to the reduced mechanical loading and characterized a rapid increase and recovery in maximum hole size within the trabecular network. This suggests that *in vivo* assessment of structural indices may be useful in determining the impact of various interventions and medical conditions. For example, it has been suggested that osteoporotic bone is associated with poor bone alignment post fracture of the distal forearm (Dias et al. 1987). Dias et al. (1987) used x-ray derived measurements of cortical bone width at the 2nd metacarpal to classify individuals as osteoporotic and determined a deformity index based on measurements of skeletal alignment on radiographs. It would be interesting to repeat this work grouping the individuals with distal radial fractures according to the World Health Organization's diagnostic criteria for osteoporosis (1994), using the same technique for quantifying

deformity, and evaluating indices of trabecular bone structure to determine the relation between bone quality and recovery post fracture.

A limitation in using indices of trabecular bone structure for diagnostic or evaluative purposes may be the negative influence which movement has on the reproducibility of the measurements as shown in Chapter 3. The finding that movement resulted in unreliable measurements has been commented on before (Sievänen et al. 1998) but no data has been published previously which characterizes this observation. As a consequence of controlled movement, the software was unable to close the cortical ring. The impact of movement on the data presented in Chapters 4 to 7 is minor. The software could not close the cortical ring in only 11 out of 407 pQCT images acquired for this thesis work. The images which were affected belonged to individuals between the ages of 63.6 and 72.4 years and may reflect age-related changes in proprioception. The required scanning time has been reduced in the latest model of the pQCT (Sievänen et al. 1998) and this should reduce the number of scans which must be eliminated due to the negative influence of movement.

While there are many factors which contribute to fracture risk, anything which compromises bone strength will increase the likelihood that the bone will break. Consequently, *in vivo* measurements of variables which quantify radial bone strength should improve the ability to identify individuals at risk for forearm fracture. One determinant of bone strength is the spatial arrangement of mineralized tissue which can be characterized using the pQCT-derived indices of trabecular bone structure proposed by Gordon et al. (1996). These *in vivo* measurements of structure are obtained at the 4% site

in the distal radius. This site is clinically relevant as it is the location of the majority of forearm fractures resulting from minimal trauma (Eastell 1996). Although the strength of the bone is probably more closely related to the 3 dimensional spatial arrangement, the indices of structure derived from pQCT images acquired in the transverse plane with an in-plane resolution of 0.36 mm and a slice thickness of 2.5 mm appear to reflect architectural qualities relevant to bone strength. *In vitro* studies are required to determine the relation between these measurements of trabecular structure at the distal radius and the amount of loading force the bone can withstand before failing. The studies presented herein suggest that this technique offers a reliable noninvasive method of characterizing the integrity of the trabecular network at the distal radius and may aid in the diagnosis of osteoporosis in individuals prior to the clinical manifestation of fracture.

APPENDIX 1. LETTERS OF PERMISSION

May 25, 1999

The Humana Press Inc.
999 Riverview Drive,
Suite 208,
Totowa, NJ 07512

Dear Publisher,

I am completing a Ph.D. thesis at McMaster University entitled "*In vivo* assessment of the impact of aging, mechanical loading, and fracture upon radial bone trabecular structure". I would like your permission to reprint portions of the following journal article in my thesis.

Gender differences in Normal Age-Dependent Patterns of Radial Bone Structure and Density: A Cross-Sectional Study Using Peripheral Quantitative Computed Tomography.
Journal of Clinical Densitometry 1999; 2(2): in press.

Please note that I am first author of this work co-authored by Drs. JD Adachi and CE Webber.

I am also requesting that you grant irrevocable, non-exclusive licence to McMaster University and to the National Library of Canada to reproduce this material as part of the thesis. Proper acknowledgement of your copyright of the reprinted material will be given in the thesis.

If these arrangements meet with your approval, please sign where indicated below and return this letter to me in the enclosed envelope. Thank you very much.

Sincerely,
Norma MacIntyre

Norma J. MacIntyre

PERMISSION GRANTED FOR THE USE REQUESTED ABOVE

The Humana Press Inc

Authorized By: Wendy A Warren WENDY A. WARREN

Title: PERMISSIONS

Date: 6/8/99

July 12, 1999

The Humana Press Inc.
999 Riverview Drive,
Suite 208,
Totowa, NJ 07512

Dear Permissions Officer,

I am completing a Ph.D. thesis at McMaster University entitled "The relation between radial bone structure and gender, aging, mechanical loading, and fracture". I would like your permission to reprint the following journal article in my thesis.

Structural Differences Between Dominant and Nondominant Radii are Detected *In Vivo* Using Peripheral Quantitative Computed Tomography. *Journal of Clinical Densitometry* 1999; 2(4): in press.

Please note that I am first author of this work co-authored by Drs. JD Adachi and CE Webber.

I am also requesting that you grant irrevocable, non-exclusive license to McMaster University and to the National Library of Canada to reproduce this material as part of the thesis. Proper acknowledgement of your copyright of the reprinted material will be given in the thesis.

If these arrangements meet with your approval, please sign where indicated below and return this letter to me in the enclosed envelope. Thank you very much.

Sincerely,

Norma MacIntyre

PERMISSION GRANTED FOR THE USE REQUESTED ABOVE
The Humana Press Inc.

Authorized By: Wendy A. Wahle HUMANA PRESS, INC

Title: Marketing Assistant / Permissions

Date: 7/28/99

APPENDIX 2. COMPONENTS OF THE HOME EXERCISE DEVICE

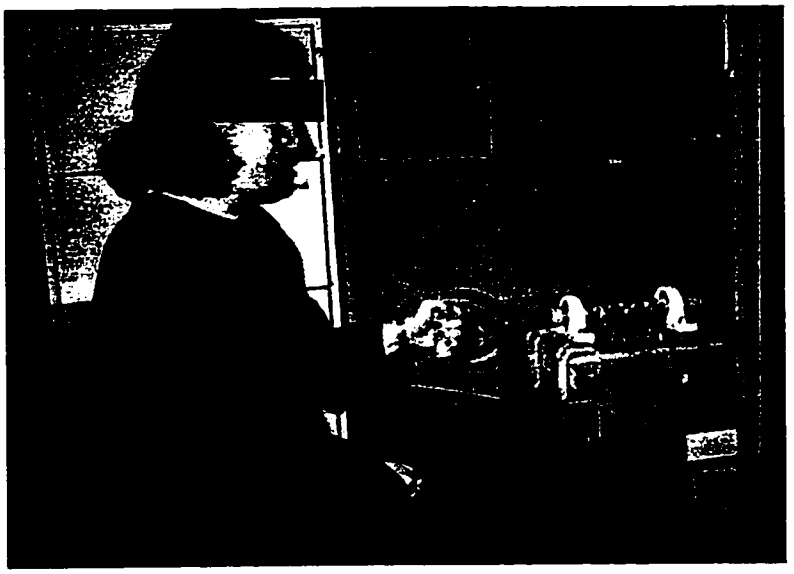

A subject demonstrates the resisted forearm pronation exercise using the home exercise device. The development of the device design was possible due to the assistance of Dr. C.J. Blimkie, Dr. C.E. Webber, John Moroz and Ray Cunningham. Mr. Bob Fraser constructed all of the exercise devices used in the study described in Chapter 6.

REFERENCES

Alfredson H, Nordström P, Lorentzon R. (1997) Bone mass in female volleyball players: a comparison of total and regional bone mass in female volleyball players and nonactive females. Calcif Tissue Int. **60**:338-342.

Alfredson H, Nordstörm P, Pietilia T, Lorentzon R. (1998) Long term loading and regional bone mass of the arm in female volleyball players. Calcif Tissue Int. **62**:303-308.

Aloia JF, Cohn SH, Ostuni JA, Cane R, Ellis K. (1978) Prevention of involutional bone loss by exercise. Ann Intern Med. **89**:356-358.

Amstutz HC, Sissons HA. (1969) The structure of the vertebral spongiosa. J Bone Joint Surg [Br]. **51**:540-50.

Augat P, Fan B, Lane NE, Lang TF, LeHir P, Lu Y, Uffmann M, Genant HK. (1998) Assessment of bone mineral at appendicular sites in females with fractures of the proximal femur. Bone. **22**:395-402.

Augat P, Fuerst T, Genant HK. (1998) Quantitative bone mineral assessment at the forearm: a review. Osteoporos Int. **8**:299-310.

Bagi CM Miller SC. (1994) Comparison of osteopenic changes in cancellous bone

induced by ovariectomy and /or immobilization in adult rats. Anat Rec. **239**:243-253.

Bassey EJ, Ramsdale SJ. (1995) Weight-bearing exercise and ground reaction forces: a 12-month randomized controlled trial of effects on bone mineral density in healthy postmenopausal women. Bone. **16**:469-476.

Bauer DC, Browner WS, Cauley JA, Orwoll ES, Scott JC, Black DM, Tao JL, Cummings SR. (1993) Factors associated with appendicular bone mass in older women. Ann Intern Med. **118**(9):657-665.

Bérard A, Bravo G, Gauthier P. (1997) Meta-analysis of the effectiveness of physical activity for the prevention of bone loss in postmenopausal women. Osteoporos Int. **7**:331-337.

Berg HE, Dudley GA, Haggmark T, Ohlsen H, Tesch PA. (1991) Effects of lower limb unloading on skeletal muscle mass and function in humans. J Appl Physiol. **70**(4):1882-1885.

Beverly M, Rider T, Evans M, Smith R. (1989) Local J Bone Miner Res.ponse to brief exercise that stresses the skeleton. Brit Med J. 299:233-235.

Bevier W, Wiswell R, Pyka G, Kozak K, Newhall K, Marcus R. (1989) Relationship of body composition, muscle strength, and aerobic capacity to bone mineral density in older men and women. J Bone Miner Res. **4**(3):421-432.

Biewener AA, Fazzalari NL, Konieczynski DD, Baudinette RV. (1996) Adaptive changes in trabecular architecture in relation to functional strain patterns and disuse. Bone. **19**:1-8.

Black DM, Cummings SR, Genant HK, Nevitt MC, Palermo L, Browner W. (1992) Axial and appendicular bone density predict fractures in older women. J Bone Miner Res. 7:633-638.

Bland JM, Altman DG. (1986) Statistical methods for assessing agreement between two methods of clinical measurement. Lancet. 1:307-310.

Bloomfield SA. (1997) Changes in musculoskeletal structure and function with prolonged bed rest. Med Sci Sports Exerc. **29**(2):197-206.

Bonjour JP, Theintz G, Buchs B, Slosman D, Clavien H, Rizzoli R. (1993) Variation in spinal and femoral bone mass gain, energy and calcium intake during adolescence. Osteoporos Int. **3**(Suppl 1):S67-S68.

Boone DC, Azen SP, Lin CM, Spence C, Baron C, Lee L. (1978) Reliability of goniometric measurements. Phys Ther. **58**:1355-1360.

Boonen S, Cheng XG, Nijs J, Nicholson PH, Verbeke G, Lesaffre E, Aerssens J, Dequeker J. (1997) Factors associated with cortical and trabecular bone loss as quantified by peripheral computed tomography (pQCT) at the ultradistal radius in aging women. Calcif Tissue Int. **60**:164-170.

Bourrin S, Palle S, Genty C, Alexandre C. (1995) Physical exercise during remobilization restores a normal bone trabecular network after tail suspension-induced osteopenia in young rats. J Bone Miner Res. **10**(5):820-828.

Bouxsein ML, Myburgh KH, van der Meulen MCH, Lindenberger E, Marcus R. (1994) Age-related differences in cross-sectional geometry of the forearm bones in healthy women. Calcif Tissue Int. **54**:113-118.

Burr D, Martin R. (1983) The effects of composition, structure and age on the torsional properties of the human radius. J Biomech. **16**:603-608.

Burr DB, Martin RB. (1989) Errors in bone remodeling: toward a unified theory of metabolic bone disease. Am J Anat. **186**(2):186-216.

Butz S, Wuster C, Scheidt-Nave C, Gotz M, Ziegler R. (1994) Forearm BMD as measure by peripheral quantitative computed tomography (pQCT) in a German reference population. Osteoporos Int. **4**:179-184.

Calbert JAL, Moysi JS, Dorado C, Rodriguez LP. (1998) Bone mineral content and density in professional tennis players. Calcif Tissue Int. **62**:491-496.

Cameron JR, Sorenson JA (1963) Measurement of bone mineral in vivo: An improved method. Science. **142**:230-232.

Carter DR, van der Meulen MCH, Beaupré GS. (1996) Mechanical factors in bone

growth and development. Bone. **18**:5S-10S.

Chilibeck P, Calder A, Sale DG, Webber C. (1993) Reproducibility of dual -energy x-ray absorptiometry. Can Assoc Radiol J. **45**(4):297-302.

Chilibeck PD, Sale DG, Webber CE. (1995) Exercise and bone mineral density. Sports Med. **19**:103-122.

Collet P, Uebelhart D, Vico L, Moro L, Hartmann D, Roth M, Alexandre C. (1997) Effects of 1- and 6-month spaceflight on bone mass and biochemistry in two humans. Bone. **20**:547-51.

Colletti LA, Edwards J, Gordon L, Shary J, Bell NH. (1989) The effects of muscle-building exercise on bone mineral density of the radius, spine, and hip in young men. Calcif Tissue Int. **45**:12-14.

Consensus Development Conference. (1993) Prophylaxis and Treatment of Osteoporosis. Am J Med. **94**:646-650.

Cortet B, Dubois P, Boutry N, Bourel P, Cotton A, Marchandise X. (1999) Image analysis of the distal radius trabecular network using computed tomography. Osteoporos Int. **9**:410-419.

Crilly RG, Delaquerriere Richardson L, Roth JH, Vandervoort AA, Hayes KC, Mackenzie RA. (1987) Postural stability and colles' fracture. Age Ageing. **16**:133-

138.

Cummings SR, Black DM, Nevitt MC, Browner W, Cauley J, Ensrud K, Genant HK, Palermo L, Scott J, Vogt TM. (1993) Bone density at various sites for prediction of hip fractures. The study of osteoporotic fractures research group. Lancet. **341**:72-75.

Currey JD. (1998) Mechanical properties of vertebrate hard tissues. Proc Inst Mech Eng [H]. **212**(6):399-411.

Düppe H, Gardsell P, Johnell O, Nilsson BE, Ringsberg K. (1997) Bone mineral density, muscle strength and physical activity. Acta Orthop Scand. **68**(2):97-103.

Dai LY, Chen DY, Wu DS, Wen Y. (1998) Osteoporosis in colles fracture. Arch Orthop Traum Surg. **117**:65-67.

Dias JJ, Wray CC, Jones JM. (1987) Osteoporosis and colles' fractures in the elderly. J Hand Surg [Br]. **12**:57-59.

Earnshaw SA, Cawte SA, Worley A, Hosking DJ. (1998) Colles' fracture of the wrist as an indicator of underlying osteoporosis in postmenopausal women: a prospective study of bone mineral density and bone turnover rate. Osteoporos Int. **8**:53-60.

Eastell R, Riggs BL, Wahner HW, O'Fallen WM, Amadio PC, Melton LJ. (1989) Colles' fracture and bone density of the ultradistal radius. J Bone Miner Res. **4**:607-613.

Eastel R. (1996) Forearm fracture. Bone. **18**:203S-207S.

Ebbesen EN, Thomsen JS, Mosekilde Li. (1997) Nondestructive determination of iliac crest cancellous bone strength by pQCT. Bone. **21**(6):535-540.

Eiken P, Kolthoff N, Barenholdt O, Hermansen F, Nielsen SP. (1994) Switching from SCA pencil-beam to fan-beam. II: Studies in vivo. Bone. **15**:671-676.

Eisman JA, Kelly PJ, Morrison NA, Pocock NA, Yeoman R, Birmingham J, Sambrook PN. (1993) Peak bone mass and osteoporosis prevention. Osteoporos Int. **1**:S56-60.

Faulkner KG, Gluer CC, Majumdar S, Lang P, Engelke K, Genant HK (1991) Non invasive measurements of bone mass, structure and strength. Current methods and experimental techniques. Am J Roentgenol. **157**:1229-1237.

Ferretti JL. (1995) Perspectives of pQCT technology associated to biomechanical studies in skeletal research employing rat models. Bone. **17**(Suppl):353-364.

Ferretti JL, Capozza RF, Zanchetta JR. (1996) Mechanical validation of a tomographic (pQCT) index for noninvasive estimation of rat femur bending strength. Bone. **18**:97-102.

Ferretti JL, Schneider P, Capozza RF, Braun M, Reiners C. (1997) Relatvie fracture risk

curves for the human distal radius calculated from pQCT determinations. J Bone Miner Res. **12**(Suppl):S264 (abstract).

Ferretti JL, Capozza RF, Cointry GR, Garcia SL, Plotkin H, Alvarez Filgueira ML, Zanchetta JR. (1998) Gender-related differences in the relationship between densitometric values of whole-body bone mineral content and lean body mass in humans between 2 and 87 years of age. Bone. **22**(6):683-690.

Ferretti JL. (1998) Biomechanical properties of bone. In: Genant HK, Guglielmi G, Jergas M (ed.) Bone Densitometry and Osteoporosis. (Springer-Verlag: Berlin Heidelberg New York) pp143-161.

Frost HM. (1981) The regional acceleratory phenomenon. Orth Clin N Amer. **12**:725-726.

Frost HM. (1987) Bone "mass" and the "mechanostat": a proposal. Anat Rec. **219**:1-9.

Frost HM. (1988) Vital biomechanics: proposed general concepts for skeletal adaptations to mechanical usage. Calcif Tissue Int. **42**:145-56.

Frost HM. (1996) A proposed general model of the mechanostat: Suggestions from a new paradigm. Anat Rec. **244**:139-142.

Frost HM, Ferretti JL, Jee WS. (1998) Perspectives: some roles of mechanical usage, muscle strength, and the mechanostat in skeletal physiology, disease, and research.

Calcif Tissue Int. **62**:1-7.

Gärdsell P, Johnell O, Nilsson BE. (1989) Predicting fractures in women using forearm bone densitometry. Calcif Tissue Int. **44**:235-242.

Gärdsell P, Johnell O, Nilsson BE. (1991) The predictive value of bone loss for fragility fractures in women: a longitudinal study over 15 years. Calcif Tissue Int. **49**:90-94.

Garland DE, Stewart CA, Adkins RH, Hu SS, Rosen C, Liotta FJ, Weinstein DA. (1992) Osteoporosis after spinal cord injury. J Orthop Res. **10**:371-378.

Garn SM. (1972) The course of bone gain and the phases of bone loss. Orthop Clin North Am. **3**:503-520.

Gasser JA. (1995) Assessing bone quantity by pQCT. Bone. **17**(Suppl):145-154.

Gatti D, Rossini M, Zamberlan N, Braga V, Fracassi E, Adami S. (1996) Effect of aging on trabecular and compact bone components of proximal and ultradistal radius. Osteoporos Int. **6**:355-360.

Genant HK, Engelke K, Fuerst T, Gluer CC, Grampp S, Harris ST, Jergas M, Lang T, Lu Y, Majumdar S, Mathur A, Takada M. (1996) Noninvasive assessment of bone mineral and structure: state of the art. J Bone Miner Res. **11**(6):707-730.

Glüer CC, Blake G, Lu Y, Blunt BA, Jergas M, Genant HK. (1995) Accurate assessment of precision errors: how to measure the reproducibility of bone densitometry techniques, Osteoporos Int. **5**:262-270.

Goeree R, O'Brien B, Pettit D, Cuddy L, Ferraz M, Adachi J. (1996) An assessment of the burden of illness due to osteoporosis in Canada. Journal of the Society for Obstetrics and Gynaecology of Canada. **18**(Suppl):15-24.

Goodship AE, Lanyon LE, McFie H. (1979) Functional adaptation of bone to increased stress. An experimental study. J Bone Joint Surg [Am]. **61**:539-46.

Gordon CL, Webber CE, Adachi JD, Christoforou N. (1996) In vivo assessment of trabecular bone structure at the distal radius from high-resolution computed tomography images. Phys Med Biol. **41**:495-508.

Gordon CL (1997) In Vivo Assessment of Trabecular Bone Structure at the Distal Radius. PhD Thesis. McMaster University, Hamilton, Ontario.

Gordon C, Webber CE, Christoforou N, Nahmias C. (1997) In vivo assessment of trabecular bone structure at the distal radius from high-resolution magnetic resonance images. Med Phys. **24**(4):585-593.

Gordon CL, Webber CE, Nicholson PS. (1998) Relation between image-based assessment of distal radius trabecular structure and compressive strength. Can Assoc Radiol J. **49**:390-397.

Grampp S, Lang P, Jergas M, Glüer CC, Mathur A, Engelke K, Genant HK. (1995) Assessment of the skeletal status by peripheral quantitative computed tomography of the forearm: short-term precision in vivo and comparison to dual X-ray absorptiometry. J Bone Miner Res. **10**:1566-76.

Gunnes M, Lehmann EH. (1996) Physical activity and dietary constituents as predictors of forearm cortical and trabecular bone gain in healthy children and adolescents: a prospective study. Acta Pædiatr. **85**:19-25.

Haapasalo H, Kannus P, Sievänen H, Heinonen A, Oja P, Vuori I. (1994) Long-term unilateral loading and bone mineral density and content in female squash players. Calcif Tissue Int. **54**:249-255.

Haidekker MA, Andresen R, Werner HJ. (1999) Relationship between structural parameters, bone mineral density and fracture load in lumbar vertebra, based on high-resolution computed tomography, quantatative computed tomography and compression tests. Osteoporos Int. **9**:433-440.

Halioua L, Anderson JJ. (1990) Age and anthropometric determinants of radial bone mass in premenopausal Caucasian women: a cross-sectional study. Osteoporos Int. **1**:50-55.

Hangartner TN. (1995) Osteoporosis due to disuse. Phys Med Rehabil Clin N Am. **6**:579-594

Hansson T, Roos B. (1986) Age changes in the bone mineral of the lumbar spine in

normal women. Calcif Tissue Int. **38**:249-51.

Harma M, Karjalainen P. (1986) Trabecular osteopenia in Colles' fracture. Acta Orthop Scand. **57**:38-40.

Hasegawa Y, Kushida K, Yamazaki K, Inoue T. (1997) Volumetric bone mineral density using peripheal quantitative computed tomography in Japanese women. Osteoporos Int. **7**:195-199.

Hawker G. (1996) Bone biology and the investigation of osteoporosis. Journal of the Society for Obstetrics and Gynaecology of Canada. **18**(Suppl):1-6.

Heaney RP, Barger-Lux MJ, Davies KM, Ryan RA, Johnson ML, Gong G. (1997) Bone dimensional change with age: interactions of genetic, hormonal, and body size variables. Osteoporos Int. **7**:426-31.

Henderson KN, Price RI, Cole JH, Gutteridge DH, Bhagat CI. (1995) Bone density in young women is associated with body weight and muscle strength but not dietary intakes. J Bone Miner Res. **10**(3):384-393.

Hernández ER, Revilla M, Seco-Durban C, Villa LF, Cortes J, Rico H. (1997) Heterogeneity of trabecular and cortical postmenopausal bone loss: a longitudinal study with pQCT. Bone. **20**(3): 283-287.

Hesp R, Klenerman L, Page L. (1984) Decreased radial bone mass in Colles' fracture.

Acta Orthop Scand. **55**:573-575.

Hinsenkamp M, Burny F, Bourgois R, Donkerwolce M. (1981) In vivo bone strain measurements: clinical results, animal experiments, and a proposal for a study of bone demineralization in weightlessness. Aviation, Space, and Environmental Medicine. **52**(2):95-103.

Horger MM. (1990) The reliability of goniometric measurements of active and passive wrist motions. Am J Occup Ther. **44**:342-348.

Hui SL, Johnston CC Jr, Mazess RB. (1985) Bone mass in normal children and young adults. Growth. **49**:34-43.

Hui SL, Slemenda CW, Johnston CC. (1988) Age and bone mass as predictors of fracture in a prospective study. J Clin Invest. **81**:1804-1809.

Johnston CC Jr, Slemenda CW. (1993) Determinants of peak bone mass. Osteoporos Int. **3**(Suppl 1):54-55.

Kannus P, Haapasalo H, Sievänen H, Oja P, Vuori I. (1994) The site-specific effects of long-term unilateral activity on bone mineral density and content. Bone. **15**:279-284.

Kannus P, Sievänen H, Jarvinen TLN, Jarvinen M, Kvist M, Oja P, Vouri I, Jozsa L. (1994) Effects of free mobilization and low-to high-intensity treadmill running on the immobilization-induced bone loss in rats. J Bone Miner Res. **9**(10):1613-1619.

Kannus P, Haapasalo H, Sankelo M, Sievänen H, Pasanen M, Heinonen A, Oja P, Vuori I. (1995) Effect of starting age of physical activity on bone mass in the dominant arm of tennis an squash players. Ann Intern Med. **123**:27-31.

Kannus P, Sievänen H, Vuori I. (1996) Physical loading, exercise, and bone. Bone **18**:1S-3S.

Kelly PJ, Twomey L, Sambrook PN, Eisman JA. (1990) Sex differences in peak adult bone mineral density. J Bone Miner Res. **5**:1169-1175.

Kelly TL, Crane G, Baran DT. (1994) Single x-ray absorptiometry of the forearm: precision, correlation, and reference data. Calcif Tissue Int. **54**:212-218.

Kerr D, Morton A, Dick I, Prince R. (1996) Exercise effects on bone mass in postmenopausal women are site-specific and load-dependent. J Bone Miner Res. **11**(2):218-225.

Kleerekoper M, Villanueva AR, Stanciu J, Rao DS, Parfitt AM. (1985) The role of three-dimensional trabecular microstructure in the pathogenesis of vertebral compression fractures. Calcif Tissue Int. **37**:594-597.

Kochersberger G, McConnell E, Kuchibhatla MN, Pieper C. (1996) The reliability, validity and stability of a measure of physical activity in the elderly. Arch Phys Med Rehab. **77**:793-795.

Kohrt WM, Ehsani AA, Birge SJ. (1997) Effects of exercise involving predominantly either joint-reaction or ground-reaction forces on bone mineral density in older women. J Bone Miner Res. **12**(8):1253-1261.

Kritz-Silverstein D, Barrett-Connor E. (1994) Grip strength and bone mineral density in older women. J Bone Miner Res. **9**(1) 45-51.

Krølner B, Pors Nielsen S. (1982) Bone mineral content of the lumbar spine in normal and osteoporotic women: cross-sectional and longitudinal studies. Clin Sci. **62**:329-36.

Krølner B, Toft B, Pors Nielsen S, Tondevold E. (1983) Physical exercise as prophylaxis against involutional vertebral bone loss: a controlled trial. Clin Sci. **64**:541-6.

Laib A, Rüegsegger P. (1999) Calibration of trabecular bone structure measurements of in vivo three-dimensional peripheral quantitative computed tomography with 28-um-resolution microcomputed tomography. Bone. **24**(1):35-39.

Lane NE, Kaneps AJ, Stover SM, Modin G, Kimmel DB. (1996) Bone mineral density and turnover following forelimb immobilization and recovery in young adult dogs. Calcif Tissue Int. **59**:401-406.

Lanyon LE, Goodship AE, Pye CJ, MacFie JH. (1982) Mechanically adaptive bone remodelling. J Biomech. **15**:141-154.

Lanyon LE, Rubin CT. (1984) Static versus dynamic loads as an influence on bone remodelling. J Biomech. **17**:892-905.

Lanyon L. (1987) Functional strain in bone tissue as an objective, and controlling stimulus for adaptive bone remodelling. J.Biomech. **20**(11/12):1083-1093.

Lanyon L. (1992) The success and failure of the adaptive response to functional load-bearing in averting bone fracture. Bone. **13**:S17-S21.

Lanyon LE. (1996) Using functional loading to influence bone mass and architecture: objectives, mechanisms, and relationship with estrogen of the mechanically adaptive process in bone. Bone. **18**:37S-343S.

Leblanc A, Schneider VS, Krebs J, Evans H, Jhingran S, Johnson P. (1987) Spinal bone mineral after 5 weeks of bed rest. Calcif Tissue Int. **41**:259-261.

Leblanc AD, Schneider VS, Evans HJ, Engelbretson DA, Krebs JM. (1990) Bone mineral loss and recovery after 17 weeks of bed rest. J Bone Miner Res. **5**(8):843-850.

Leboff MS, Fuleihan GE, Angell JE, Chung S, Curtis K. (1992) Dual-energy x-ray absorptiometry of the forearm: reproducibility and correlation with single-photon absorptiometry. J Bone Miner Res. **7**:841-846.

Leterme D, Casasnovas B. (1999) Adaptation of rat lateral gastrocnemius muscle motor units during hindlimb unloading. Eur J Appl Physiol. **79**:312-317.

Li XJ, Jee WSS, Chow JSY, Woodbury Dm. (1990) Adaptation of cancellous bone to aging and immobilization in the rat: a single photon absorptiometry and histomorphometry study. Anat Rec. **227**:12-24.

Löfman O, Larsson L, Ross I, Toss G, Berglund K. (1997) Bone mineral density in normal Swedish women. Bone. **20**(2):167-174.

Lohman T, Going S, Pamenter R, Hall M, Boyden T, Houtkooper L, Ritenbaugh C, Bare L, Hill A, Aickin M. (1995) Effects of resistance training on regional and total bone mineral density in premenopausal women: a randomized prospective study. J Bone Miner Res. **10**(7):1015-1024.

Louis O, Willnecker J, Soykens S, Van den Winkel P, Osteaux M. (1995) Cortical thickness assessed by peripheral quantitative computed tomography: accuracy evaluated on radius specimens. Osteoporos Int. **5**:446-449.

MacDougall JD, Ward GR, Sale G, Sutton JR. (1977) Biochemical adaptation of human skeletal muscle to heavy resistance training and immobilization. J. Appl. Physiol.: Respirat. Environ. Exercise Physiol. **43**(4):700-703.

MacDougall JD, Elder GCB, Sale DG, Moroz JR, Sutton JR. (1980) Effects of strength training and immobilization on human muscle fibres. Eur J Appl Physiol. **43**:25-34.

MacIntyre NJ, Adachi JD, Webber CE. (1999) Gender differences in normal age-dependent patterns of radial bone structure and density: A cross-sectional study using

peripheral quantitative computed tomography. Journal of Clinical Densitometry. **2**:163-173

Maeda H, Kimmel DB, Raab DM, Lane NE. (1993) Musculoskeletal recovery following hindlimb immobilization in adult female rats. Bone. **14**:153-159.

Majumdar S, Newitt D, Mathur A, Osman D, Gies A, Chiu E, Lotz J, Kinney J, Genant H. (1996) Magnetic resonance imaging of the trabecular bone structure in the distal radius: relationship with x-ray tomographic microscopy and biomechanics. Osteoporos Int. **6**:376-385.

Majumdar S, Genant HK, Grampp S, Newitt DC, Truong V-H, Lin JC, Mathur A. (1997) Correlation of trabecular bone structure with age, bone mineral density, and osteoporotic status: in vivo studies in the distal radius using high resolution magnetic resonance imaging. J Bone Miner Res. **12**(1):111-118.

Mallmin H, Ljunghall S. (1994) Distal radius fracture is an early sign of general osteoporosis: bone mass measurements in a population-based study. Osteoporos Int. **4**:357-361.

Marshall D, Johnell O, Wedel H. (1996) Meta-analysis of how well measures of bone mineral density predict occurance of osteoporotic fractures. Brit Med J. **312**:1254-1259.

Martin D, Notelovitz M (1993) Effects of aerobic training on bone mineral density of

postmenopausal women. J Bone Miner Res. **8**:931-6.

Martin JC, Reid DM. (1999) Radial bone mineral density and estimated rates of change in normal Scottish women: assessment by peripheral quantitative computed tomography. Calcif Tissue Int. **64**:126-132.

Mathiowetz V, Weber K, Volland G, Kashman N. (1984) Reliability and validity of grip and pinch strength evaluations. J Hand Surg **9A**:222-226

Matkovic V, Jelic T, Wardlaw GM, Ilich JZ, Goel PK, Wright JK, Andon MB, Smith KT, Heaney RP. (1994) Timing of peak bone mass in caucasian females and its implication for the prevention of osteoporosis. J Clin. Invest. **93**:799-808.

Mazess RB, Barden HS. (1988) Measurement of bone by dual-photon absorptiometry (DPA) and dual-energy X-ray absorptiometry (DEXA). Ann Chir Gynaecol. 77:197-203.

Mazess RB, Barden HS. (1990) Interrelationships among bone densitometry sites in normal young women. Bone Miner **11**:347-56.

Mazess RB, Barden HS. (1991) Bone density in premenopausal women: effects of age, dietary intake, physical activity, smoking, and birth-control pills. Am J Clin Nutr. **53**:132-42.

Mellish RW, Garrahan NJ, Compston JE. (1989) Age-related changes in trabecular width

and spacing in human iliac biopsies. Bone Miner **6**:331-338.

Melton LJ, Chao EYS, Lane J. (1995) Biomechanical aspects of fractures. In: Riggs BL, Melton LJ. (eds). Osteoporosis: Etiology, Diagnosis, and Management. 2nd Edition. pp 111-131. Raven Press, New York.

Melton LJ, Ehrischilles EA, Lane AW, Riggs BL (1992) How many women have osteoporosis? J Bone Miner Res. **9**:1005-1010.

Miles MP, Clarkson PM, Bean M, Ambach K, Mulroy J, Vincent K. (1993) Muscle function at the wrist following 9 d of immobilization and suspension. Med Sci Sports Exerc. **26**(5):615-623.

Morgan DB, Spiers FW, Pulvertaft CN, Fourman P. (1967) The amount of bone in the metacarpal and the phalanx according to age and sex. Clin Radiol. **18**:101-108.

Mosekilde L, Mosekilde L. (1986) Normal vertebral body size and compressive strength: relations to age and to vertebral and iliac trabecular bone compressive strength. Bone. **7**:207-12.

Mosekilde Li, Mosekilde Le, Danielsen CC. (1987) Biomechanical competence of vertebral trabecular bone in relation to ash density and age in normal individuals. Bone. **8**:79-85.

Mosekilde Li. (1988) Age-related changes in vertebral trabecular bone architecture -

assessed by a new method. Bone. **9**:247-250.

Mosekilde Li. (1989) Sex differences in age-related loss of vertebral trabecular bone mass and structure - biomechanical consequences. Bone. **10**:425-432.

Mosekilde L, Mosekilde L (1990) Sex differences in age-related changes in vertebral body size, density and biomechanical competence in normal individuals. Bone. **11**(2):67-73.

Mosekilde L. (1993) Normal age-related changes in bone mass, structure, and strength - consequences of the remodelling process. Dan Med Bull. **40**:65-83.

Müller R, Hahn M, Vogel m, Delling G, Rüegsegger P. (1996) Morphometric analysis of noninvasively assessed bone biopsies: comparison of high- resolution computed tomography and histologic sections. Bone. **18**(3):215-220.

Müller R, Hildebrand T, Hauselmann HJ, Rüesegger P. (1996) In vivo reproducibility of three-dimensional structural properties of noninvasive bone biopsies using 3 D-pCQT. J Bone Miner Res. **11**(11):1745-1750.

Müller R, Van Campenhout H, Van Damme B, Van Der Perre G, Dequeker J, Hildebrand T, Rüegsegger P. (1998) Morphometric analysis of human bone biopsies: a quantitative structural comparison of histological sections and micro-computed tomography. Bone. **23**(1):59-66.

Nelson ME, Fisher EC, Dilmanian FA, Dallal GE, Evans WJ. (1991) A 1-y walking program and increased dietary calcium in postmenopausal women: effects on bone. Am J Clin Nutr. **53**:1304-11.

Nijs J, Westhovens R, Joly J, Cheng XG, Borghs H, Dequeker J. (1998) Diagnostic sensitivity of peripheral quantitative computed tomography measurements at ultradistal and proximal radius in postmenopausal women. Bone. **22**(6):659-664.

Nordström P, Nordström G, Lorentzon, R. (1997) Correlation of bone density to strength and physical activity in young men with a low or moderate level of physical activity. Calcif Tissue Int. **60**:332-337.

Norkin C, White D. 1995 Measurement of Joint Motion. A Guide to Goniometry. 2nd edition. pp 74 - 116. Philadelphia PA, Davis Co.

Notelovitz M, Martin D, Tesar R, Khan FY, Probart C, Fields C, McKenzie L. (1991) Estrogen therapy and variable-resistance weight training increase bone mineral in surgically menopausal women. J Bone Miner Res. **6**(6):583-589.

O'Connor JA, Lanyon LE, MacFie H. (1982) The influence of strain rate on adaptive bone remodelling. J Biomech. **15**:767-81.

Ooms ME, Lips P, Van Lingen A, Valkenburg HA. (1993) Determinants of bone mineral density and risk factors for osteoporosis in healthy elderly women. J Bone Miner Res. **8**:669-675.

Ott SM. (1993) When bone mass fails to predict bone failure. Calcif Tissue Int. **53** (Suppl 1):S7-S13.

Owen RA, Melton LJ 3d, Ilstrup DM, Johnson KA, Riggs BL. (1982) Colles' fracture and subsequent hip fracture risk. Clin Orthop. **171**:37-43.

Palle S, Vico L, Bourrin S, Alexandre C. (1992) Bone tissue response to four-month antiorthostatic bedrest: a bone histomorphometric study. Calcif Tissue Int. **51**:189-194.

Parfitt AM. (1979) Quantum concept of bone remodeling and turnover: implications for the pathogenesis of osteoporosis. Calcif Tissue Int. **28**:1-5.

Parfitt AM, Mathews CH, Villanueva AR, Kleerekoper, Frame B, Rao DS. (1983) Relationship between surface, volume, and thickness of iliac trabecular bone in aging and in osteoporosis. J Clin Invest. **72**:1396-1409.

Parfitt AM. (1984) The cellular basis of bone remodelling: the quantum concept reexamined in light of recent advances in the cell biology of bone. Calcif Tissue Int. **36**:S37-S45.

Parfitt AM. (1994) the two faces of growth: benefits and risks to bone integrity. Osteoporos Int. **4**:382-398.

Pocock NA, Eisman JA, Yeates MG, Sambrook PN, Eberl S. (1986) Physical fitness is a

major determinant of femoral neck and lumbar spine bone mineral density. J Clin Invest.**78**:618-621.

Pocock NA, Eisman JA, Hopper JL, Yeates MG, Sambrook PN, Eberl S. (1987) Genetic determinants of bone mass in adults. A twin study. J Clin Invest. **80**:706-10.

Pocock N, Eisman J, Gwinn T, Sambrook P, Kelly P, Freund J, Yeates M. (1989) Muscle strength, physical fitness and weight but not age predict femoral neck bone mass. J Bone Miner Res. **4**:441-448.

Preisinger E, Alacamlioglu Y, Pils K, Saradeth T, Schneider B. (1995) Therapeutic exercise in the prevention of bone loss. Am J Phys Med Rehabil. **74**(2):120-123.

Prince RL, Price RI, Ho S. (1988) Forearm bone loss in hemiplegia: a model for the study of immobilization osteoporosis. J Bone Miner Res. **3**(3):305-310.

Prince RL, Smith M, Dick IM, Price RI, Webb PG, Henderson NK, Harris MM. (1991) Prevention of postmenopausal osteoporosis. New Engl J Med. **325**(17):1189-1195.

Pruitt LA, Jackson RD, Bartels RL, Lehnhard HJ. (1992) Weight-training effects on bone mineral density in early postmenopausal women. J Bone Miner Res. **7**(2):179-183.

Rüegsegger P, Durand E, Dambacher A. (1991) Differential effects of aging and disease on trabecular and compact bone density of the radius. Bone. **12**:99-105.

Raab DM, Smith EL, Crenshaw TD, Thomas DP. (1990) Bone mechanical properties after exercise training in young and old rats. J Appl Physiol. **68**:130-4.

Raab-Cullen DM, Akhter MP, Kimmel DB, Recker RR. (1994) Bone response to alternate -day mechanical loading of the rat tibia. J Bone Miner Res. **9**(2):203-211.

Recker RR, Davies KM, Hinders SM, Heaney RP, Stegman MR, Kimmel DB. (1992) Bone gain in young adult women. JAMA. **268**(17):2403-2408.

Recker RR, Kimmel DB, Parfitt AM, Davies KM, Keshawarz N, Hinders S. (1988) Static and tetracycline-based bone histomorphometric data from 34 normal postmenopausal females. J Bone Miner Res. **3**:133-144.

Rico H, González-Riola J, Revilla M, Villa LF, Gómez-Castresana F, Escribano J. (1994) Cortical versus trabecular bone mass: influence of activity on both bone components. Calcif Tissue Int. **54**:470-472.

Riggs BL, Melton LJ. (1986) Involutional osteoporosis N Engl J Med. **314**:1676-1686.

Riggs BL, Wahner HW, Melton LJ 3rd, Richelson LS, Judd HL, O'Fallon WM. (1987) Dietary calcium intake and rates of bone loss in women. J Clin Invest. **80**:979-82.

Riggs BL, Melton LJ (eds). (1995) Osteoporosis: Etiology, Diagnosis, and Management. (2nd edition). Raven Press, New York.

Rikli RE, McManis BG. (1990) Effects of exercise on bone mineral content in postmenopausal women. Res Q Exerc Sport. **61**(3):243-249.

Rothert ML, Holmes-Rovner M, Rovner D, Kroll J, Breer L, Talarczyk G, Schmitt N, Padonu G, Wills C.(1997) An educational intervention as decision support for menopausal women. Res Nurs Health. **20**:377-87.

Rubin CT, Lanyon LE. (1984) Regulation of bone formation by applied dynamic loads. J Bone Joint Surg. **66A**(3):397-402.

Rubin CT, Lanyon L. (1985) Regulation of bone mass by mechanical strain magnitude. Calcif Tissue Int. **37**:411-417.

Ryan AS, Treuth MS, Hunter GR, Elahi D. (1998) Resistive training maintains bone density in postmenopausal women. Calcif Tissue Int. **62**:295-299.

Sale DG, McComas J, MacDougall JD, Upton AR. (1982) Neuromuscular adaptation in human thenar muscles following strength training and immobilization. J Appl Physiol: Respirat Environ Exercise Physiol. **53**(2):419-424.

Sandler RB, Cauley JA, Hom DL, Sashin D, Kriska AM. (1987) The effects of walking on the cross-sectional dimensions of the radius in postmenopausal women. Calcif Tissue Int. **41**:65-69.

Sandler RB, Cauley JA, Sashin D, Scialabba MA, Kriska AM. (1989) The effect of grip

strength on radial bone in postmenopausal women. J Orthop Res. 7:440-444.

Sargeant AJ, Davies CTM, Edwards RHT, Maunder C, Young A. (1976) Functional and structural changes after disuse of human muscle. Clin Sci Mol Med. **52**:337-342.

Sato Y, Maruoka H, Oizumi K, Kikuyama M. (1996) Vitamin D deficiency and osteopenia in the hemiplegic limbs of stroke patients. Stroke. **27**(12):2183-2187.

Schlenker RA, VonSeggen WW. (1976) The distribution of cortical and trabecular bone mass along the lengths of the radius and ulna and the implications for *in vivo* bone mass measurements. Calcif Tissue Res. **20**:41-52.

Schneider P, Börner W, Mazess RB, Barden H. (1988) The relationship of peripheral to axial bone density. Bone Miner. **4**:279-287.

Schneider P, Reiners C. (1998) Peripheral quantitative computed tomography. In: Genant HK, Guglielmi G, Jergas M. (ed.). pp349-363. Bone densitometry and osteoporosis. Springer-Verlag, Berlin.

Schneider VS, McDonald J. (1984) Skeletal calcium homeostasis and countermeasures to prevent disuse osteoporosis. Calcif Tissue Int. **36**:5151-5154.

Schultheis L. (1991) The mechanical control system of bone in weightlessness spaceflight and in aging. Exp Gerontol. **26**:203-214.

Seeman E. (1994) Peak bone density in women with fractures: contribution of low peak bone density and rapid bone loss. Osteoporos Int. **3**(Suppl 1):S15-S25.

Shimegi S, Yanagita M, Okano H, Yamada M, Fukui H, Fukumura Y, Ibuki Y, Kojima I. (1994) Physical exercise increases bone mineral density in postmenopausal women. Endocr J. **41**:49-56.

Shrout PE, Fleiss JL. (1979) Intraclass correlations: uses in assessing rater reliability. Psychol Bull. **86**(2):420-428.

Sievänen H, Kannus P, Heinonen A, Oja P, Vuori I. (1994) Bone mineral density and muscle strength of lower extremities after long-term strength training, subsequent knee ligament injury and rehabilitation: a unique 2-year follow-up of a 26-year-old female student. Bone. **15**(1):85-90.

Sievänen H, Kannus P, Nieminen V, Heinonen A, Oja P, Vuori I. (1996) Estimation of various mechanical characteristics of human bones using dual energy x-ray absorptiometry: methodology and precision. Bone. **18**(1):17S-27S.

Sievänen H, Heinonen A, Kannus P. (1996) Adaptation of bone to altered loading environment: a biomechanical approach using x-ray absorptiometric data from the patella of a young woman. Bone. **19**(1):55-59.

Sievänen H, Koskue V, Rauhio A, Kannus P, Heinonen A, Vouri I. (1998) Peripheral quantitative computed tomography in human long bones: evaluation of in vitro and in

vivo precision. J Bone Miner Res. **13**(5):871-882.

Simkin A, Ayalon J, Leichter I. (1987) Increased trabecular bone density due to bone-loading exercises in postmenopausal osteoporotic women. Calcif Tissue Int. **40**:59-63.

Sinaki M, Wahner H, Offord K. (1989) Relationship between grip strength and related regional bone mineral content. Arch Phys Med Rehabil. **70**:823-826.

Sinaki M, Wahner HW, Bergstralh EJ, Hodgson F, Offord KP, Squires RW, Swee RG, Kao PC. (1996) Three-year controlled , randomized trial of the effect of dose-specified loading and strengthening exercises on bone mineral density of spine and femur in nonathletic, physically active women. Bone. **19**(3)233:244.

Sinaki M, Fitzpatrick LA, Ritchie C, Montesano A, Wahner HW. (1998) Site-specificity of bone mineral density and muscle strength in women. Am J Phys Med Rehabil. **77**(6):470-476.

Smith DA, Hosie CJ, Deacon AD, Hamblen DL. (1990) Quantitative gamma-ray computed tomography of the radius in normal subjects and osteoporotic patients Br J Radiol. **63**:776-82.

Smith EL, Smith PE, Ensign CJ, Shea MM. (1984) Bone involution decrease in exercising middle-aged women. Calcif Tissue Int. **36**:S129-S138.

Smith EL, Gilligan C, McAdam M, Ensign CP, Smith P. (1989) Deterring bone loss by exercise intervention in premenopausal and postmenopausal women. Calcif Tissue Int. **44**:312-321.

Snow CM. (1996) Exercise and bone mass in young and premenopausal women. Bone. **1**:51S-55S.

Snow-Harter C, Bouxsein M, Lewis B, Charette S, Weinstein P, Marcus R. (1990) Muscle strength as a predictor of bone mineral density in young women. J Bone Miner Res. **5**(6):589-595.

Spadaro JA, Werner FW, Brenner RA, Fortino MD, Fay LA, Edwards WT. (1994) Cortical and trabecular bone contribute strength to the oseteopenic distal radius. J Orthop Res. **12**:211-218.

Tsuji S, Tsunoda N, Yata H, Katsukawa F, Onishi S, Yamazaki H. (1995) Relation between grip strength and radial bone mineral density in young athletes. Arch Phys Med Rehabil. **76**:234-238.

Turner CH, Akhter MP, Raab DM, Kimmel DB, Recker RR. (1991) A noninvasive, in vivo model for studying strain adaptive bone modeling. Bone. **12**:73-79.

Turner CH, Burr DB. (1993) Basic biomechanical measurements of bone: a tutorial. Bone. **14**:595-608.

Turner CH. (1998) Three rules for bone adaptation to mechanical stimuli. Bone. **3**:399-407.

Tuukkanen J, Peng Z, Vaananen HK. (1992) The effect of training on the recovery from immobilization-induced bone loss in rats. Acta Physiol Scand. **145**:407-411.

Tylavsky FA, Bortz AD, Hancock RL, Anderson JJ. (1989) Familial resemblance of radial bone mass between premenopausal mothers and their college-age daughters. Calcif Tissue Int. **45**:265-72.

Vesterby A, Gundersen HJ, Melsen F, Mosekilde L. (1989) Normal postmenopausal women show iliac crest trabecular thinning on vertical sections. Bone. **10**:333-339.

Vesterby A, Gundersen HJG, Melsen F. (1989) Star volume of marrow space and trabeculae of the first lumbar vertebra: sampling efficiency and biological variation. Bone. **10**:7-13.

Vico L, Chappard D, Alexandre C, Palle S, Minaire P, Riffat G, Morukov B, Rakhmanov S. (1987) Effects of a 120 day period of bed-rest on bone mass and bone cell activities in man: attempts at countermeasure. Bone Miner. **2**:383-394.

Vico L, Pouget JF, Calmels P, Chatard JC, Rehailia M, Minaire P, Geyssant A, Alexandre C. (1995) The relations between physical ability and bone mass in women aged over 65 years. J Bone Miner Res. **10**:374-383.

Vico L, Lafage-Proust M-H, Alexandre C. (1998) Effects of gravitational changes on the bone system in vitro and in vivo. Bone. **22**(5):95S-100S.

Vogel JM, Whittle MW. (1976) Bone mineral changes: the second manned skylab mission. Aviation, Space, and Environmental Medicine. **47**(4):396-400.

Von Wowern N, Storm TL, Olgaard K. (1988) Bone mineral content by photon absorptiometry of the mandible compared with that of the forearm and the lumbar spine. Calcif Tissue Int. **42**:157-161.

Walters J, Koo WWK, Bush A, Hammami M. (1998) Effect of hand dominance on bone mass measurement in sedentary individuals. Journal of Clinical Densitometry. **1**:359-367.

Wapniarz M, Lehmann R, Reincke M, Schönau E, Klein K, Allolio B. (1997) Determinants of radial bone density as measured by pQCT in pre- and postmenopausal women: the role of bone size. J Bone Miner Res. **12**(2):248-254.

Webber CE. (1998) Uncertainties in bone mineral density T scores. Clin Invest Med. **21**:88-93.

Weinstein RS, New KD, Sappington LJ. (1991) Dual-energy x-ray absorptiometry versus single photon absorptiometry. Calcif Tissue Int. **49**:313-316.

Whitehouse WJ. (1977) Cancellous bone in the anterior part of the iliac crest. Calcif

Tissue Res. **23**:67-76.

World Health Organization. Assessment of fracture risk and its application to screening for postmenopausal osteoporosis. Technical Reports series No 843 of a WHO study group. WHO, Geneva. 1994

Young DR, Nilklowitz WJ, Steele CR. (1983) Tibial changes in experimental disuse osteoporosis in the monkey. Calcif Tissue Int. **35**:304-308.

Young DR, Niklowitz WJ, Brown RJ, Jee WSS. (1986) Immobilization-associated osteoporosis in primates. Bone. **7**:109-117.